Selecting Centrifugal Pumps

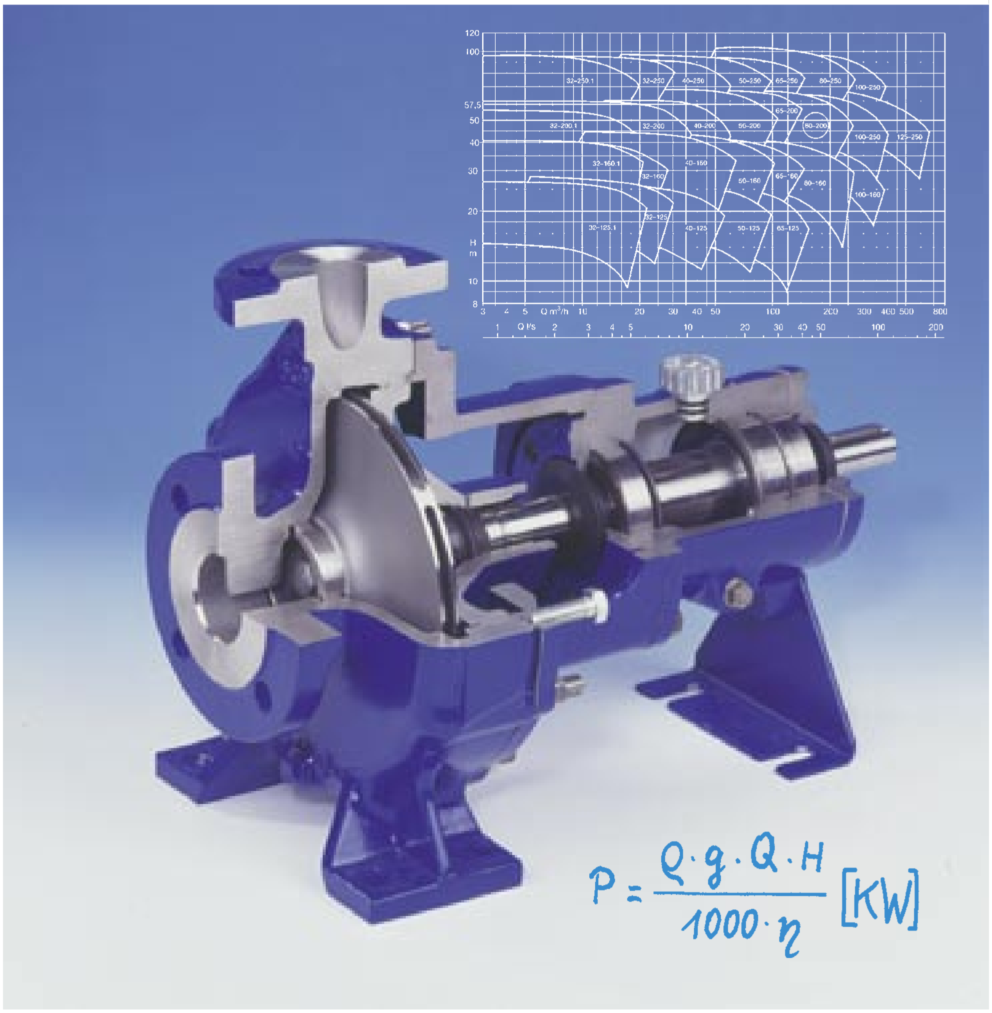

Published by:
**KSB Aktiengesellschaft,
Communications (V5),
67225 Frankenthal / Germany**

4th completely revised and expanded edition 2005

Layout, drawings and composition:
KSB Aktiengesellschaft,
Media Production V51

ISBN 3-00-017841-4

Contents

Table of contents

Contents

Tables

1 Nomenclature

A	m^2	Area
A	m	Distance between measuring point and pump flange
a	m, mm	Width of a rectangular elbow
B	m, mm	Vertical distance from suction pipe to floor
C_v	gpm	Flow coefficient for valves, defined as the flow of water at 60 °F in US gallons/minute at a pressure drop of 1 lb/in^2 across the valve
c_D		Resistance coefficient of a sphere in water flow
c_T	(%)	Solids content in the flow
D	m (mm)	Outside diameter; maximum diameter
DN	(mm)	Nominal diameter
d	m (mm)	Inside diameter; minimum diameter
d_s	m (mm)	Grain size of solids
d_{50}	m (mm)	Mean grain size of solids
F	N	Force
f		Throttling coefficient of an orifice
f_H		Conversion factor for head (KSB system)
f_Q		Conversion factor for flow rate (KSB system)
f_η		Conversion factor for efficiency (KSB system)
g	m/s^2	Gravitational constant = 9.81 m/s^2
H	m	Head; discharge head
H_{geo}	m	Geodetic head
H_s	m	Suction lift
$H_{s\ geo}$	m	Vertical distance between water level and pump reference plane for suction lift operation
$H_{z\ geo}$	m	Vertical distance between pump reference plane and water level for positive inlet pressure operation
H_L	m	Head loss
H_0	m	Shut-off head (at Q = 0)
I	A	Electric current (amperage)
K		Dimensionless specific speed, type number
k	mm, µm	Mean absolute roughness
k		Conversion factors k_Q, k_H, k_η (HI method)
k_v	m^3/h	Metric flow factor for valves, defined as the flow of water at 20 °C in cubic metres per hour at a pressure drop of 1 bar
L	m	Length of pipe
L_s	m	Straight length of air-filled pipe
M	Nm	Moment
$NPSH_r$	m	NPSH required by the pump
$NPSH_a$	m	NPSH available
N_s		Specific speed in US units
n	min^{-1} (rpm) s^{-1} (rev/s)	Speed of rotation
n_q	min^{-1}	Specific speed in metric units
P	kW (W)	Power; input power

p_e		Pressure in suction or inlet tank
PN	(bar)	Nominal pressure
Δp	bar (Pa)	Pressure rise in the pump; pressure differential ($Pa \equiv N/m^2$)
p	bar (Pa)	Pressure ($Pa \equiv N/m^2 = 10^{-5}$ bar)
p_b	mbar (Pa)	Atmospheric pressure (barometric)
p_L	bar (Pa)	Pressure loss
p_v	bar (Pa)	Vapour pressure of fluid pumped
Q	m^3/s, m^3/h	Flow rate / capacity (also in litre/s)
q_{air}	%	Air or gas content in the fluid pumped
Q_{off}	m^3/h	Flow rate at switch-off pressure
Q_{on}	m^3/h	Flow rate at start-up pressure
R	m (mm)	Radius
Re		Reynolds number
S	m	Submergence (fluid level above pump); immersion depth
s	mm	Wall thickness
s’	m	Difference of height between centre of pump impeller inlet and centre of pump suction nozzle
T	Nm	Torque
t	°C	Temperature
U	m	Length of undisturbed flow
U	m	Wetted perimeter of a flow section
V_B	m^3	Suction tank volume
V_N	m^3	Useful volume of pump sump
v	m/s	Flow velocity
w	m/s	Settling velocity of solids
y	mm	Travel of gate valve; distance to wall
Z	1/h	Switching cycle (frequency of starts)
z		Number of stages
$z_{s,d}$	m	Height difference between pump discharge and suction nozzles
α	°	Angle of change in flow direction; opening angle
δ	°	Angle of inclination
ζ		Loss coefficient
η	(%)	Efficiency
η	Pa s	Dynamic viscosity
λ		Pipe friction factor
ν	m^2/s	Kinematic viscosity
ϱ	kg/m^3	Density
τ	N/m^2	Shear stress
τ_f	N/m^2	Shear stress at yield point
φ		Temperature factor; opening angle of a butterfly valve; cos φ: power factor of asynchronous motors
ψ		Head coefficient (dimensionless head generated by impeller)

Indices, Subscripts

a	At outlet cross-section of the system; branching off
Bl	Referring to orifice bore
d	On discharge side; at discharge nozzle; flowing through
dyn	Denoting dynamic component
E	At the narrowest cross-section of valves (Table 5)
E	At suction pipe or bell-mouth inlet
e	At inlet cross-section of system, e.g. in suction or inlet tank
f	Referring to carrier fluid
H	Horizontal
in	Referring to inlet flow
K	Referring to curvature
L	Referring to losses
m	Mean value
max	Maximum value
min	Minimum value
N	Nominal value
opt	Optimum value; at best efficiency point (BEP)
P	Referring to pump
p	Referring to pressure
r	Reduced, for cutdown impeller or impeller vanes
s	On suction side; at suction nozzle
s	Referring to solids
stat	Static component
sys	Referring to system / installation
t	Referring to impeller prior to trimming
V	Vertical
w	Referring to water
z	Referring to viscous fluid
0	Basic position, referred to individual sphere
1, 2, 3	Consecutive numbers; items
I, II	Number of pumps operated

2
Pump Types

Typical selection criteria for centrifugal pumps are their design data (flow rate or capacity Q, discharge head H, speed of rotation n and NPSH), the properties of the fluid pumped, the application, the place of installation and the applicable regulations, specifications, laws and codes. KSB offers a broad range of pump types to meet the most varied requirements.

Main design features for classification are:

– the number of stages (single-stage / multistage),

– the position of the shaft (horizontal / vertical),

– the pump casing (radial, e.g. volute casing / axial, e.g. tubular casing),

– the number of impeller entries (single entry / double entry),

– the type of motor (dry motor / dry rotor motor, e.g. submerged motor / wet rotor motor, e.g. canned motor, submersible motor).

These features usually determine what a pump type or series looks like. An overview of typical designs according to classification features is given below (Table 1 and Figs. 1a to 1p).

Other pump classification features include:

– the mode of installation, which is dealt with in section 7.1,

– the nominal diameter (for the pump size, as a function of the flow rate),

– the rated pressure (for the wall thickness of casings and flanges),

– the temperature (for example for the selection of cooling equipment for shaft seals),

– the fluid pumped (abrasive, aggressive, toxic fluids),

– the type of impeller (radial flow / axial flow depending on the specific speed),

– the self-priming ability,

– the casing partition, the position of the pump nozzles, an outer casing, etc.

Table 1: Centrifugal pump classification

Number of stages	Single stage						Multistage	
Shaft position	Horizontal			Vertical			Horiz.	Vertic.
Casing design	Radial		Axial	Radial		Axial	Stage casing	
Impeller entries	1	2	1	1	2	1	1	1
Motor type, Fig. 1..								
Dry (standardized) motor	a	b	c	d	e	f	g	h
Magnetic drive	i							
Submerged dry rotor motor (See 3.3.2)			j	k		l		m
Wet rotor motor (See 3.3.2)	n						o	p

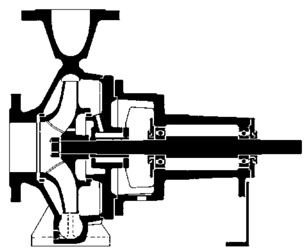
a

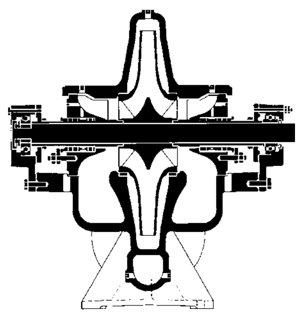
b

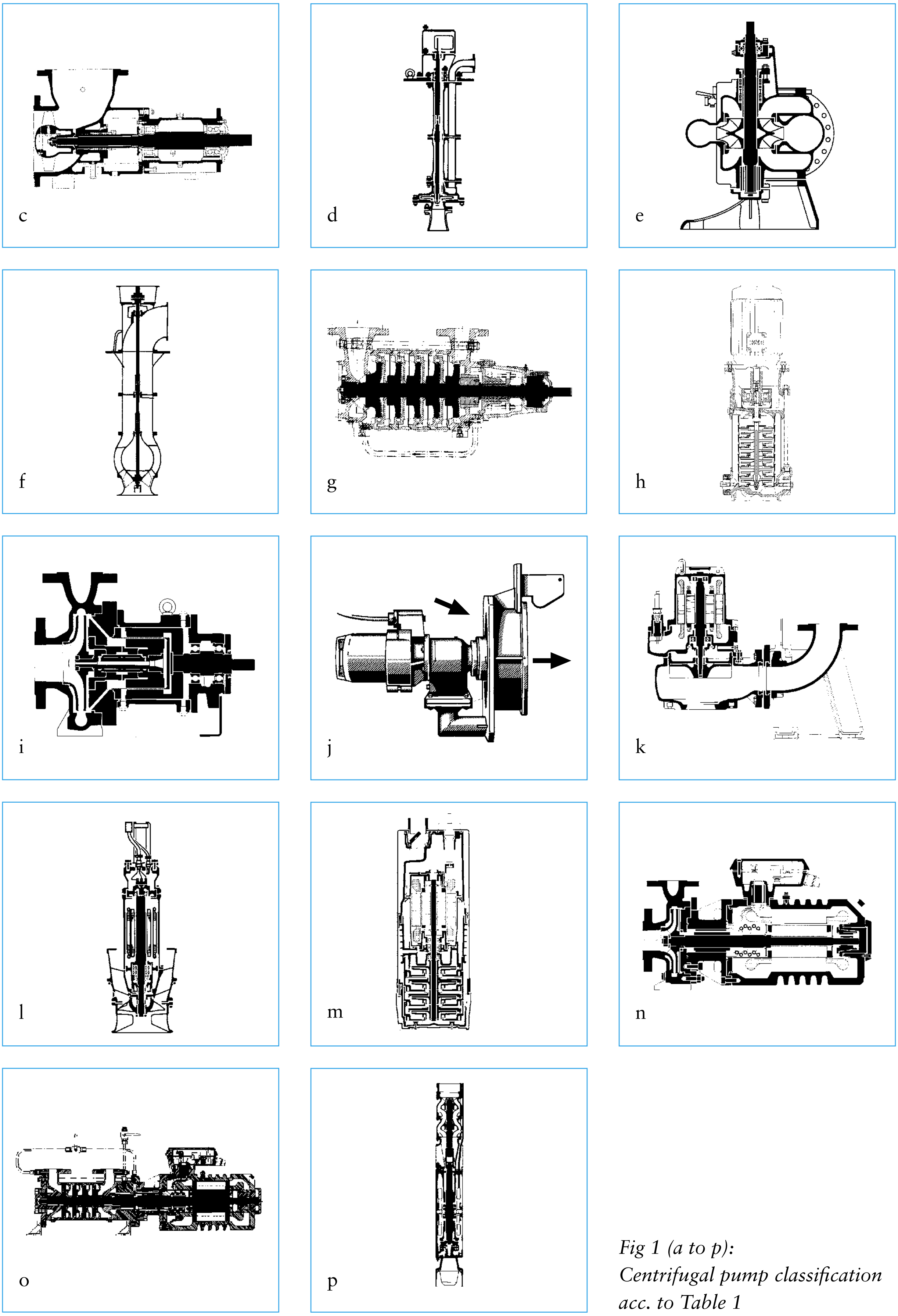

Fig 1 (a to p):
Centrifugal pump classification
acc. to Table 1

3 Selection for Pumping Water

This section applies mainly to pumping water; the particularities of pump selection for other media are treated in sections 4, 5 and 6.

3.1 Pump Data

3.1.1 Pump Flow Rate

The pump flow rate or capacity Q is the useful volume of fluid delivered to the pump discharge nozzle in a unit time in m^3/s (l/s and m^3/h are also used in practice, as are GPM in the US). The flow rate changes proportionally to the pump speed of rotation. Leakage flow as well as the internal clearance flows are not considered part of the pump flow rate.

3.1.2 Developed Head and Developed Pressure of the Pump

The total developed head H of a pump is the useful mechanical energy in Nm transferred by the pump to the flow, per weight of fluid in N, expressed in Nm/N = m (also used to be called "metres of fluid")[1)]. The head develops proportionally to the square of the impeller's speed of rotation and is independent of the density ϱ of the fluid being pumped. A given centrifugal pump will impart the same head H to various fluids (with the same kinematic viscosity ν) regardless of their density ϱ. This statement applies to all centrifugal pumps.

The total developed head H manifests itself according to Bernoulli's equation (see section 3.2.1.1) as

– the pressure head H_p proportional to the pressure difference between discharge and suction nozzles of the pump,

– the geodetic head $z_{s,d}$ (Figs. 8 and 9), i.e., the difference in height between discharge and suction nozzles of the pump and

– the difference of the kinetic energy head $(v_d^2\text{-}v_s^2)/2g$ between the discharge and suction nozzles of the pump.

The pressure rise Δp in the pump (considering the location of the pressure measurement taps according to section 7.3!) is determined solely by the pressure head H_p along with the fluid density ϱ according to the equation

$$\Delta p = \varrho \cdot g \cdot [H - z_{s,d} - (v_d^2 - v_s^2)/2g] \qquad (1)$$

where

ϱ Density of the fluid being pumped in kg/m^3

g Gravitational constant $9.81\ m/s^2$

H Total developed head of the pump in m

$z_{s,d}$ Height difference between pump discharge and suction nozzles in m (see Figs. 8 and 9)

v_d Flow velocity in the discharge nozzle $= 4\ Q/\pi d_d^2$ in m/s

v_s Flow velocity in the suction nozzle $= 4\ Q/\pi d_s^2$ in m/s

Q Flow rate of the pump at the respective nozzle in m^3/s

d Inside diameter of the respective pump nozzle in m

Δp Pressure rise in N/m^2 (for conversion to bar: 1 bar = 100 000 N/m^2)

High-density fluids therefore increase the pressure rise and the pump discharge pressure. The discharge pressure is the sum of the pressure rise and the inlet pressure and is limited by the strength of the pump casing. The effect of temperature on the pump's strength limits must also be considered.

3.1.3 Efficiency and Input Power

The input power P of a pump (also called brake horsepower) is the mechanical power in kW or W taken by the shaft or coupling. It is proportional to the third power of the speed of rotation and is given by one of the following equations:

[1)] In the US, the corresponding units are ft-lbf/lbm, i. e. 1 foot head = 1 foot-pound-force per pound mass; the numerical value of head and specific work are identical.

$$P = \frac{\varrho \cdot g \cdot Q \cdot H}{\eta} \text{ in W} = \frac{\varrho \cdot g \cdot Q \cdot H}{1000 \cdot \eta} \text{ in kW} = \frac{\varrho \cdot Q \cdot H}{367 \cdot \eta} \text{ in kW} \quad \textbf{(2)}$$

where

ϱ	Density in kg/m^3	in kg/dm^3	in kg/dm^3
Q	Flow rate in m^3/s	in m^3/s	in m^3/h

g Gravitational constant = 9.81 m/s^2
H Total developed head in m
η Efficiency between 0 and <1 (not in %)

The pump efficiency η is given with the characteristic curves (see section 3.1.6).

The pump input power P can also be read with sufficient accuracy directly from the characteristic curves (see section 3.1.6) for density ϱ = 1000 kg/m^3. For other densities ϱ, the input power P must be changed in proportion.

Pumping media which are more viscous than water (see section 4) or have high concentrations of entrained solids (see section 6) will require a higher input power. This is, for example, the case when pumping sewage or waste water, see section 3.6.

The pump input power P is linearly proportional to the fluid density ϱ. For high-density fluids the power limits of the motor (section 3.3.3) and the torque limits (for the loading on coupling, shaft and shaft keys) must be considered.

3.1.4 Speed of Rotation

When using three-phase current motors (asynchronous squirrel-cage motors to IEC standards) the following speeds of rotation are taken as reference for pump operation:

Table 2: Reference speeds of rotation

Number of poles	2	4	6	8	10	12	14
Frequency	Reference speeds for the characteristic curve documentation in min^{-1} (rpm)						
For 50 Hz	2900	1450	960	725	580	480	415
For 60 Hz	3500	1750	1160	875	700	580	500

In practice the motors run at slightly higher speeds (which depend on the power output and on the make) [1], which the pump manufacturer may consider for the pump design and selection when the customer agrees. In this case, the affinity laws described in section 3.4.3 are to be applied. The characteristic curves of submersible motor pumps and submersible borehole pumps have already been matched to the actual speed of rotation.

When using motor speed controllers (for example phase angle control for ratings up to a few kW or, in most other cases, frequency inverters), gearboxes, belt drives or when using turbines or internal combustion engines as drivers, other pump speeds are possible.

3.1.5 Specific Speed and Impeller Type

The specific speed n_q is a parameter derived from a dimensional analysis which allows a comparison of impellers of various pump sizes even when their operating data differ (flow rate Q_{opt}, developed head H_{opt}, rotational speed n at the point of best efficiency η_{opt}). The specific speed can be used to classify the optimum impeller design (see Fig. 2) and the corresponding pump characteristic curve (see section 3.1.6, Fig. 5).

n_q is defined as the theoretical rotational speed at which a geometrically similar impeller would run if it were of such a size as to produce 1 m of head at a flow rate of 1 m^3/s at the best efficiency point. It is expressed in the same units as the speed of rotation. The specific speed can be made a truly dimensionless characteristic parameter while retaining the same numerical value by using the definition in the right-hand version of the following equation [2]:

$$n_q = n \cdot \frac{\sqrt{Q_{opt}/1}}{(H_{opt}/1)^{3/4}} \qquad = 333 \cdot n \cdot \frac{\sqrt{Q_{opt}}}{(g \cdot H_{opt})^{3/4}} \tag{3}$$

where	Q_{opt}	in m^3/s	Q_{opt}	in m^3/s	= Flow rate at η_{opt}
	H_{opt}	in m	H_{opt}	in m	= Developed head at η_{opt}
	n	in rpm	n	in rev/s	= Pump speed
	n_q	in metric units	n_q	Dimensionless parameter	
			g	Gravitational constant 9.81 m/s^2	

For multistage pumps the developed head H_{opt} at best efficiency for a **single** stage and for double-entry impellers, the optimum flow rate Q_{opt} for only **one** impeller half are to be used.

As the specific speed n_q increases, there is a continuous change from the originally radial exits of the impellers to "mixed flow" (diagonal) and eventually axial exits (see Fig. 2). The diffuser elements of radial pump casings (e.g. volutes) become more voluminous as long as the flow can be carried off radially. Finally only an axial exit of the flow is possible (e.g. as in a tubular casing).

Approximate reference values:

n_q up to approx.	25	Radial high head impeller
up to approx.	40	Radial medium head impeller
up to approx.	70	Radial low head impeller
up to approx.	160	Mixed flow impeller
approx. from	140 to 400	Axial flow impeller (propeller)

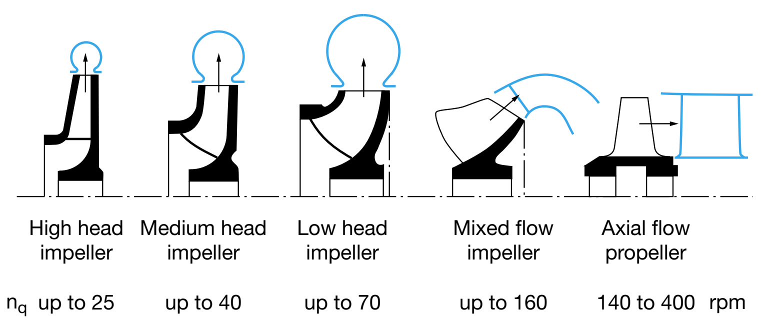

Fig. 2: Effect of the specific speed n_q on the design of centrifugal pump impellers. The diffuser elements (casings) of single stage pumps are outlined.

Using Fig. 3 it is possible to determine n_q graphically. Further types of impellers are shown in Fig. 4: Star impellers are used in self-priming pumps. Peripheral impellers extend the specific speed range to lower values down to approximately n_q = 5 (peripheral pumps can be designed with up to three stages). For even lower specific speeds, rotary (for example progressive cavity pumps with n_q = 0.1 to 3) or reciprocating positive displacement pumps (piston pumps) are to be preferred.

The value of the specific speed is one of the influencing parameters required when converting the pump characteristic curves for pumping viscous or solids-laden media (see sections 4 and 6).

In English-language pump literature the true dimensionless specific speed is sometimes designated as the "type number K". In the US, the term N_s is used, which is calculated using gallons/min (GPM), feet and rpm. The conversion factors are:

$$K = n_q / 52.9 \qquad N_s = n_q / 51.6 \tag{4}$$

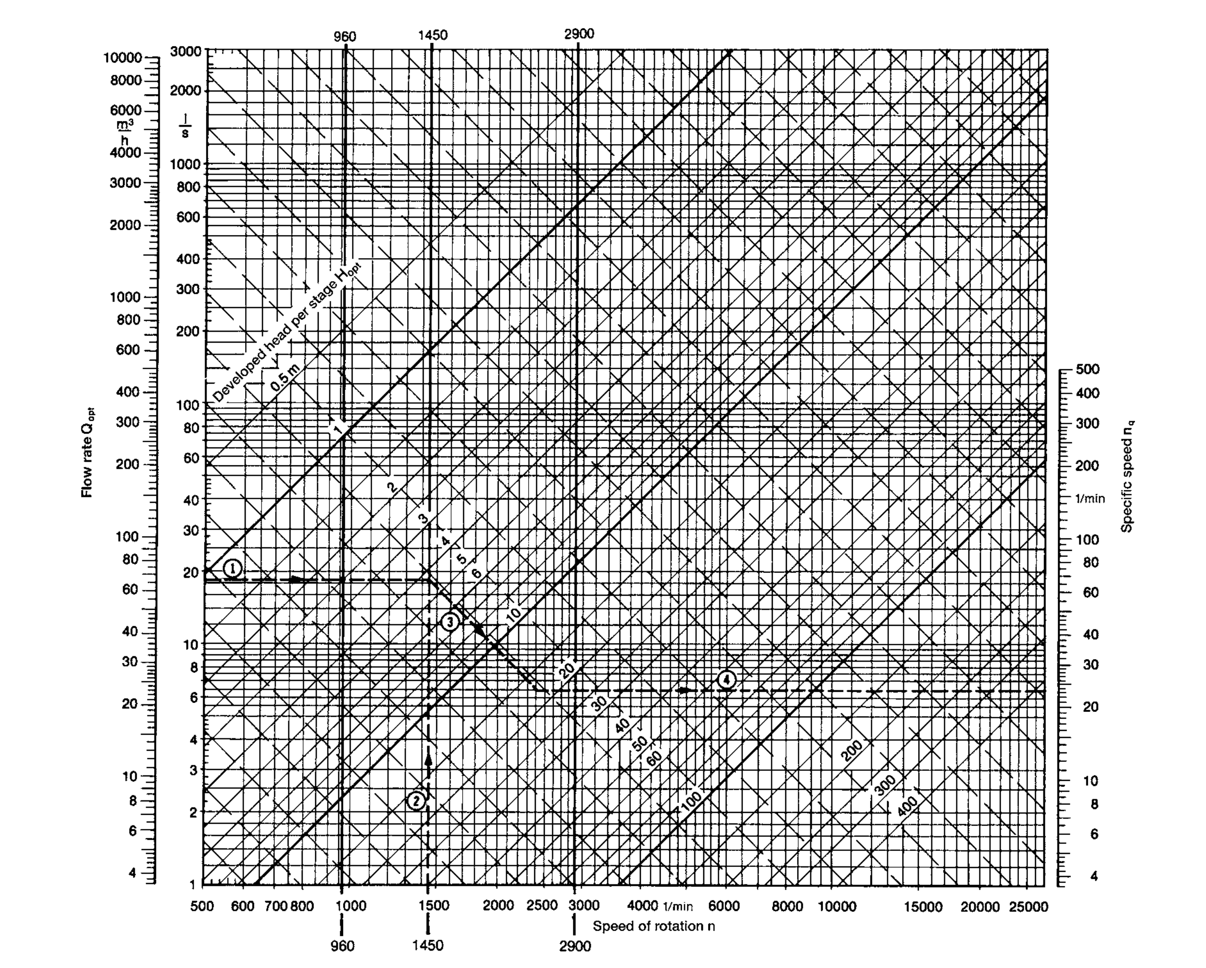

Fig. 3: Nomograph to determine specific speed n_q (enlarged view on p. 80)
Example: Q_{opt} = 66 m^3/h = 18.3 l/s; n = 1450 rpm, H_{opt} = 17.5 m. Found: n_q = 23 (metric units).

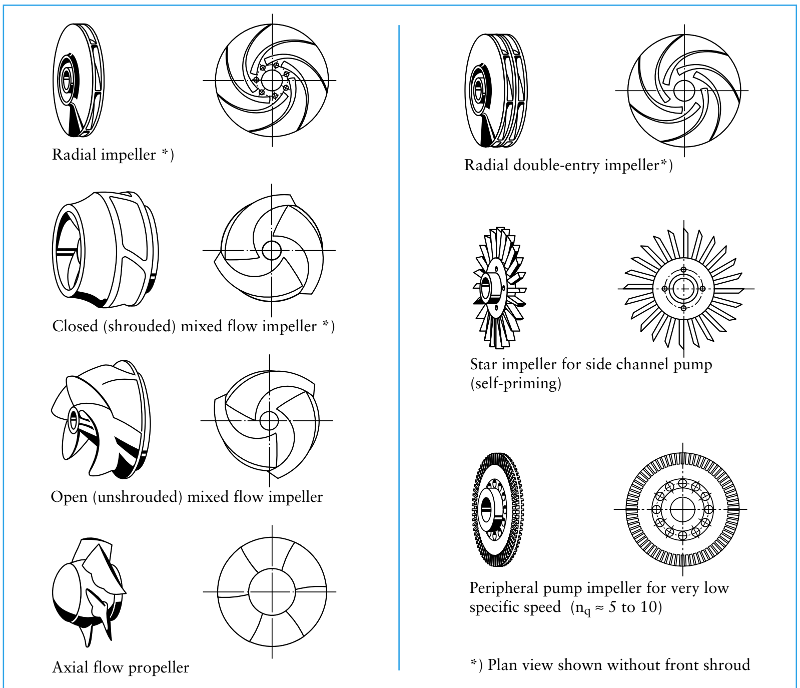

3.1.6 Pump Characteristic Curves

Unlike positive displacement pumps (such as piston pumps), centrifugal pumps deliver a variable flow rate Q (increasing with decreasing head H) when operating at constant speed. They are therefore able to accommodate changes in the system curve (see section 3.2.2). The input power P and hence the efficiency η as well as the $NPSH_r$ (see section 3.5.4) are dependent on the flow rate.

Fig. 4: Impeller types for clear liquids

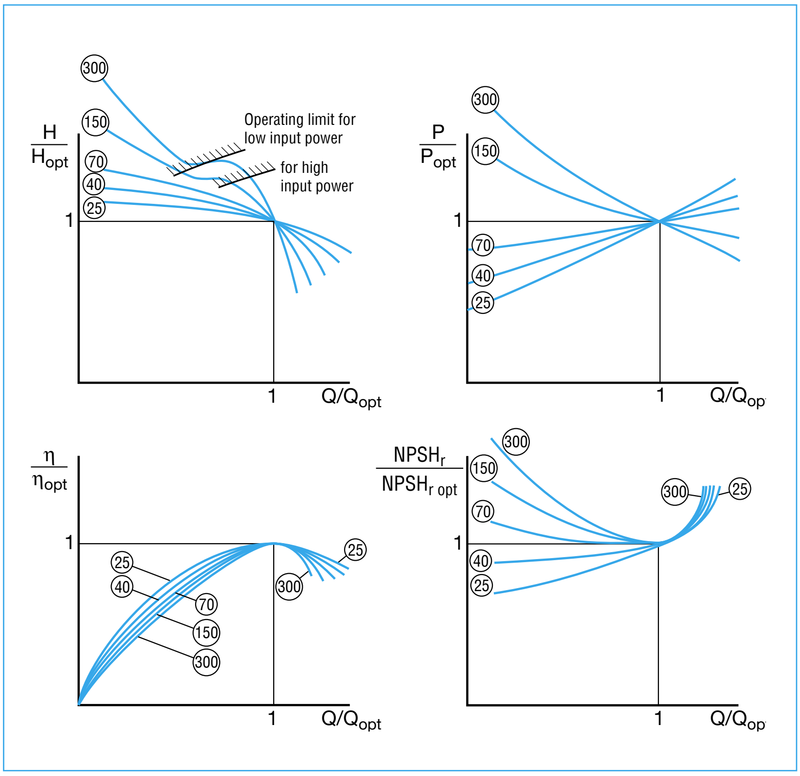

Fig. 5: Effect of specific speed n_q on centrifugal pump characteristic curves (Not drawn to scale! For NPSH$_r$, see section 3.5.4).

The relationship of these values is shown graphically in the pump characteristic curves, whose shape is influenced by the specific speed n_q and which document the performance of a centrifugal pump (see Fig. 5 for a comparison of characteristics and Fig. 6 for examples). The head curve of the pump is also referred to as the H/Q curve.

The H/Q curve can be steep or flat. For a steep curve, the flow rate Q changes less for a given change of developed head ΔH than for a flat curve (Fig. 7). This can be advantageous when controlling the flow rate.

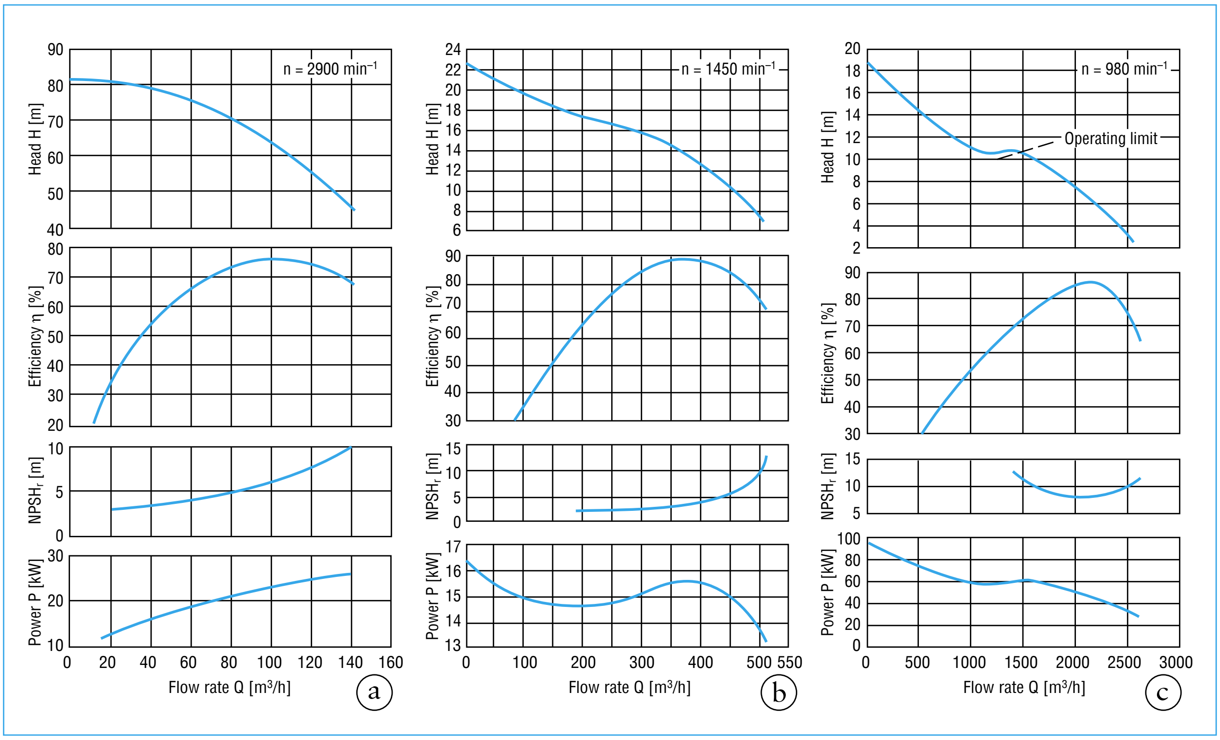

Fig. 6: Three examples of characteristic curves for pumps of differing specific speeds.
a: radial impeller, $n_q \approx 20$; b: mixed flow impeller, $n_q \approx 80$; c: axial flow impeller, $n_q \approx 200$.
(For NPSH$_r$ see section 3.5.4)

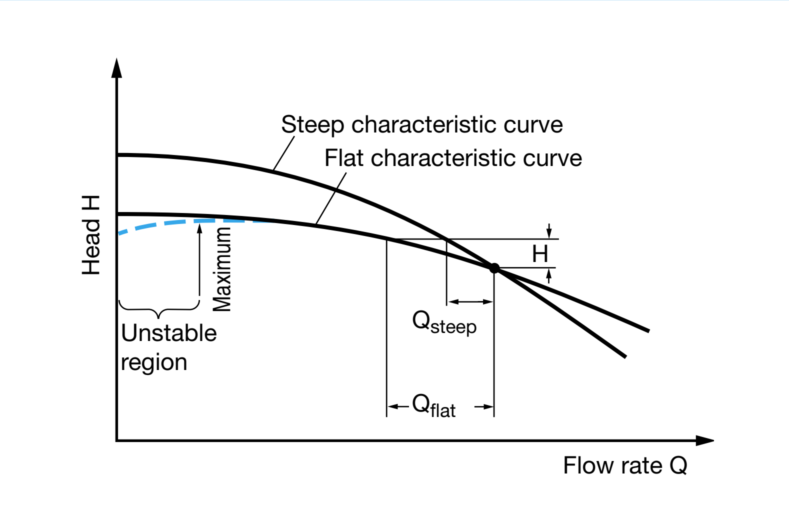

Fig. 7: Steep, flat or unstable characteristic curve

H/Q characteristics normally have a stable curve, which means that the developed head falls as the flow rate Q increases. For low specific speeds, the head H may – in the low flow range – drop as the flow rate Q decreases, i. e., the curve is unstable (shown by the dash line in Fig. 7). This type of pump characteristic curve need only be avoided when two intersections with the system curve could result, in particular when the pump is to be used for parallel operation at low flow rates (see section 3.4.4) or when it is pumping into a vessel which can store energy (accumulator filled with gas or steam). In all other cases the unstable curve is just as good as the stable characteristic.

Unless noted otherwise, the characteristic curves apply for the density ϱ and the kinematic viscosity ν of cold, deaerated water.

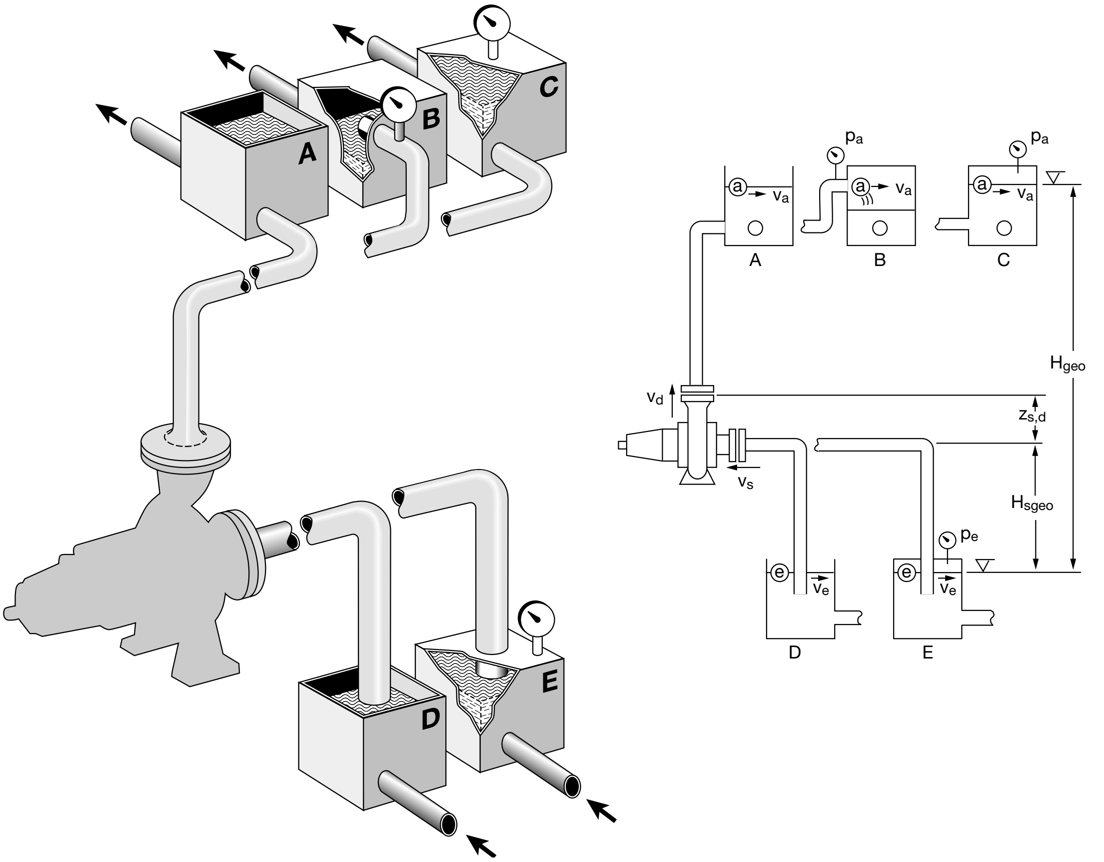

Fig. 8: Centrifugal pump system with variously designed vessels in suction lift operation
A = Open tank with pipe ending below the water level
B = Closed pressure vessel with free flow from the pipe ending above the water level
C = Closed pressure vessel with pipe ending below the water level
D = Open suction/inlet tank
E = Closed suction/inlet tank

v_a and v_e are the (usually negligible) flow velocities at position a in tanks A and C and at position e in tanks D and E. In case B, v_a is the non-negligible exit velocity from the pipe end at a.

3.2 System Data

3.2.1 System Head

3.2.1.1 Bernoulli's Equation

Bernoulli's equation expresses the equivalence of energy in geodetic (potential) energy, static pressure and kinetic energy form. The system head H_{sys} for an assumed frictionless, inviscid flow is composed of the following three parts (see Figs. 8 and 9):

- H_{geo} (geodetic head) is the difference in height between the liquid level on the inlet and discharge sides. If the discharge pipe ends above the liquid level, the centre of the exit plane is used as reference for the height (see Figs 8B and 9B).
- $(p_a - p_e)/(\varrho \cdot g)$ is the pressure head difference between the inlet and outlet tank, applic-

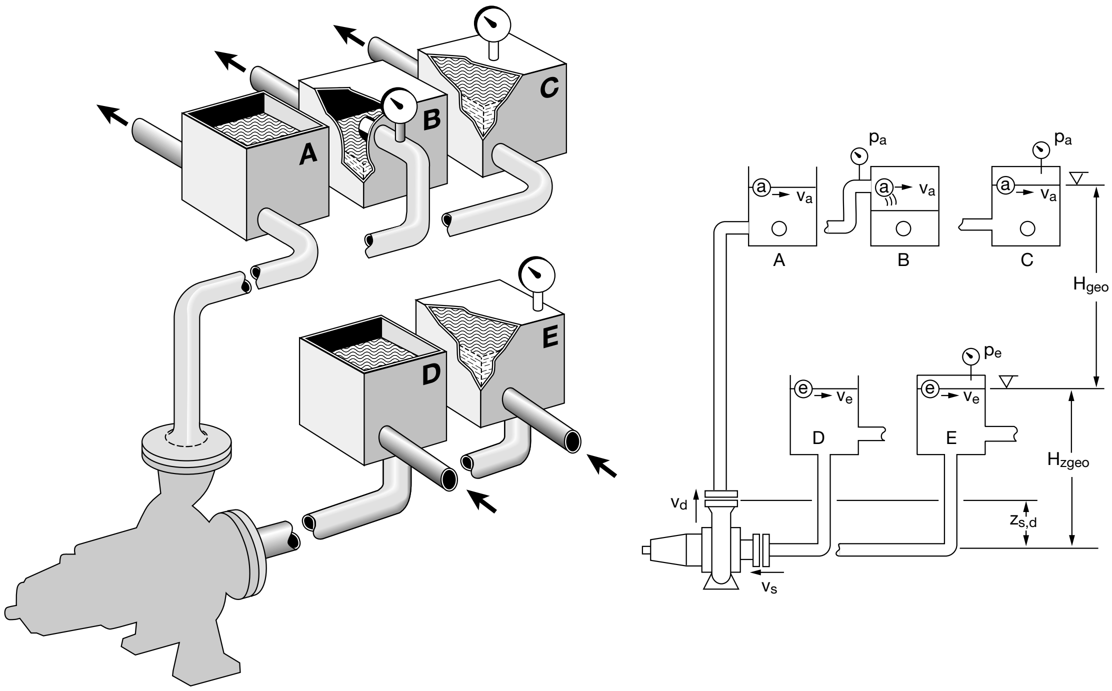

Fig. 9: Centrifugal pump system with variously designed vessels in suction head (positive inlet pressure) operation. Legend as in Fig. 8.

able when at least one of the tanks is closed as for B, C or E (see Figs. 8B, C, E, 9B, C, E).

- $(v_a^2 - v_e^2)/2g$ is the difference in the velocity heads between the tanks.

For a physically real flow, the friction losses (pressure head losses) must be added to these components:

$\sum H_L$ is the sum of the head losses (flow resistance in the piping, valves, fittings, etc in the suction and discharge lines as well as the entrance and exit losses, see section 3.2.1.2), and is referred to as the system pressure loss.

The sum of all four components yields the system head H_{sys}:

$$H_{sys} = H_{geo} + (p_a - p_e)/(\varrho \cdot g) + (v_a^2 - v_e^2)/2g + \sum H_L \quad \textbf{(5)}$$

where
all the heads H are in m,
all the pressures p are in Pa (1 bar = 100 000 Pa),
all velocities v are in m/s,
the density ϱ is in kg/m^3,
the gravitational constant is g = 9.81 m/s^2.

The difference of the velocity heads can often be neglected in practice. When at least one tank is closed as for B, C or E (see Figs. 8B, C, E, 9B, C, E), Eq. 5 can be simplified as

$$H_{sys} \approx H_{geo} + (p_a - p_e)/(\varrho \cdot g) + \sum H_L \qquad (6)$$

and further simplified when both tanks are open as for A and D (see Figs. 8A, D and 9A, D) as

$$H_{sys} \approx H_{geo} + \sum H_L \qquad (7)$$

3.2.1.2 Pressure Loss Due to Flow Resistances

The pressure loss p_L is caused by wall friction in the pipes and flow resistances in valves, fittings, etc. It can be calculated from the head loss H_L, which is independent of the density ϱ, using the following equation:

$$p_L = \varrho \cdot g \cdot H_L \qquad (8)$$

where
- ϱ Density in kg/m^3
- g Gravitational constant 9.81 m/s^2
- H_L Head loss in m
- p_L Pressure loss in Pa (1 bar = 100 000 Pa)

3.2.1.2.1 Head Loss in Straight Pipes

The head loss for flow in straight pipes with circular cross-sections is given in general by

$$H_L = \lambda \cdot \frac{L}{d} \cdot \frac{v^2}{2g} \qquad (9)$$

where
- λ Pipe friction factor according to Eqs. (12) to (14)
- L Length of pipe in m
- d Pipe inside diameter in m
- v Flow velocity in m/s (= 4Q/πd^2 for Q in m^3/s)
- g Gravitational constant 9.81 m/s^2

Fig. 10: Pipe friction factor λ as a function of the Reynolds number Re and the relative roughness d/k (enlarged view on p. 81)

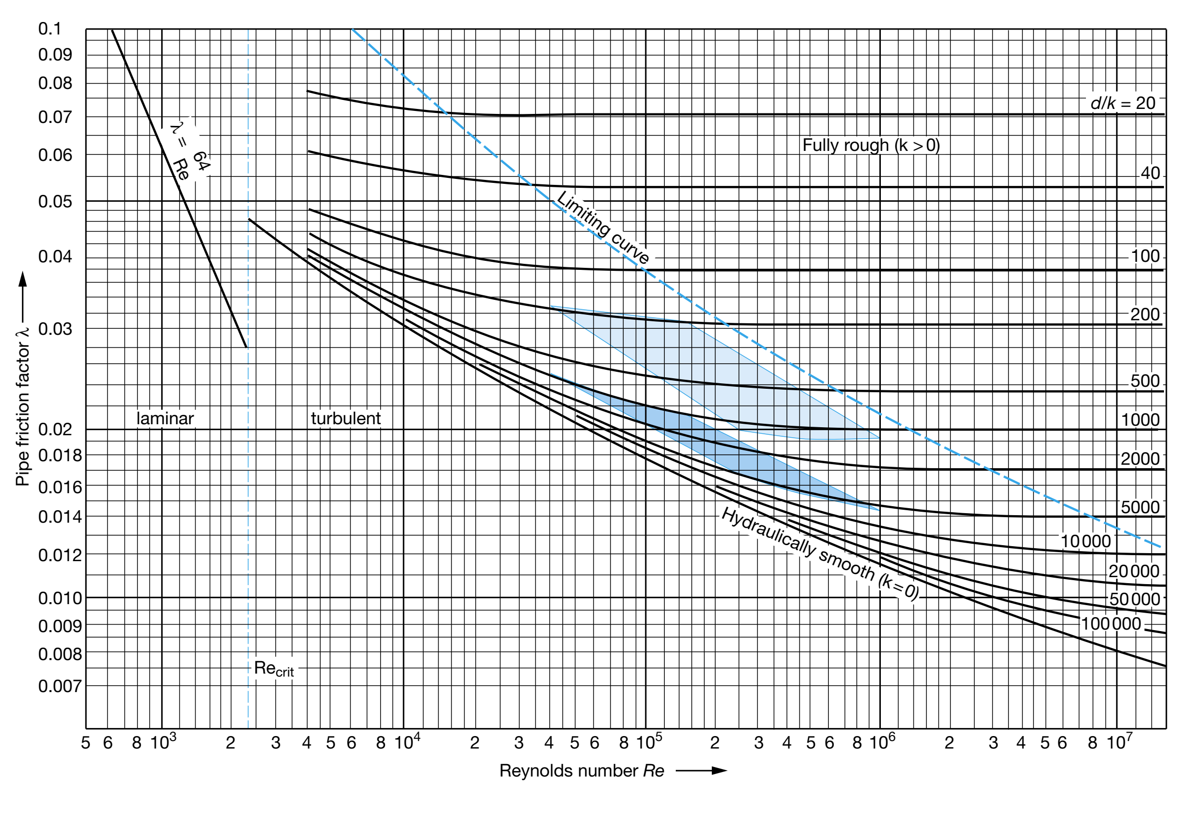

For pipes with non-circular cross-sections the following applies:

$$d = 4A/U \qquad (10)$$

where
A Cross-sectional flow area in m^2
U Wetted perimeter of the cross-section A in m; for open channels the free fluid surface is not counted as part of the perimeter.

Recommended flow velocities

for cold water

Inlet piping	0.7 – 1.5 m/s
Discharge piping	1.0 – 2.0 m/s

for hot water

Inlet piping	0.5 – 1.0 m/s
Discharge piping	1.5 – 3.5 m/s

The pipe friction factor λ has been determined experimentally and is shown in Fig. 10. It varies with the flow conditions of the liquid and the relative roughness d/k of the pipe surface. The flow conditions are expressed according to the affinity laws (dimensional analysis) using the Reynolds' number Re. For circular pipes, this is:

$$Re = v \cdot d/\nu \qquad (11)$$

where
v Flow velocity in m/s ($= 4Q/\pi d^2$ for Q in m^3/s)
d Pipe inside diameter in m
ν Kinematic viscosity in m^2/s (for water at 20 °C exactly $1.00 \cdot (10)^{-6}$ m^2/s).

For non-circular pipes, Eq. 10 is to be applied for determining d.

For hydraulically smooth pipes (for example drawn steel tubing or plastic pipes made of polyethylene (PE) or polyvinyl chloride (PVC)) or for laminar flow, λ can be calculated:

In the laminar flow region (Re <2320) the friction factor is independent of the roughness:

$$\lambda = 64/Re \qquad (12)$$

For turbulent flow (Re > 2320) the test results can be represented by the following empirical relationship defined by Eck (up to Re < 10^8 the errors are smaller than 1%):

$$\lambda = \frac{0.309}{(\lg \frac{Re}{7})^2} \qquad (13)$$

In Fig. 10 it can be seen that the pipe friction factor depends on another dimensionless parameter, the relative roughness of the pipe inner surface d/k; k is the average absolute roughness of the pipe inner surface, for which approximate values are given in Table 3. Note: both d and k must be expressed in the same units, for example mm!

As shown in Fig. 10, above a limiting curve, λ is dependent only on the relative roughness d/k. The following empirical equation by Moody can be used in this region:

$$\lambda = 0.0055 + 0.15/\sqrt[3]{(d/k)} \qquad (14)$$

For practical use, the head losses H_L per 100 m of straight steel pipe are shown in Fig. 11 as a function of the flow rate Q and pipe inside diameter d. The values are valid only for cold, clean water or for fluids with the same kinematic viscosity, for completely filled pipes and for an absolute roughness of the pipe inner surface of k = 0.05 mm, i.e., for new seamless or longitudinally welded pipes. (For the pipe inside diameters, see Table 4).

The effect of an increased surface roughness k will be demonstrated in the following for a frequently used region in Fig. 11 (nominal diameter 50 to 300 mm, flow velocity 0.8 to 3.0 m/s). The **dark-shaded region in Fig. 11 corresponds to** the similarly marked region in **Fig. 10** for an absolute roughness k = 0.05 mm. For a **roughness increased by a factor 6** (slightly incrusted old steel pipe with k = 0.30 mm), the **pipe friction factor** λ (proportional to the head loss H_L) in the lightly shaded region in Fig. 10 is **only 25% to 60%** higher than before.

For sewage pipes the increased roughness caused by soiling must be taken into consideration (see section 3.6). For pipes with a large degree of incrustation, the actual head loss can only be determined experimentally. Deviations from the nominal diameter change the head loss considerably, since the pipe inside diameter enters Eq. (9) to the 5th power! (For example, a 5% reduction in the inside diameter changes the head loss by 30%). **Therefore the nominal diameter may not be used as the pipe inside diameter for the calculations!**

Table 3: Approximate average roughness height k (absolute roughness) for pipes

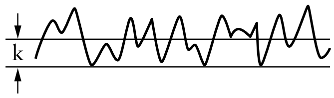

Pipe material	Condition of pipe interior		
Steel	new,	seamless	skin
			acid-cleaned
			galvanized
		longitudinally welded,	skin
			bituminized
			galvanized
			cemented
		riveted	
	used,	moderately rusty	
		slight incrustation	
		heavy incrustation	
		after cleaning	
Asbestos cement	new		
Heavy clay (drainage)	new		
Concrete	new,	unfinished	
		with smooth finish	
Spun concrete	new,	unfinished	
		with smooth finish	
Reinforced concrete	new,	with smooth finish	
All concretes	used,	with smooth finish	
Metal pipes		drawn	
Glass, plastic			
Rubber tubing	new,	not embrittled	
Wood	new		
	after long exposure to water		
Masonry			

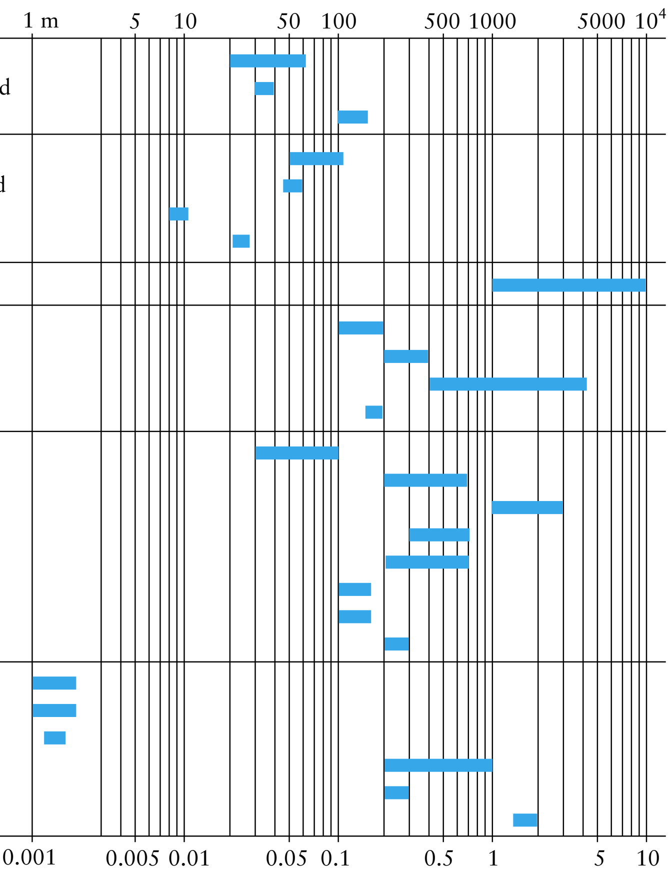

Table 4: Inside diameter d and wall thickness s in mm and weight of typical commercial steel pipes and their water content in kg/m to ENV 10 220 (formerly DIN ISO 4200). D = outside diameter, s = wall thickness

DN	D	All dimensions in mm Seamless s *	d	Welded s **	d	Seamless pipe weight in kg/m Pipe	Water	Welded pipe weight in kg/m Pipe	Water
15	21.3	2.0	17.3	1.8	17.7	0.952	0.235	0.866	0.246
20	26.9	2.0	22.9	1.8	23.3	1.23	0.412	1.11	0.426
25	33.7	2.3	29.1	2.0	29.7	1.78	0.665	1.56	0.692
32	42.4	2.6	37.2	2.3	37.8	2.55	1.09	2.27	1.12
40	48.3	2.6	43.1	2.3	43.7	2.93	1.46	2.61	1.50
50	60.3	2.9	54.5	2.3	55.7	4.11	2.33	3.29	2.44
65	76.1	2.9	70.3	2.6	70.9	4.71	3.88	5.24	3.95
80	88.9	3.2	82.5	2.9	83.1	6.76	5.34	6.15	5.42
100	114.3	3.6	107.1	3.2	107.9	9.83	9.00	8.77	9.14
125	139.7	4.0	131.7	3.6	132.5	13.4	13.6	12.1	13.8
150	168.3	4.5	159.3	4.0	160.3	18.2	19.9	16.2	20.2
200	219.1	6.3	206.5	4.5	210.1	33.1	33.5	23.8	34.7
250	273.0	6.3	260.4	5.0	263.0	41.4	53.2	33.0	54.3
300	323.9	7.1	309.7	5.6	312.7	55.5	75.3	44.0	76.8
350	355.6	8.0	339.6	5.6	344.4	68.6	90.5	48.3	93.1
400	406.4	8.8	388.8	6.3	393.8	86.3	118.7	62.2	121.7
500	508.0	11.0	486.0	6.3	495.4	135	185.4	77.9	192.7
600	610.0	12.5	585.0	6.3	597.4	184	268.6	93.8	280.2

* above nominal diameter DN 32 identical to DIN 2448

** above nominal diameter DN 25 identical to DIN 2458

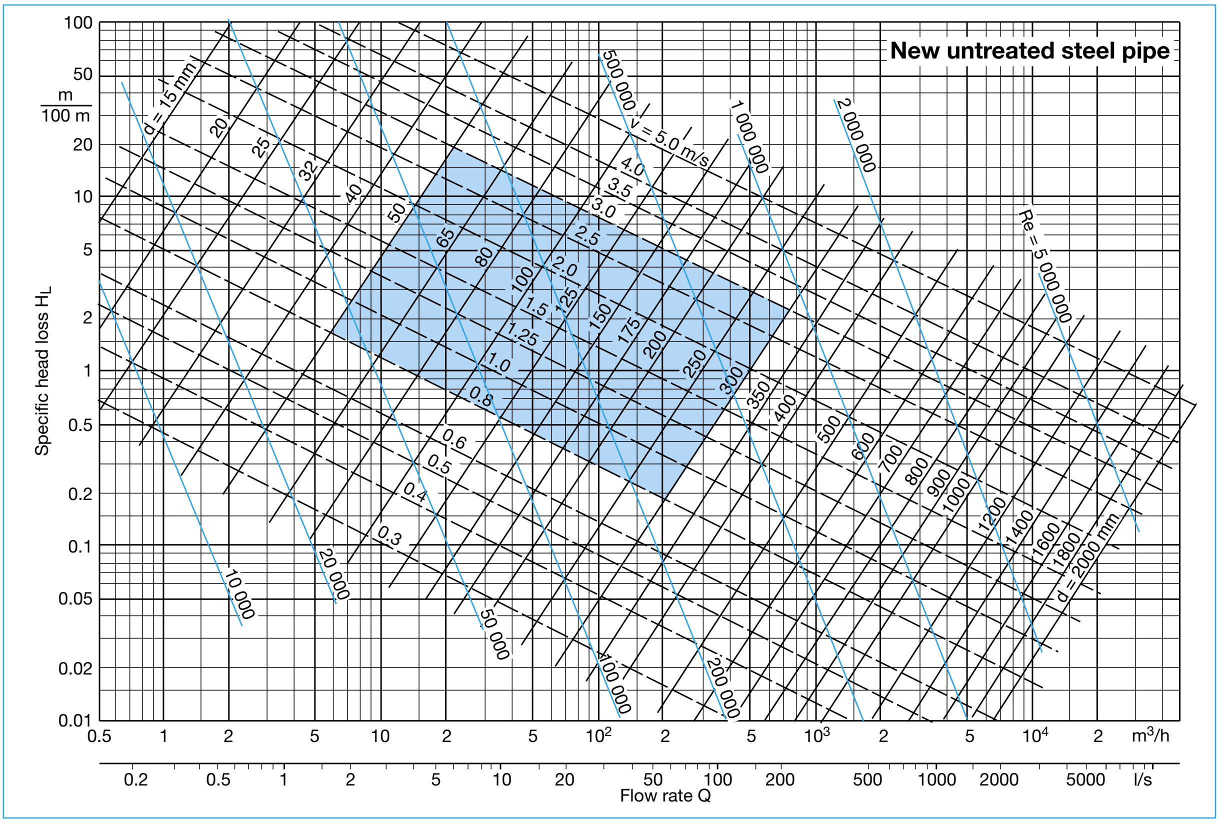

Fig. 11: Head losses H_L for new steel pipes (k = 0.05 mm) *(enlarged view on p. 82)*

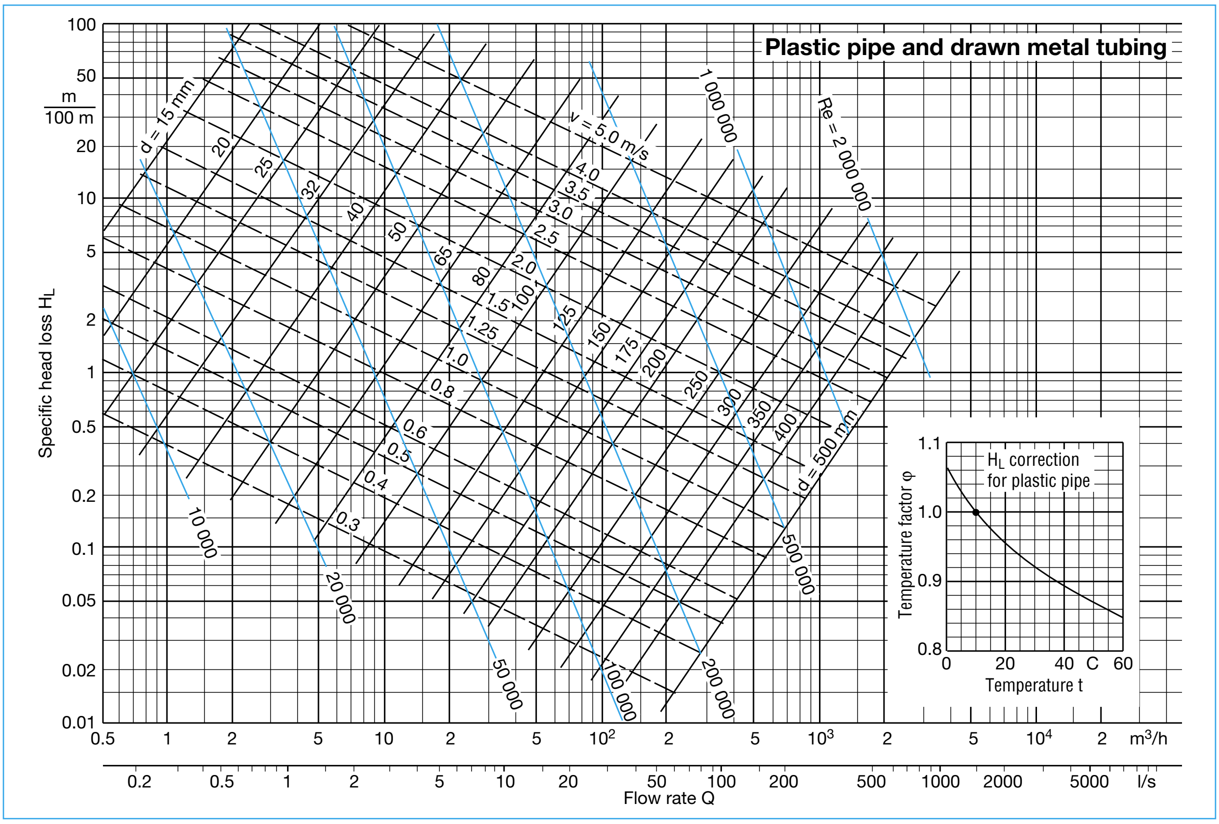

Fig. 12: Head losses H_L for hydraulically smooth pipes (k = 0) *(enlarged view on p. 83). For plastic pipe when t ≠ 10 °C multiply by the temperature factor φ.*

The head losses H_L in plastic (for example PE or PVC) pipes or smooth drawn metal piping are very low thanks to the smooth pipe surface. They are shown in Fig. 12 and valid for water at 10 °C. At other temperatures, the loss for plastic pipes must be multiplied with a temperature correction factor indicated in Fig. 12 to account for their large thermal expansion. For sewage or other untreated water, an additional 20–30% head loss should be taken into consideration for potential deposits (see section 3.6).

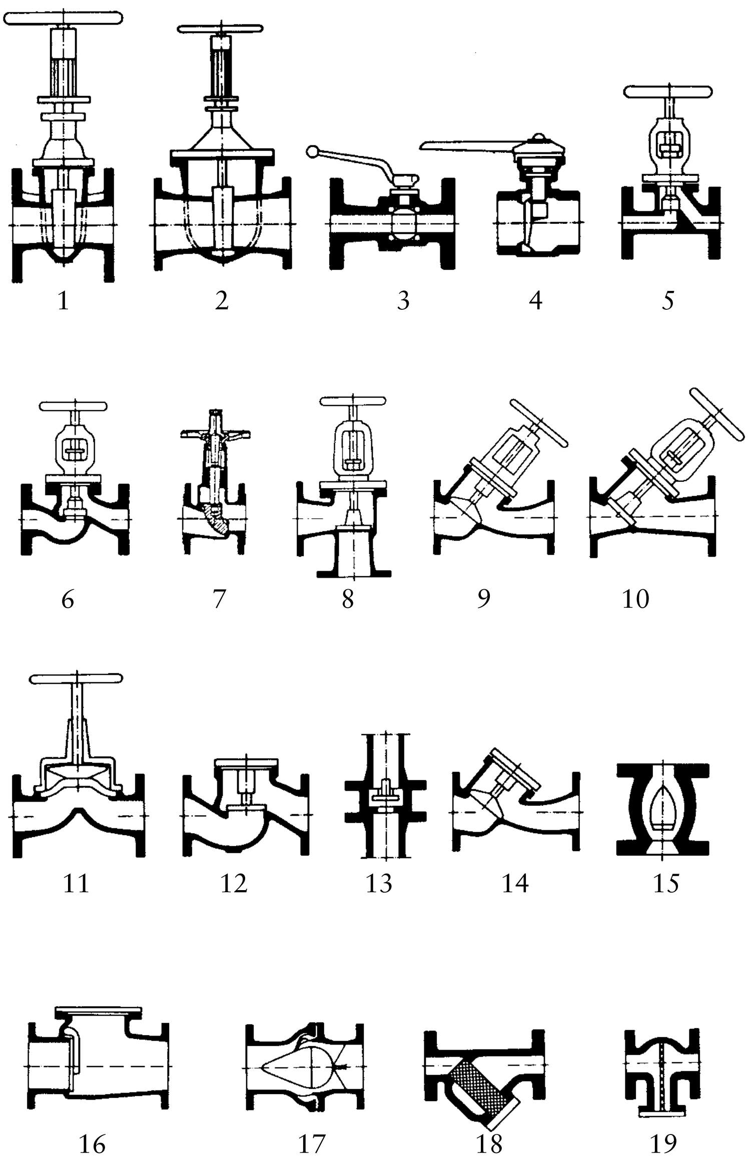

Fig. 13: Schematic representation of the valve designs listed in Table 5

3.2.1.2.2 Head Loss in Valves and Fittings

The head loss in valves and fittings is given by

$$H_L = \zeta \cdot v^2/2g \qquad (15)$$

where

ζ Loss coefficient

v Flow velocity in a characteristic cross-section A (for example the flange) in m/s

g Gravitational constant 9.81 m/s^2

Tables 5 to 8 and Figures 13 to 15 contain information about the various loss coefficients ζ for valves and fittings for operation with cold water.

The minimum and maximum in Table 5 bracket the values given in the most important technical literature and apply to valves which have a steady approach flow and which are fully open. The losses attributable to straightening of the flow disturbances over a length of pipe equivalent to 12 x DN downstream of the valve are included in the ζ value in accordance with VDI/VDE 2173 guidelines. Depending on the inlet and exit flow conditions, the valve models used and the development objectives (i.e. inexpensive vs. energy-saving valves), the loss values can vary dramatically.

Table 5: Loss coefficients ζ for various types of valves and fittings (referred to the velocity of flow in the line connection nominal diameter DN)

	Type of valve / fitting		Design	Loss coefficient ζ for DN = 15	20	25	32	40	50	65	80	100	125	150	200	250	300	400	500	600	800	1000	Comment
Shut-off valves	Slide disc valves (d_E = DN)	min	1	0.1																		0.1	For d_E < DN cf. footnote 1)
		max		0.65	0.6	0.55	0.5	0.5	0.45	0.4	0.35	0.3										0.3	
	Round-body gate valves (d_E = DN)	min	2						0.25	0.24	0.23	0.22	0.21	0.19	0.18	0.17	0.16	0.15	0.13	0.12	0.11	0.11	
		max							0.32	0.31	0.30	0.28	0.26	0.25	0.23	0.22	0.20	0.19	0.18	0.16	0.15	0.14	
	Ball and plug valves (d_E = DN)	min	3	0.10	0.10	0.09	0.09	0.08	0.08	0.07	0.07	0.06	0.05	0.05	0.04	0.03	0.03	0.02					For d_E < DN ζ = 0.4 to 1.1
		max		0.15														0.15					
	Butterfly valves PN 2.5 10	min	4					0.90	0.59	0.38	0.26	0.20	0.14	0.12	0.09	0.06						0.06	
		max						1.20	1.00	0.80	0.70	0.62	0.56	0.50	0.42	0.40	0.37	0.33	0.33	0.33	0.30	0.28	
	Butterfly valves PN 16 25	min							2.04	1.80	1.55	1.30	1.08	0.84	0.75	0.56	0.48	0.40				0.40	* Also for PN 40
		max							2.50*	2.30*	2.10*	1.90*	1.70*	1.50*	1.30	1.10	0.90	0.83	0.76	0.71	0.67*	0.63*	
	Globe valves, forged	min	5			6.0			6.0														
		max				6.8			6.8														
	Globe valves, cast	min	6	3.0													3.0						ζ = 2 to 3 can be achieved for optimized valve
		max		6.0													6.0						
	Compact valves	min	7	0.3	0.4	0.6	0.6	1.0	1.1						1.1								
		max		0.3	0.9	1.9				1.9	2.2	2.2	2.3	2.5	2.5								
	Angle valves	min	8	2.0														2.0					
		max		3.1			3.1	3.4	3.8	4.1	4.4	4.7	5.0	5.3	5.7	6.0	6.3	6.6					
	Y-valves	min	9	1.5													1.5						
		max		2.6													2.6						
	Straight-through valves	min	10	0.6														0.6					
		max		1.6														1.6					
	Diaphragm valves	min	11	0.8										0.8									
		max		2.7										2.7									
Non-return valves	Non-return valves, straight seat	min	12	3.0											3.0								
		max		6.0											6.0								
	Non-return valves, axial	min	13	3.2					3.2	3.7	5.0	7.3	4.3				4.3						Axially expanded as from DN 125
		max		3.4	3.4	3.5	3.6	3.8	4.2	5.0	6.4	8.2	4.6				4.6						
	Non-return valves, slanted seat	min	14	2.5	2.4	2.2	2.1	2.0	1.9	1.7	1.6	1.5					1.5						
		max		3.0													3.0						
	Foot valves	min	15						1.0	0.9	0.8	0.7	0.6	0.5	0.4	0.4	0.4	(7.0)	(6.1)	(5.5)	(4.5)	(4.0)	( ) In groups
		max							3.0								3.0						
	Swing check valves	min	16	0.5				0.5	0.4								0.4	0.3				0.3	Swing check valves without levers and weights 2)
		max		3.0																		3.0	
	Hydrostops v = 4 m/s		17						0.9			3.0		3.0	2.5	2.5	1.2	2.2					
	v = 3 m/s								1.8			4.0		4.5	4.0	4.0	1.8	3.4					
	v = 2 m/s								5.0			6.0		8.0	7.5	6.5	6.0	7.0					
	Filters		18					2.8									2.8						In clean condition
	Strainers		19					1.0									1.0						

1) If the narrowest shut-off diameter d_E is smaller than the line connection nominal diameter DN. the loss coefficient ζ must be increased by $(DN/d_E)^x$ with x = 5 to 6.
2) When the valve is partially open, i.e. low flow velocities, the loss coefficients increase to the "max" values. With increasing flow velocities v (in m/s) the loss coefficients decrease roughly as ζ 3/v.
See Fig. 13 for designs.

Table 6: Loss coefficients ζ in elbows and bends

Round elbow	α	15°		30°		45°		60°		90°	
		Surface smooth	rough	Surface smooth	rough	Surface smooth	rough	Surface smooth	rough	Surface smooth	rough
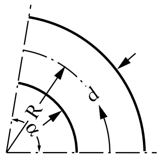	ζ for R = 0	0.07	0.10	0.14	0.20	0.25	0.35	0.50	0.70	1.15	1.30
	ζ for R = d	0.03	–	0.07	–	0.14	0.34	0.19	0.46	0.21	0.51
	ζ for R = 2 d	0.03	–	0.06	–	0.09	0.19	0.12	0.26	0.14	0.30
	ζ for R 5 d	0.03	–	0.06	–	0.08	0.16	0.10	0.20	0.10	0.20
Welded bend 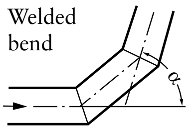	Number of circum-ferential welds	–	–	–	–	2	–	3	–	3	–
	ζ	–	–	–	–	0.15	–	0.20	–	0.25	–

Note: For the branch fittings in Table 7 and the adapters of Table 8, one must differentiate between the **irreversible** pressure loss (reduction in pressure)

$$p_L = \zeta \cdot \varrho \cdot v_1^2/2 \qquad (16)$$

where

p_L Pressure loss in Pa
ζ Loss coefficient
ϱ Density in kg/m³
v Flow velocity in m/s

and the **reversible** pressure change of the frictionless flow according to Bernoulli's equation (see 3.2.1.1):

$$p_2 - p_1 = \varrho \cdot (v_1^2 - v_2^2)/2 \qquad (17)$$

For accelerated flows (for example a reduction in the pipe diameter), $p_2 - p_1$ is always negative, for decelerated flows (e.g. pipe expansion) it is always positive. When calculating the net pressure change as the arithmetic sum of p_L and $p_2 - p_1$, the pressure losses from Eq. 16 are always to be subtracted.

Often the so-called k_v value is used instead of the loss coef-

Table 7: Loss coefficients ζ for fittings

Combinations of pipe bends (elbows):

The ζ value of the single 90° elbow should not be doubled, but only be multiplied by the factors indicated to obtain the pressure loss caused by the combination of elbows illustrated.

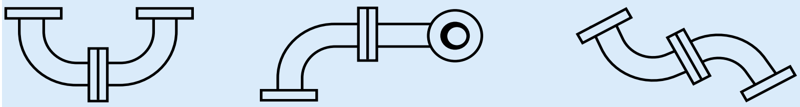

Expansion joints:

Bellows-type expansion joint with/without guide pipe	ζ ≈ 0.3/2.0
Compensation tube bend	ζ ≈ 0.6 to 0.8
Creased compensation tube bend	ζ ≈ 1.3 to 1.6
Bellows-type compensation tube bend	ζ ≈ 3.2 to 4

Inlet pipe fittings:

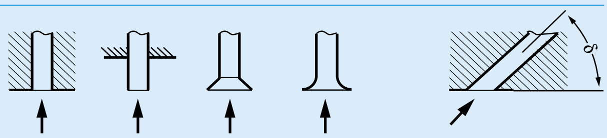

Inlet edge						
Sharp	ζ ≈	0.5	3			for δ = 75° 60° 45°
Chamfered	ζ ≈	0.25	0.55	0.20	0.05	ζ ≈ 0.6 0.7 0.8

Discharge pipe fittings:

ζ ≈ 1 downstream of an adequate length of straight pipe with an approximately uniform velocity distribution in the outlet cross-section
ζ ≈ 2 for a very irregular velocity distribution, for example immediately downstream of a pipe fitting or a valve, etc.

Continued on next page

Table 8: Loss coefficients ζ for adapters

Expansion		Contraction	
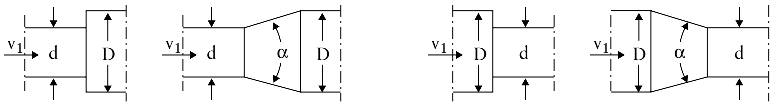			
Type I	II	III	IV

Type		d/D	0.5	0.6	0.7	0.8	0.9
I		ζ ≈	0.56	0.41	0.26	0.13	0.04
II for	α = 8°	ζ ≈	0.07	0.05	0.03	0.02	0.01
	α = 15°	ζ ≈	0.15	0.11	0.07	0.03	0.01
	α = 20°	ζ ≈	0.23	0.17	0.11	0.05	0.02
III		ζ ≈	4.80	2.01	0.88	0.34	0.11
IV for	20° < α < 40°	ζ ≈	0.21	0.10	0.05	0.02	0.01

Table 7 (continued)

Flow meters:

Short Venturi tube α = 30°

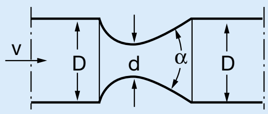

Standard orifice

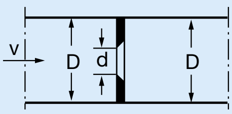

ζ is referred to the velocity v at diameter D.

Diameter ratio d/D	= 0.30	0.40	0.50	0.60	0.70	0.80
Area ratio $m = (d/D)^2$	= 0.09	0.16	0.25	0.36	0.49	0.64
Short Venturi tube	ζ ≈ 21	6	2	0.7	0.3	0.2
Standard orifice	ζ ≈ 300	85	30	12	4.5	2

Water meters (volume meters) ζ ≈ 10

For domestic water meters, a max. pressure drop of 1 bar is specified for the rated load. In practice, the actual pressure loss is seldom higher.

Branch fittings (of equal diameter)

Note:

The loss coefficients ζ_a for the branched-off flow Q_a or ζ_d for the main flow $Q_d = Q - Q_a$ refer to the velocity of the total flow Q in the branch. On the basis of this definition, ζ_a or ζ_d may have negative values; in this case, they are indicative of a pressure **gain** instead of a pressure **loss**. This is not to be confused with the reversible pressure **changes** according to Bernoulli's equation (see notes to Tables 7 and 8).

Q_a/Q =		0.2	0.4	0.6	0.8	1
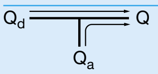 Q_d, Q, Q_a	ζ_a ≈	−0.4	0.08	0.47	0.72	0.91
	ζ_d ≈	0.17	0.30	0.41	0.51	–
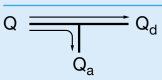 Q, Q_d, Q_a	ζ_a ≈	0.88	0.89	0.95	1.10	1.28
	ζ_d ≈	−0.08	−0.05	0.07	0.21	–
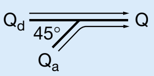 Q_d, 45°, Q, Q_a	ζ_a ≈	−0.38	0	0.22	0.37	0.37
	ζ_d ≈	0.17	0.19	0.09	−0.17	–
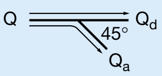 Q, 45°, Q_d, Q_a	ζ_a ≈	0.68	0.50	0.38	0.35	0.48
	ζ_d ≈	−0.06	−0.04	0.07	0.20	–

ficient ζ when calculating the pressure loss for water in valves:

$$p_L = (Q / k_v)^2 \cdot \varrho / 1000 \quad (18)$$

where

Q Volume rate of flow in m^3/h (!)

ϱ Density of water in kg/m^3

p_L Pressure loss in bar (!)

The k_v value is the flow rate in m^3/h which would result from a pressure drop of 1 bar through the valve for cold water. It correlates with the pressure loss p_L in bar with the flow rate Q in m^3/h. The notation k_{vs} is used for a fully open valve.

Conversion for cold water:

$$\zeta \approx 16 \cdot d^4/k_v^2 \quad (19)$$

where

d Reference (nominal) diameter of the valve in cm (!)

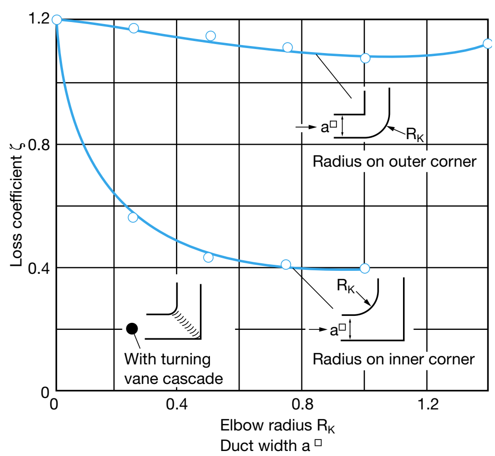

Fig. 14: Effect of rounding off the inner and outer side of elbows in square ducts on the loss coefficient ζ

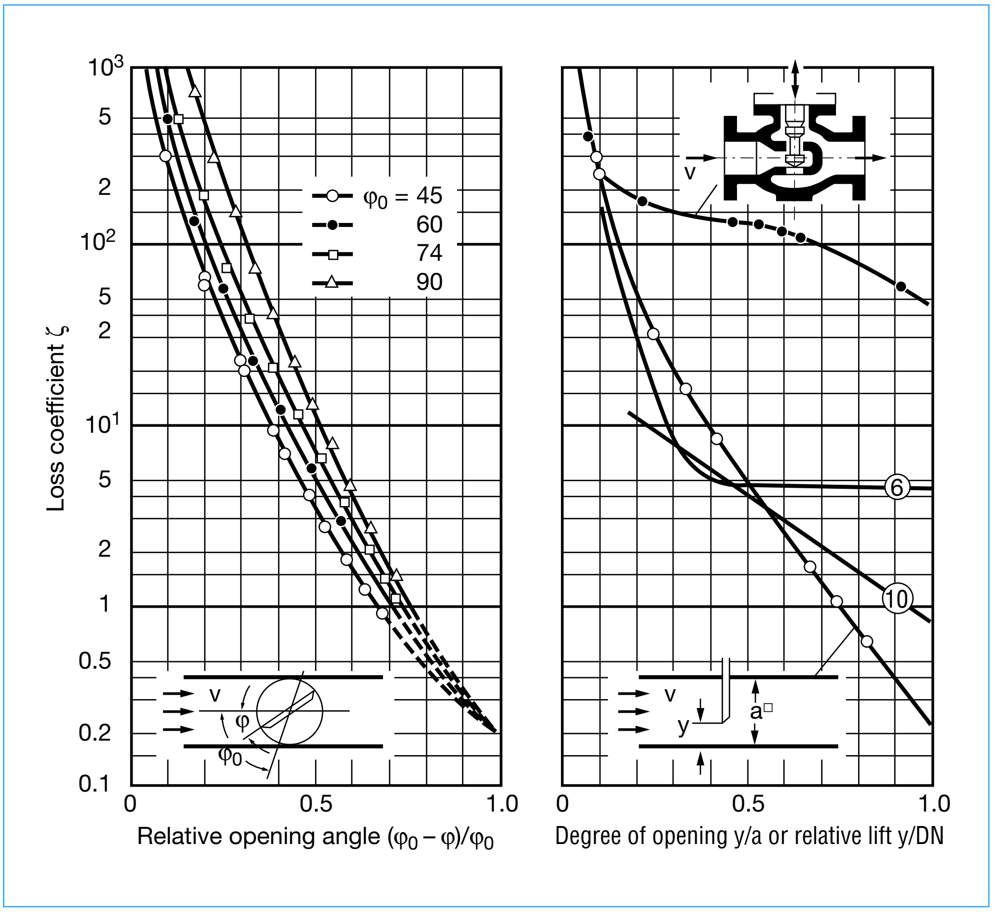

Fig. 15: Loss coefficients ζ of butterfly valves, globe valves and gate valves as a function of the opening angle or degree of opening (The numbers designate the types illustrated in Fig. 13)

3.2.2 System Characteristic Curve

The system characteristic curve plots the head H_{sys} required by the system as a function of the flow rate Q. It is composed of the so-called "static" and "dynamic" components (see Fig. 16)[3].

The static component consists of the geodetic head H_{geo} and the pressure head difference $(p_a-p_e)/(\varrho \cdot g)$ between the inlet

Fig. 16: System characteristic curve H_{sys} with static and dynamic components

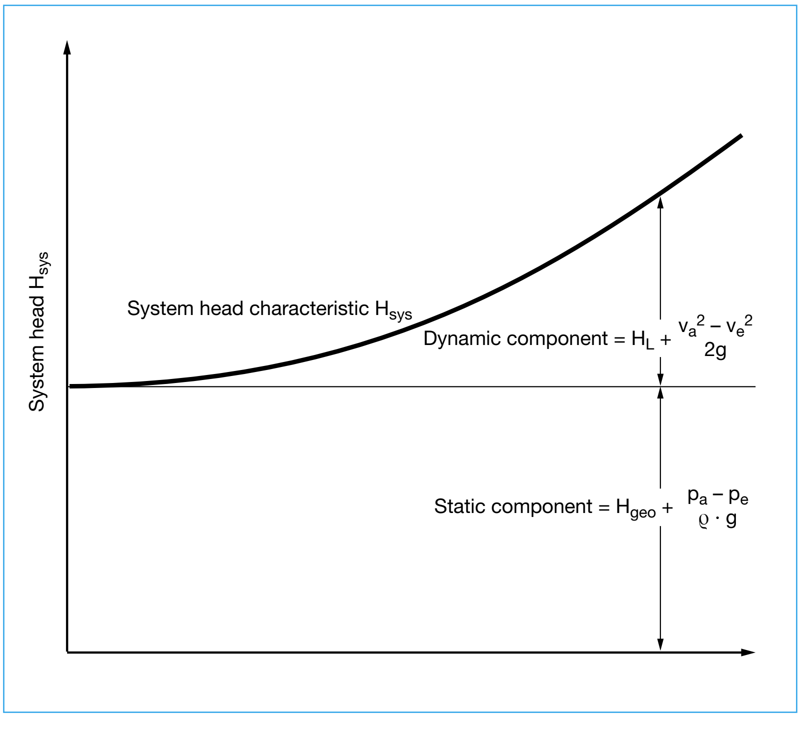

[3] One must be careful to distinguish between this use of "static" and "dynamic" components and the precisely defined "static head" and "dynamic head" used in fluid dynamics, since the "dynamic component" of the system head curve consists of both "static head" (i.e. pressure losses) and "dynamic head" (i.e. velocity or kinetic energy head).

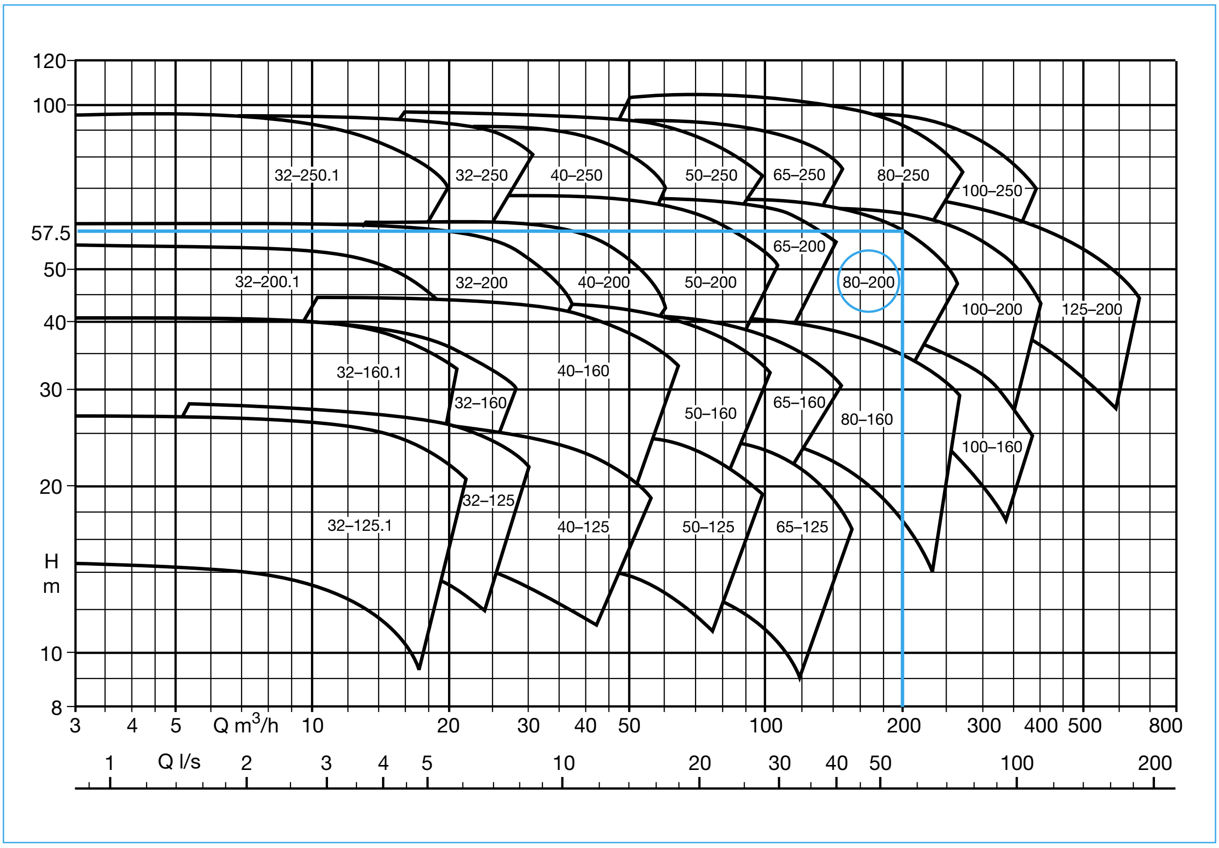

Fig. 17: Selection chart for a volute casing pump series for n = 2900 rpm
(First number = nominal diameter of the discharge nozzle, second number = nominal impeller diameter)

and outlet tanks, which are independent of the flow rate. The pressure head difference is zero when both tanks are open to the atmosphere.

The dynamic component consists of the head loss H_L, which increases as the square of the flow rate Q (see section 3.2.1.2), and of the change in velocity head $(v_a^2-v_e^2)/2g$ between the inlet and outlet cross-sections of the system. Two points are sufficient to calculate this parabola, one at Q = 0 and one at any point Q > 0.

For pipe systems connected one after the other (series connection) the individual system curves H_{sys1}, H_{sys2} etc. are plotted as functions of Q, and the heads for each flow rate are added to obtain the total system curve $H_{sys} = f(Q)$.

For branched piping systems the system curves H_{sys1}, H_{sys2}, etc. of the individual branches between the flow dividers are each calculated as functions of Q. The flow rates Q_1, Q_2, etc. of all branches in parallel for each given head H_{sys} are then added to determine the total system curve $H_{sys} = f(Q)$ for all the branches together. The sections before and after the flow dividers must be added as for a series connection.

3.3 Pump Selection

3.3.1 Hydraulic Aspects

The data required for selecting a pump size, i.e. the flow rate Q and the head H of the desired operating point are assumed to be known from the system characteristic curve; the electric mains frequency is also given. With these values it is possible to choose the pump size, the speed of rotation and, if necessary, the number of stages, from the selection chart in the sales literature (see Figs. 17 and 19). Further details of the chosen pump such as the efficiency η, the input power P, the required $NPSH_r$ (see section 3.5.4) and the reduced impeller diameter D_r can then be determined from

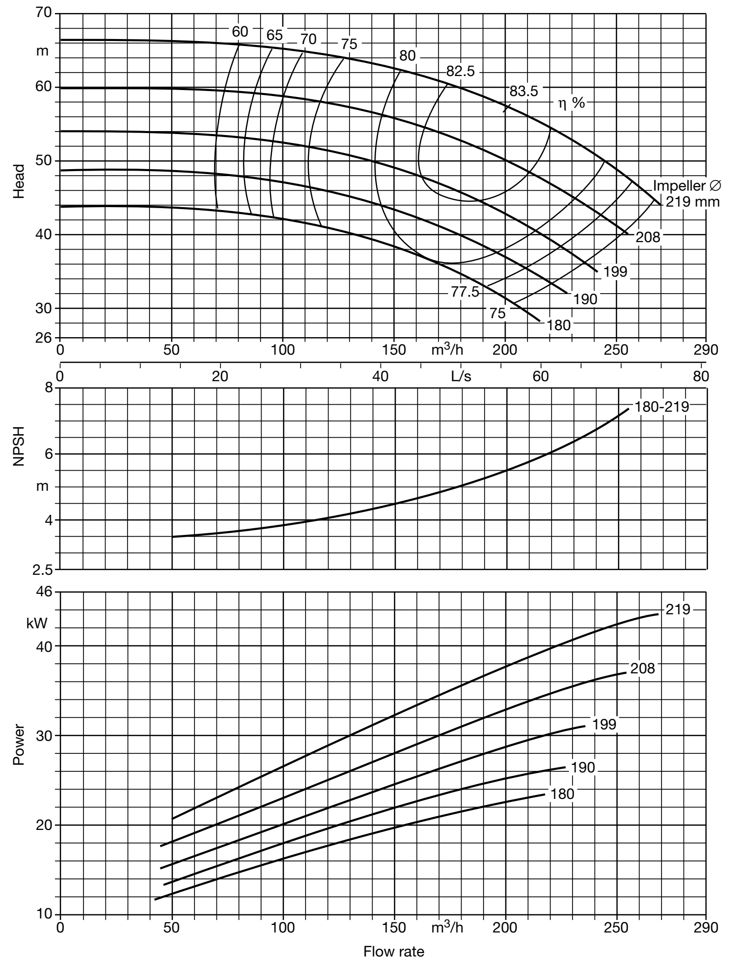

Fig. 18: Complete characteristics of a centrifugal pump

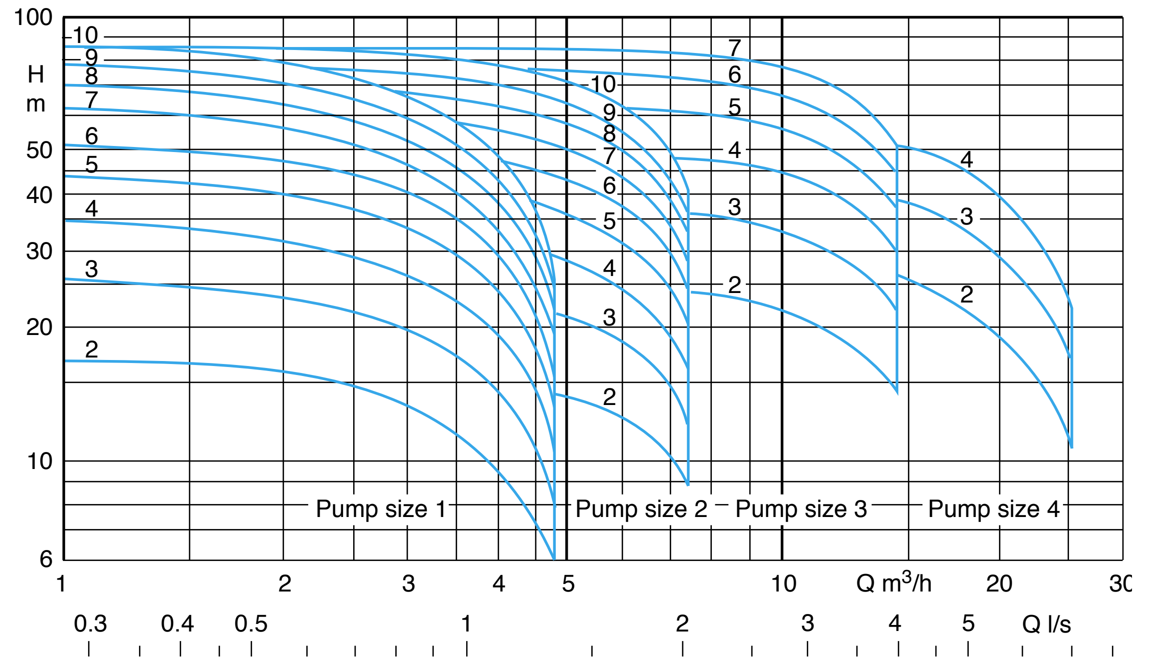

Fig. 19: Selection chart for a multistage pump series for n = 2900 rpm

the individual characteristic curve (for example see Fig. 18).

If there are no specific reasons for doing otherwise, a pump should be selected so that the operating point lies near its best efficiency point Q_{opt} (= flow rate at which efficiency is highest, BEP). The limits Q_{min} and Q_{max} (for example due to vibration behaviour, noise emission as well as radial and axial forces) are given in the product literature or can be determined by inquiry [1].

To conclude the selection, the NPSH conditions must be checked as described in section 3.5.

A multistage pump is chosen using the same general procedure; its selection chart shows the number of stages in addition to the pump size (Fig. 19).

For **pumps operating in series** (one after the other) the developed **heads** H_1, H_2, etc. of the individual characteristic curves must be added (after subtracting any head losses which occur between them) to obtain the total characteristic H = f(Q).

For **pumps operating in parallel,** the individual characteristics H_1, H_2, etc. = f(Q) are first reduced by the head losses occurring up to the common node (head loss H_L calculation according to section 3.2.1.2) and plotted versus Q. Then the flow rates Q of the reduced characteristics are added to produce the effective characteristic curve of a “virtual” pump. This characteristic interacts with the system curve H_{sys} for the rest of the system through the common node.

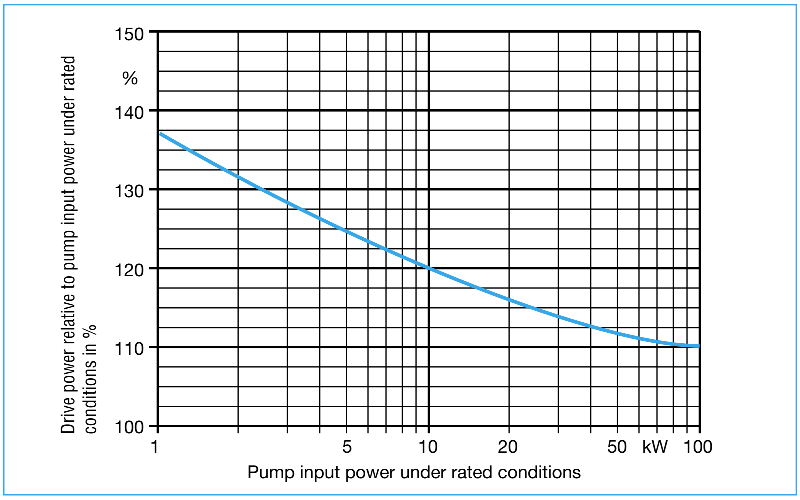

Fig. 20: Drive power as a function of rated pump input power at the operationg point
Example as per ISO 9905, 5199 and 9908 (Class I, II and III)

3.3.2 Mechanical Aspects

When selecting a pump the mechanical aspects require attention in addition to the hydraulics. Several examples are:

– the effects of the maximum discharge pressure and temperature of the fluid pumped on the operating limits,

– the choice of the best shaft sealing method and cooling requirements,

– the vibration and noise emissions,

– the choice of the materials of construction to avoid corrosion and wear while keeping in mind their strength and temperature limits.

These and other similar requirements are often specific to certain industries and even to individual customers and must be addressed using the product literature [1] or by consulting the design department.

3.3.3 Motor Selection

3.3.3.1 Determining Motor Power

Operation of a centrifugal pump is subject to deviations from rated speed and fluctuations in the flow volume handled, and, consequently, changes in the operating point (see section 3.4.1). In particular if steep power curves are involved (see Figs. 5 and 6), this may result in a higher required pump input power P than originally specified. For practical purposes, a safety allowance is therefore added when the appropriate motor size is selected. Safety allowances may be specified by the purchaser, or laid down in technical codes, see Fig. 20. The safety allowances stipulated by individual associations are shown in the relevant type series literature [1] or the customer’s specification.

When energy-saving control methods are used (e.g., speed control systems), the maximum power peaks which may possibly occur must be taken into account.

If a pump is selected for a product with a density lower than that of water, the motor power required may have to be determined on the basis of the density of water (for example, during the performance test or acceptance test in the test bay).

Typical efficiencies η and power factors cos φ of standardized IP 54 motors at 50 Hz are shown in Fig. 21, and the curves of efficiency η and power factor cos φ as a function of relative motor load P/PN in Fig. 22.

Table 9 lists types of enclosure that provide protection of electric motors against ingress of foreign objects or water, and of persons against accidental contact.

The specific heat build-up in both electric motors and flexible couplings during start-up as well as the risk of premature contactor wear limit the frequency of starts. Reference values for the maximum permissible number of starts Z are given in table 10, unless otherwise specified.

Submersible motor pumps (Figs. 1j to 1m) are ready-assembled pump units whose motors need not be selected individually [7]. Their electrical characteristics are given in the type series literature. The motor is filled with air and can be operated submerged in the product handled thanks to a – in most cases – double-acting shaft seal with a paraffin oil barrier.

Table 9: Types of enclosure for electric motors to EN 60 529 and DIN/VDE 0530, Part 5

The type of protective enclosure is indicated by the IP code as follows:

Code letters (International Protection)	IP
First digit (0 to 6 or X if not applicable)	X
Second digit (0 to 8 or X if not applicable)	X

Alternatively letters A, B, C, D and H, M, S, W – for special purposes only.

Key to digits:		Protection of electrical equipment against ingress of solid objects	Protection of persons against accidental contact by
First digit	0	(not protected)	(not protected)
	1	> 50 mm in dia.	back of the hand
	2	> 12.5 mm in dia.	finger
	3	> 2.5 mm in dia.	tool
	4	> 1.0 mm in dia.	wire
	5	protected against dust (limited ingress permitted, no harmful deposits)	wire
	6	totally protected against dust	wire
		Protection against ingress of water with harmful consequences	
Second digit	0	(not protected)	
	1	vertical dripwater	
	2	dripwater up to 15° from the vertical	
	3	sprays (60° from the vertical)	
	4	sprays (all directions)	
	5	low-pressure jets of water	
	6	strong jets of water (heavy sea)	
	7	temporary flooding	
	8	permanent flooding	

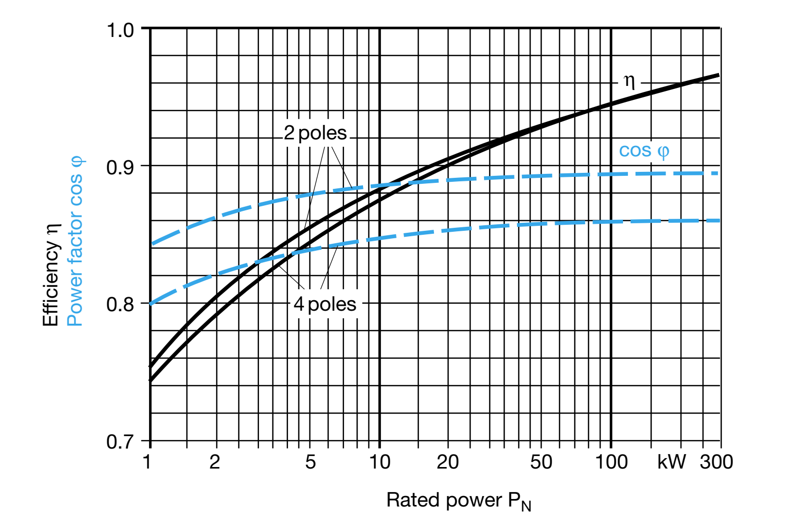

Fig. 21: Typical efficiencies η and power factors cos φ of standardized motors, IP 54 enclosure, at 50 Hz as a function of motor power P_N

Table 10: Permissible frequency of starts Z per hour for electric motors

Motor installation	Dry	Wet (submersible motors)
Motors up to 4 kW	15	30
Motors up to 7.5 kW	15	25
Motors up to 11 kW	12	25
Motors up to 30 kW	12	20
Motors above 30 kW	10	10

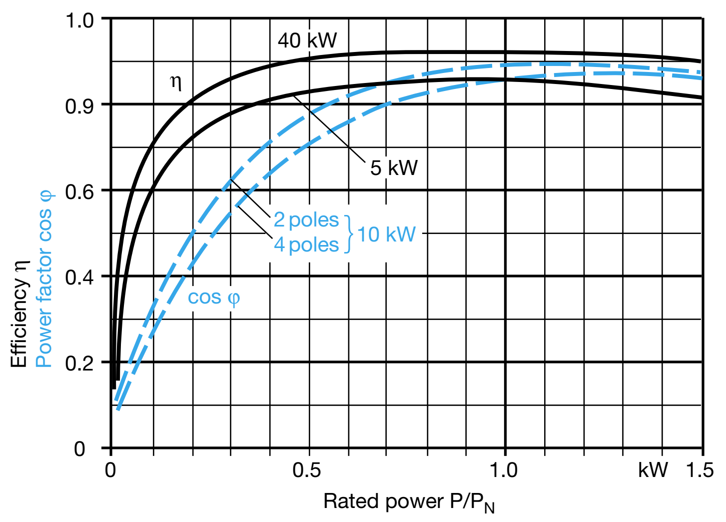

Fig. 22: Curve of efficiency η and power factor cos φ of standardized IP 54 motors plotted over relative motor power P/P_N

Submersible borehole pumps, which are mostly used for extracting water from wells, are another type of ready-assembled units whose motors need not be selected individually (Fig. 1p). On these pumps, the rotor and the windings are immersed in water [7]. Their electrical characteristics and permissible frequency of starts are indicated in the type series literature [1].

3.3.3.2 Motors for Seal-less Pumps

Seal-less pumps are frequently used for handling aggressive, toxic, highly volatile or valuable fluids in the chemical and petrochemical industries. They include magnetic-drive pumps (Fig. 1f) and canned motor pumps (Figs. 1n and 1o). A mag-drive pump is driven by a primary magnetic field rotating outside its flameproof enclosure and running in synchronization with the secondary magnets inside the enclosure [12].

The primary component in turn is coupled to a commercial dry driver. The impeller of a canned motor pump is mounted directly on the motor shaft, so that the rotor is surrounded by the fluid pumped. It is separated from the stator windings by the can [7].

Seal-less pump sets are generally selected with the help of computerized selection programs, taking into account the following considerations:

- The rotor is surrounded by the fluid pumped, whose kinematic viscosity υ (see section 4.1) must be known, as it influences friction losses and therefore the motor power required.
- Metal cans or containment shrouds (for example made of 2.4610) cause eddy current losses, resulting in an increase in the motor power required. Non-metal shrouds in mag-drive pumps do not have this effect.
- The vapour pressure of the fluid pumped must be known, so as to avoid bearing damage caused by dry running when the fluid has evaporated. It is advisable to install monitoring equipment signalling dry running conditions, if any.
- Data on specific fluid properties such as its solids content and any tendency to solidify or polymerize or form incrustations and deposits, need to be available at the time of selection.

3.3.3.3 Starting Characteristics

The pump torque Tp transmitted by the shaft coupling is directly related to the power P and speed of rotation n. During pump start-up, this torque follows an almost parabolical curve as a function of the speed of rotation [10], as shown in Fig. 23. The torque provided by the asynchronous motor must, however, be higher so as to enable the rotor to run up to duty speed. Together with the voltage, this motor torque has a direct effect on the motor's current input, and the latter in turn on heat build-up in the motor windings. The aim, therefore, is to prevent unwanted heat build-up in the motor by limiting the run-up period and/or current inrush [2] (see also Table 11).

Table 11: Starting methods for asynchronous motors

Starting method	Type of equipment	Current input (mains load)	Run-up time	Heat build-up in motor during start-up	Mechanical loading	Hydraulic loading	Cost relation	Recommended motor designs	Comments
D. o. l.	Contactor (mechanical)	4–8 · I_N	Approx. 0.5–5 s	High	Very high	Very high	1	All	Mostly limited to ≤4 kW by energy supply companies
Star-delta	Contactor combination (mechanical)	1/3 of d. o. l. values	Approx. 3–10 s	High	Very high	Very high	1.5–3	All; canned motors and submersible motors subject to a major drop in speed during switchover	Usually stipulated for motors >4 kW by energy supply companies
Reduced voltage	Autotransformer, mostly 70% tapping	0.49 times the d. o. l. values	Approx. 3–10 s	High	High	High	5–15	All	No currentless phase during switchover (gradually replaced by soft starters)
Soft start	Soft starter (power electronics)	Continuously variable; typically 3 · I_N	Approx. 10–20 s	High	Low	Low	5–15	All	Run-up and run-down continuously variable via ramps for each individual load appllication; no hydraulic surges
Frequency inverter	Frequency inverter (power electronics)	1 · I_N	0–60 s	Low	Low	Low	Approx. 30	All	Too expensive to use solely for run-up and run-down purposes; better suited for open- or closed-loop control

In the case **of d.o.l. starting** (where the full mains voltage is instantly applied to the motor once it is switched on), the full starting torque is instantly available and the unit runs up to its duty speed in a very short period of time. For the motor itself, this is the most favourable starting method. But at up to 4–8 times the rated current, the starting current of the d.o.l. method places a high load on the electricity supply mains, particularly if large motors are involved, and may cause problematic voltage drops in electrical equipment in their vicinity. For motor operation on public low-voltage grids (380 V), the regulations laid down by the energy supply companies for d.o.l. starting of motors of 5.5 kW and above must be complied with. If the grid is not suitable for d.o.l starting, the motor can be started up with reduced voltages, using one of the following methods:

Star-delta starting is the most frequent, since most inexpensive, way of reducing the starting current. During normal operation, the motor runs in delta, so that the full mains voltage (for example 400 V) is applied to the motor windings. For start-up, however, the windings are star-connected, so that the voltage at the windings is reduced by a factor of 0.58 relative to the mains voltage. This reduces the starting current and torque to one third of the values of d.o.l. starting, resulting in a longer start-up process.

The motor runs up in star connection beyond pull-out torque up to the maximum speed of rotation at point B’ in Fig. 23. Then, switchover to delta is effected and the motor continues to accelerate up to rated speed. During the switchover period of approx. 0.1 s, the current supply to the motor is interrupted and the speed drops. On pump sets with a low moment of inertia (canned motors and submersible motors), this speed reduction may be so pronounced that switchover to delta may result in almost the full starting current being applied after all, same as with d.o.l. starting.

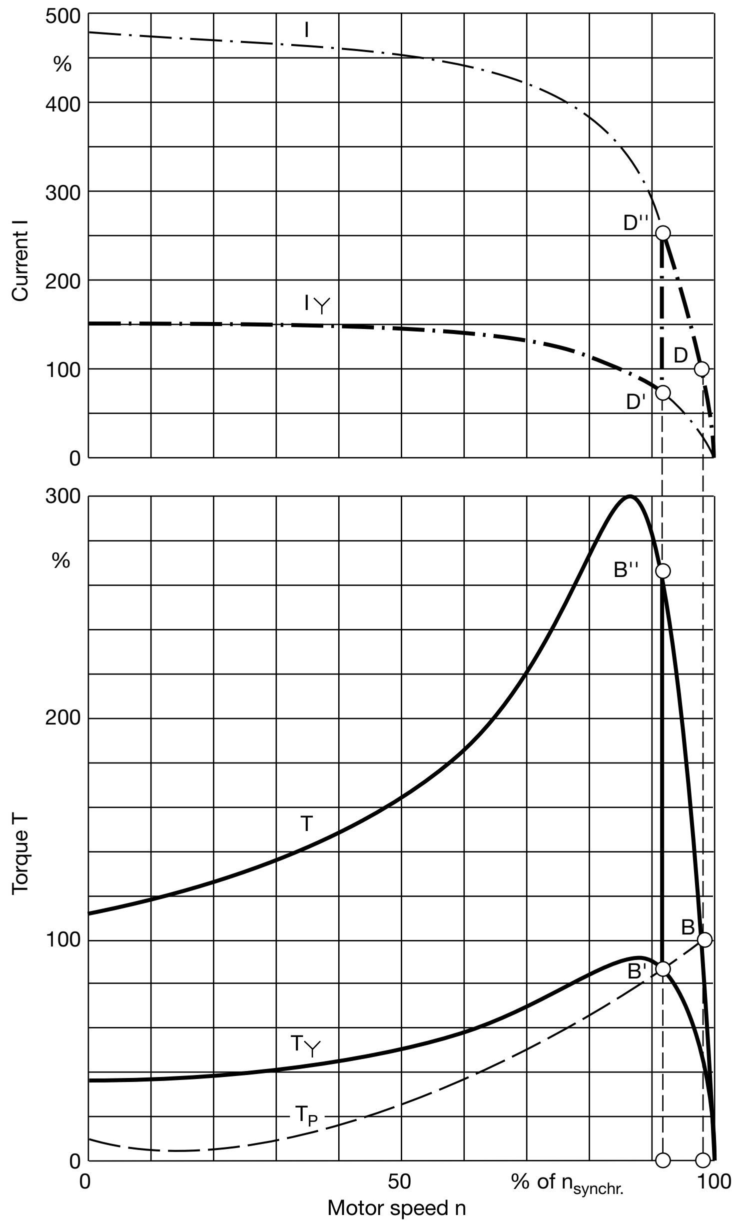

Fig. 23: Starting curve for current I and torque T of squirrel-cage motors in star-delta connection
(Y = star connection; Δ = delta connection; P = pump)

An **autotransformer** also serves to reduce voltage at the motor windings and – unlike star-delta starting – allows selection of the actual voltage reduction. A 70% tapping of the transformer, for instance, will bring down the start-up torque and current supplied by the mains to 49% of the values for d.o.l. starting. The fact that current supply is never interrupted is another advantage of autotransformers.

Soft starters are used for electronic continuous variation of the voltage at the motor windings in accordance with the dimmer principle. This means that the start-up time and starting current can be freely selected within the motor's permissible operating limits (heat losses due to slip!). Special constraints regarding the frequency of starts (contrary to Table 10) have to be heeded [1].

Frequency inverters (usually for open- or closed-loop control) provide a soft starting option without the need for any additional equipment. For this purpose, the output frequency and voltage of the frequency inverter (see section 3.4.3) are increased continuously from a minimum value to the required value, without exceeding the motor's rated current.

3.4 Pump Performance and Control [4], [6], [8]

3.4.1 Operating Point

The operating point of a centrifugal pump, also called its duty point, is given by the intersection of the pump characteristic curve (see section 3.1.6) with the system characteristic curve (see section 3.2.2). The flow rate Q and the developed head H are both determined by the intersection. To change the operating point either the system curve or the pump curve must be changed.

A **system characteristic curve** for pumping water can only be changed

- by changing the flow resistance (for example, by changing the setting of a throttling device, by installing an orifice or a bypass line, by rebuilding the piping or by its becoming incrusted) and/or
- by changing the static head component (for example, with a different water level or tank pressure).

A **pump characteristic curve** can be changed

- by changing the speed of rotation (see section 3.4.3),
- by starting or stopping pumps operated in series or parallel (see sections 3.4.4 or 3.4.5),
- for pumps with radial impellers, by changing the impeller's outside diameter (see section 3.4.6),
- for pumps with mixed flow impellers, by installing or changing the setting of installed pre-swirl control equipment (see section 3.4.8),
- for axial flow (propeller) pumps, by changing the blade pitch setting (see section 3.4.9).

Please note: the effect of these measures for changing the characteristic curve can only be predicted for non-cavitating operation (see section 3.5).

3.4.2 Flow Control by Throttling

Changing the flow rate Q by operating a throttle valve is the simplest flow control method not only for a single adjustment of the flow rate but also for its continuous control, since it requires the least investment. But it is also the most energy wasting method, since the flow energy is converted irreversibly to heat.

Fig. 24 illustrates this process: by intentionally increasing the system resistance (for example by throttling a valve on the

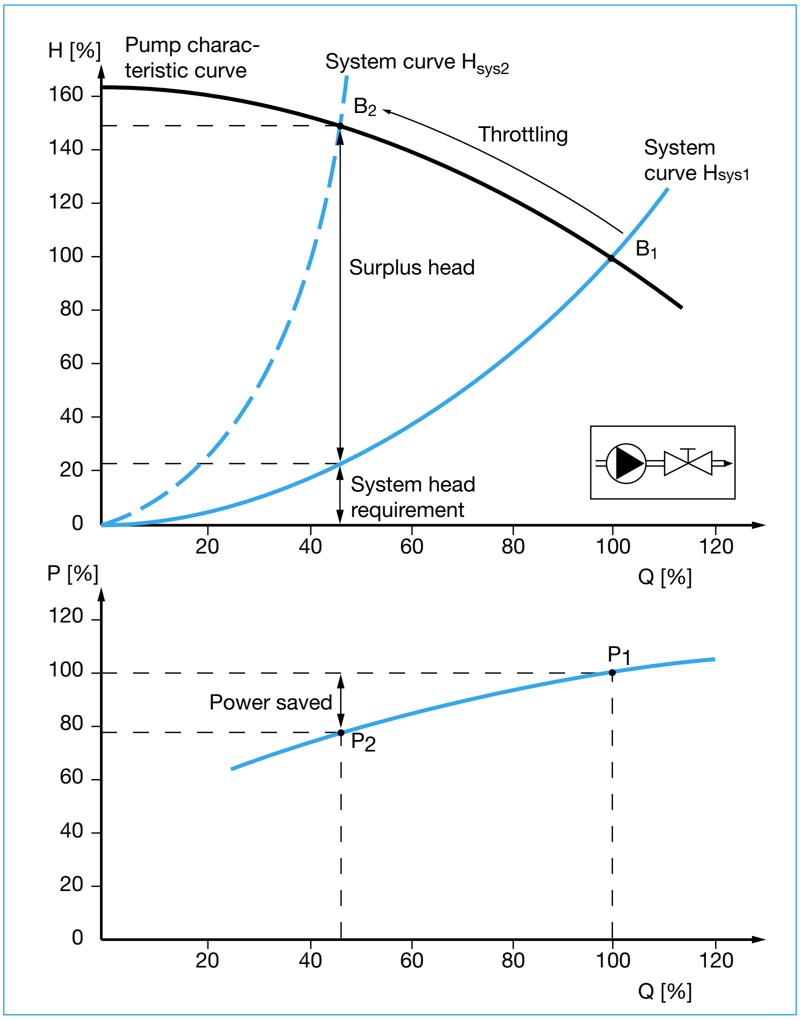

Fig. 24: Change of the operating point and power saved by throttling a pump whose power curve has a positive slope

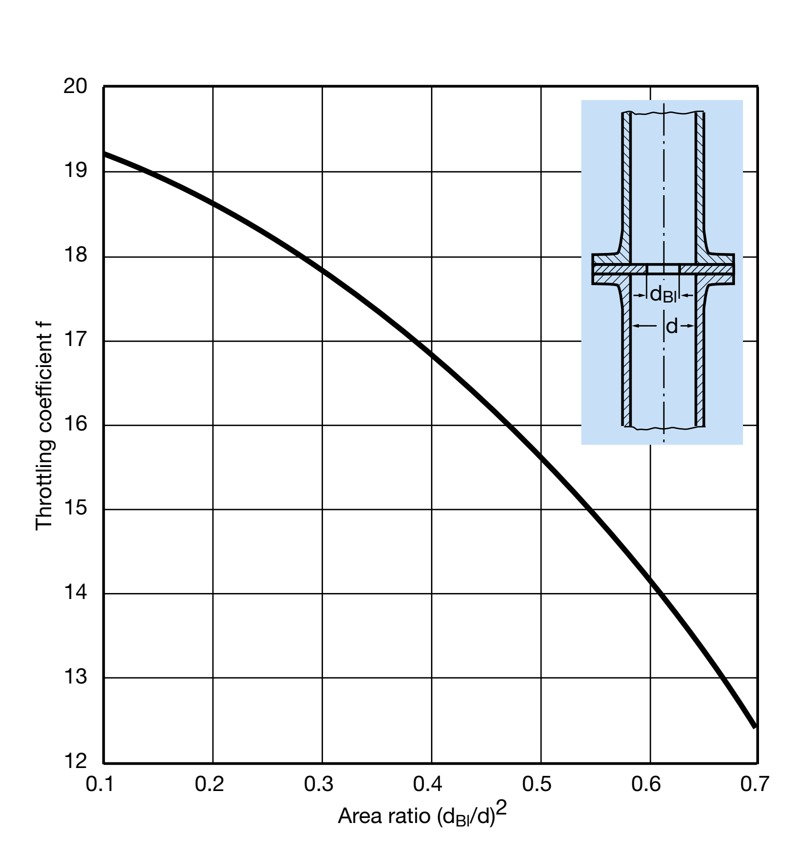

Fig. 25: Orifice plate and its throttling coefficient f

pump discharge side) the original system curve H_{sys1} becomes steeper and transforms into H_{sys2}. For a constant pump speed, the operating point B_1 on the pump characteristic moves to B_2 at a lower flow rate. The pump develops a larger head than would be necessary for the system; this surplus head is eliminated in the throttle valve. The hydraulic energy is irreversibly converted into heat which is transported away by the flow. This loss is acceptable when the control range is small or when such control is only seldom needed. The power saved is shown in the lower part of the figure; it is only moderate compared with the large surplus head produced.

The same is principally true of the installation of a fixed, **sharp-edged orifice plate** in the discharge piping, which can be justified for low power or short operating periods. The necessary hole diameter d_{Bl} of the orifice is calculated from the head difference to be throttled ΔH, using the following equation:

$$d_{Bl} = f \cdot \sqrt{Q/\sqrt{g \cdot \Delta H}} \qquad \textbf{(20)}$$

where

- d_{Bl} Hole diameter of the orifice in mm
- f Throttling or pressure drop coefficient acc. to Fig. 25
- Q Flow rate in m^3/h
- g Gravitational constant 9.81 m/s^2
- ΔH Head difference to be throttled in m

Since the area ratio $(d_{Bl}/d)^2$ must be estimated in advance, an iterative calculation is necessary (plotting the calculated vs. the estimated diameter d_{Bl} is recommended so that after two iterations the correct value can be directly interpolated, see example calculation 8.20).

3.4.3 Variable Speed Flow Control

At various speeds of rotation n, a centrifugal pump has different characteristic curves, which are related to each other by the affinity laws. If the characteristics H and P as functions of Q are known for a speed n_1, then all points on the characteristic curve for n_2 can be calculated by the following equations:

$$Q_2 = Q_1 \,.\, n_2/n_1 \qquad \textbf{(21)}$$

$$H_2 = H_1 \cdot (n_2/n_1)^2 \qquad \textbf{(22)}$$

$$P_2 = P_1 \cdot (n_2/n_1)^3 \qquad \textbf{(23)}$$

Eq. (23) is valid only as long as the efficiency η does not decrease as the speed n is reduced. With a change of speed, the operating point is also shifted (see section 3.4.1). Fig. 26 shows the H/Q curves for several speeds of rotation; each curve has an intersection with the system characteristic H_{sys1}. The operating point B moves along this system curve to smaller flow rates when the speed of rotation is reduced.

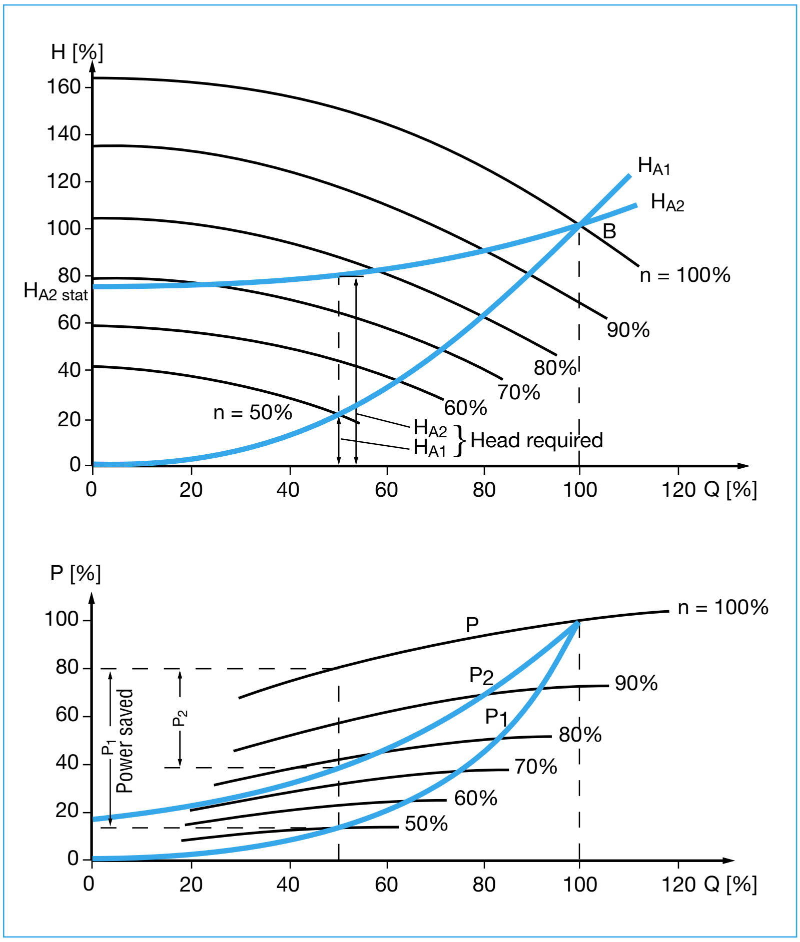

Fig. 26: Operation of a variable speed pump for different system characteristic curves H_{sys1} and H_{sys2} (Power savings ΔP_1 and ΔP_2 at half load each compared with simple throttling)

If the system curve is a parabola through the origin as for H_{sys1} in the example, the developed head H according to Eq. (22) is reduced to one fourth its value and the required driving power in Eq. (23) to one eighth its value when the speed is halved. The lower part of Fig. 26 shows the extent of the savings ΔP_1 compared with simple throttling.

If the system curve is a parabola with a large static head component as for H_{sys2}, it is possible that the pump characteristic at reduced speed has no intersection with it and hence, that no operating point results; the lower speed range is then of no use and could be eliminated. The potential power savings ΔP_2 at a given flow rate Q are less than for the system curve H_{sys1} as shown in the lower part of the diagram [4]. The improvement compared with throttling decreases as the static head component $H_{sys,stat}$ increases (i.e., for a lower dynamic head component $H_{sys,dyn}$).

Variation of the speed usually means varying the electrical driving frequency, which must be considered when choosing the motor. The expenditure for variable speed drives is not low, but it is amortized quickly for pumps which are used often and which are frequently required to run at reduced flows with small static head component $H_{sys,stat}$ [8]. This is particularly the case for pumps in heating systems.

3.4.4 Parallel Operation of Centrifugal Pumps

Where **one** pump is unable to deliver the required flow Q at the operating point, it is possible to have two or more pumps working in parallel in the same piping system, each with its own non-return valve (Fig. 27). Parallel operation of pumps is easier when their shutoff heads H_0 are all equal, which is the case for identical pumps. If the shutoff heads H_0 differ, the lowest shutoff head marks the point on the common H/Q curve for the minimum flow rate Q_{min}, below which no parallel operation is possible, since the non-return valve of the pump with smaller shutoff head will be held shut by the other pump(s).

During parallel pumping it must be kept in mind that after stopping one of two identical centrifugal pumps (Fig. 27), the flow rate Q_{single} of the remaining pump does not fall to half of $Q_{parallel}$, but rather increases to more than half. The remaining pump might then immediately run at an operating point B_{single} above its design point, which must be considered when checking the NPSH values (see section 3.5) and the drive power (see section 3.1.3). The reason for this behaviour is the parabolic shape of the system characteristic H_{sys}. For the same reason, the reverse procedure of taking a second identical pump on line does not double the flow rate Q_{single} of the pump that was already running, but rather increases the flow rate less than that:

$$Q_{parallel} < 2 \cdot Q_{single} \qquad (24)$$

This effect when starting or stopping one additional pump is more intense when the system curve is steeper or when the pump characteristic is flatter. As long as both pumps I and II are running, the total flow rate $Q_{parallel}$ is the sum of Q_I and Q_{II}, i.e.:

$$Q_{parallel} = Q_I + Q_{II} \qquad (25)$$

To compute the characteristic curve for parallel operation see section 3.3.1.

Starting or stopping individual pumps operated in parallel does save energy, but it allows only a stepped control of the flow rate. For continuously variable control, at least one of the pumps must be fitted with a variable speed drive or a control valve must be installed in the common discharge piping [4].

If centrifugal pumps running at fixed speeds and having unstable characteristics (see Fig. 7 in section 3.1.6) are run in parallel, difficulties can arise when bringing another pump online.

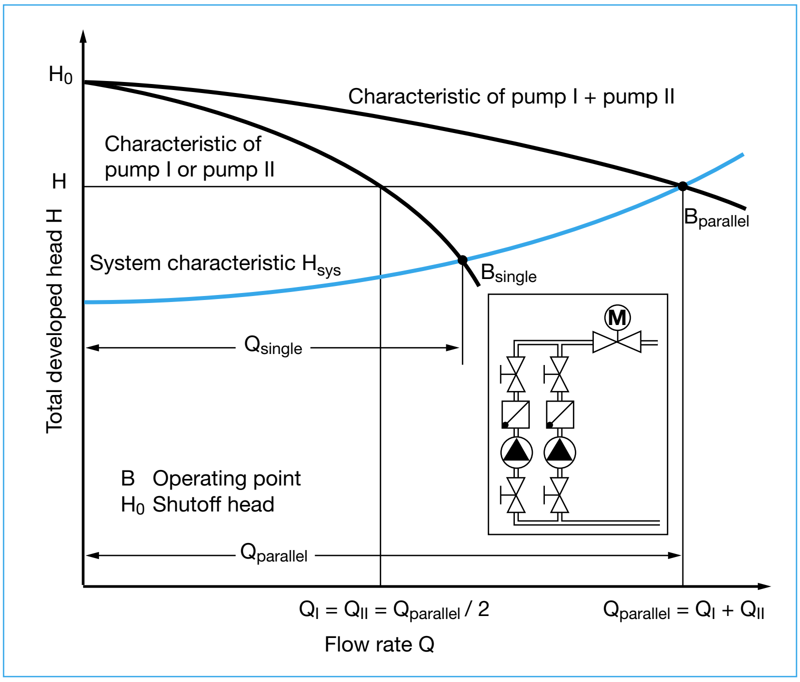

Fig. 27: Parallel operation of 2 identical centrifugal pumps with stable characteristic curves

The problems occur when the developed head H_1 of the pump running is larger than the shut-off head (i.e., the developed head at Q = 0) of the pump to be started; the second pump is unable to overcome the pressure on its non-return valve (Fig. 28, System curve H_{sys1}). Pumps with unstable characteristics are not suitable for such a low flow operation. (For a lower system curve H_{sys2} they would be perfectly able to operate properly since the developed head H_2 of the pump running is lower than the shutoff head H_0 of the pump to be started).

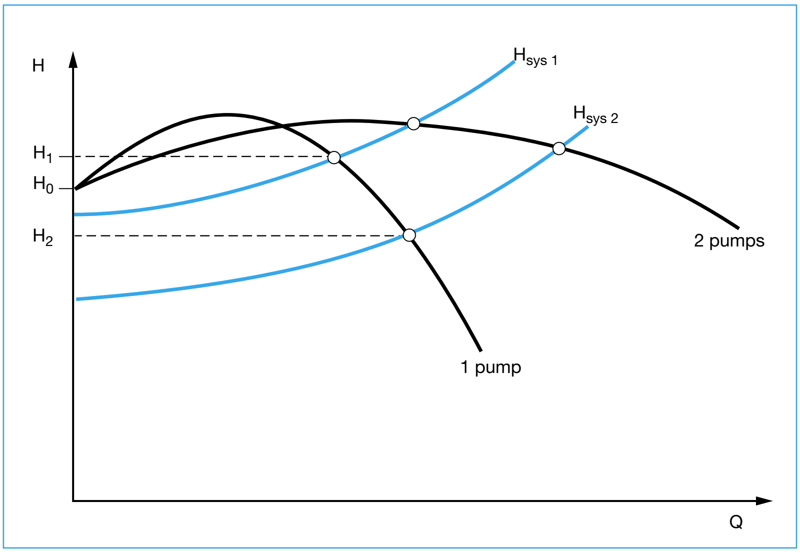

Fig. 28: Parallel operation of 2 identical centrifugal pumps with unstable characteristics

3.4.5 Series Operation

In series operation, the pumps are connected one after the other so that the developed heads can be added for a given flow rate. This means that the discharge pressure of the first pump is the inlet pressure for the second pump, which must be considered for the choice of shaft seal and for the strength of the casing. For this reason multistage pumps are usually used for such applications (except for the hydraulic transport of solids, see section 6). They do not pose these shaft sealing problems.

3.4.6 Turning Down Impellers

If the flow rate or developed head of a radial or mixed flow centrifugal pump are to be reduced **permanently,** the outside diameter D of the impeller should be reduced. The reduction should be limited to the value for which the impeller vanes still overlap when viewed radially. The documentation of the pump characteristics (Fig. 18) usually shows curves for several diameters D (in mm).

Impellers made from hard materials, such as those used for solids-handling pumps, or from stainless steel sheet metal, as well as single vane impellers (Fig. 43) and star or peripheral pump impellers **cannot** be turned down. (The same is true for under-filing as described in section 3.4.7). For multistage pumps, usually only the vanes but not the shrouds of the impellers are cut back. It is sometimes possible to simply remove the impeller and diffuser of one stage of a multistage pump and replace them with a blind stage (two concentric cylindrical casings to guide the flow) instead of cutting back the impeller vanes. Impellers with a non-cylindrical exit section are either turned down or have only their blades cut back as specified in the characteristic curve literature (for example, as shown in Fig. 29).

If the impeller diameter only needs to be reduced slightly, a rule of thumb can be applied. An exact calculation cannot be made, since the geometrical similarity of the vane angle and exit width are not preserved when turning down the impeller. The following approximate relationship exists between Q, H and the impeller diameter D to be found (averaged, if required):

$$(D_t/D_r)^2 \approx Q_t/Q_r \approx H_t/H_r \quad (26)$$

where subscript $_t$ designates the condition before the reduction

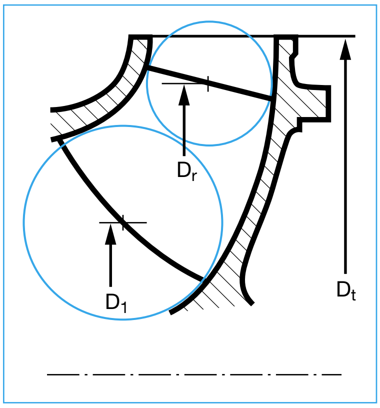

Fig. 29: Contour for cutting back the vanes of an impeller with a mixed flow exit

of the impeller outer diameter and index $_r$ the condition after the reduction. The required (average) reduced diameter results as:

$$D_r \approx D_t \cdot \sqrt{(Q_r/Q_t)} \approx D_t \cdot \sqrt{(H_r/H_t)} \quad \textbf{(27)}$$

The parameters needed to determine the reduced diameter can be found as shown in Fig. 30: in the H/Q curve (linear scales required!) a line is drawn connecting the origin (careful: some scales do not start at zero!) and the new operating point B_r. The extension of the line intersects the characteristic curve for full diameter D_t at the point B_t. In this way the values of Q and H with the subscripts $_t$ and $_r$ can be found, which are used with Eq. (27) to find the desired reduced diameter D_r.

The ISO 9906 method is more accurate, but also more involved through the consideration of the average diameter D_1 of the impeller leading edge (subscript $_1$), valid for $n_q < 79$ and for a change of diameter $< 5\%$, as long as the vane angle and the impeller width remain constant. Thus using the nomenclature of Figs. 29 and 30:

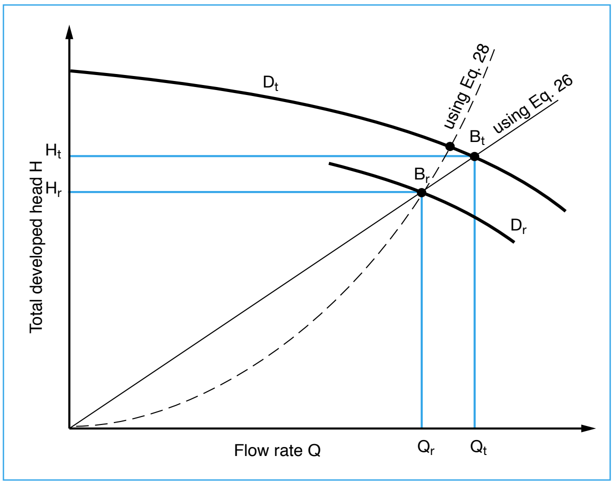

Fig. 30: Determination of the reduced impeller diameter D_r

$$(D_r^2 - D_1^2)/(D_t^2 - D_1^2) = H_r/H_t = (Q_r/Q_t)^2 \quad (28)$$

A solution is only possible when D_1 is known and when a parabola $H \sim Q^2$ is drawn through the reduced operating point B_r (with H_r and Q_r), not a line as in Fig. 30, which intersects the base H/Q curve for diameter D_t at a different point B_t (with different H_t and Q_t).

3.4.7 Under-filing of Impeller Vanes

A small, permanent increase of the developed head at the best efficiency point (up to 4 – 6%) can be achieved for radial impellers by filing the back sides of the backward-curved vanes, i.e., by sharpening the vanes on the concave side, as shown in Fig. 31. The shutoff head does not change. This method is suitable for minor final corrections.

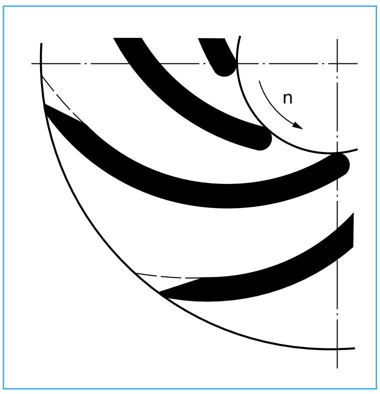

Fig. 31: Under-filed vanes of a radial impeller

3.4.8 Pre-Swirl Control of the Flow

For tubular casing pumps with mixed flow impellers, the pump characteristic can be influenced by changing the pre-rotation in the impeller inlet flow. Such pre-swirl control equipment is often fitted to control the flow rate. The various characteristic curves are then shown in the product literature labelled with the control setting (Fig. 32).

3.4.9 Flow Rate Control or Change by Blade Pitch Adjustment

The characteristic curves of axial flow (propeller) pumps can be altered by changing the setting of the propeller blade pitch. The setting can be fixed and firmly bolted or a device to change the blade pitch during operation can be used to control the flow rate. The blade pitch angles are

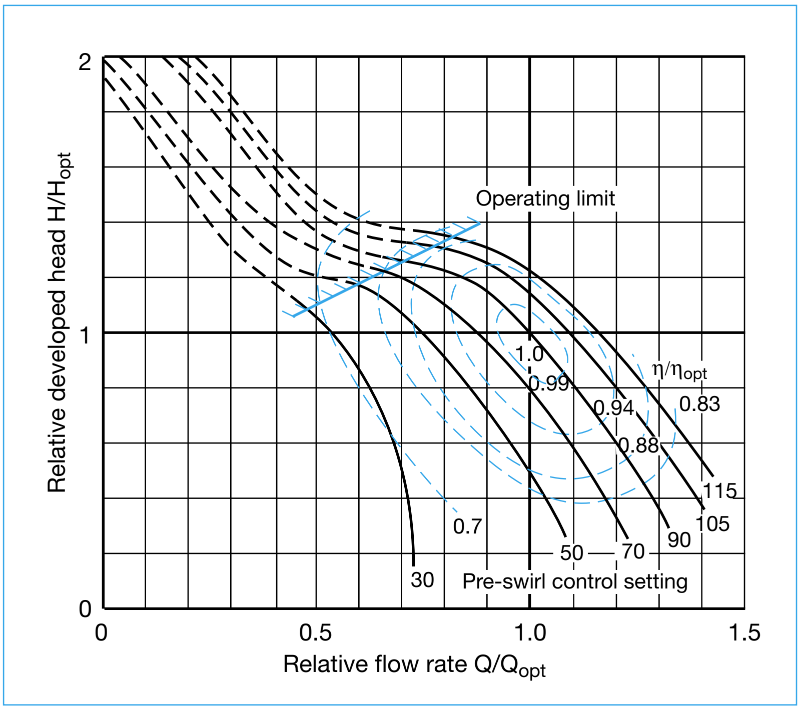

Fig. 32: Characteristic curve set of a centrifugal pump with pre-swirl control equipment, $n_q \approx 160$

shown in the product literature with their respective characteristic curves (see Fig. 33).

3.4.10 Flow Control Using a Bypass

The system characteristic curve can be made steeper by closing a throttle valve, but it can also be made flatter by opening a bypass in the discharge piping as shown in Fig. 34. The pump operating point moves from B_1 to a larger flow rate B_2. The bypass flow rate is controlled and can be fed back into the inlet tank without being used directly. From the point of view of saving energy, this type of control only makes sense when the power curve falls for increasing pump flow rates ($P_1 > P_2$), which is the case for high specific speeds (mixed and axial flow propeller pumps).

For these types of pumps, controlling the flow by pre-swirl control or by changing the blade pitch is even more economical, however. The expenditure for a bypass and control valve is not small [4]. This method is also suitable for preventing pumps from operating at unacceptably low flow rates (see operating limits in Figs. 5 and 6c as well as in Figs. 32 and 33).

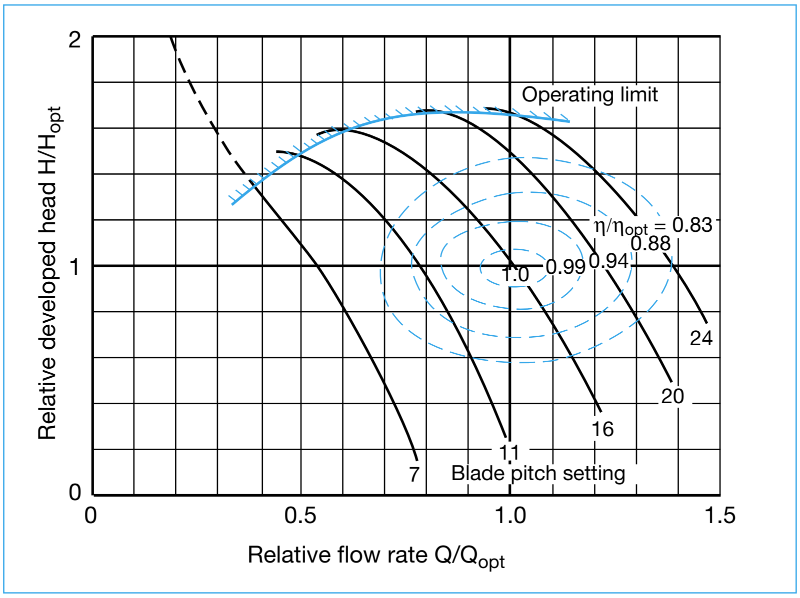

Fig. 33: Characteristic curve set of an axial flow pump with blade pitch adjustment, $n_q \approx 200$

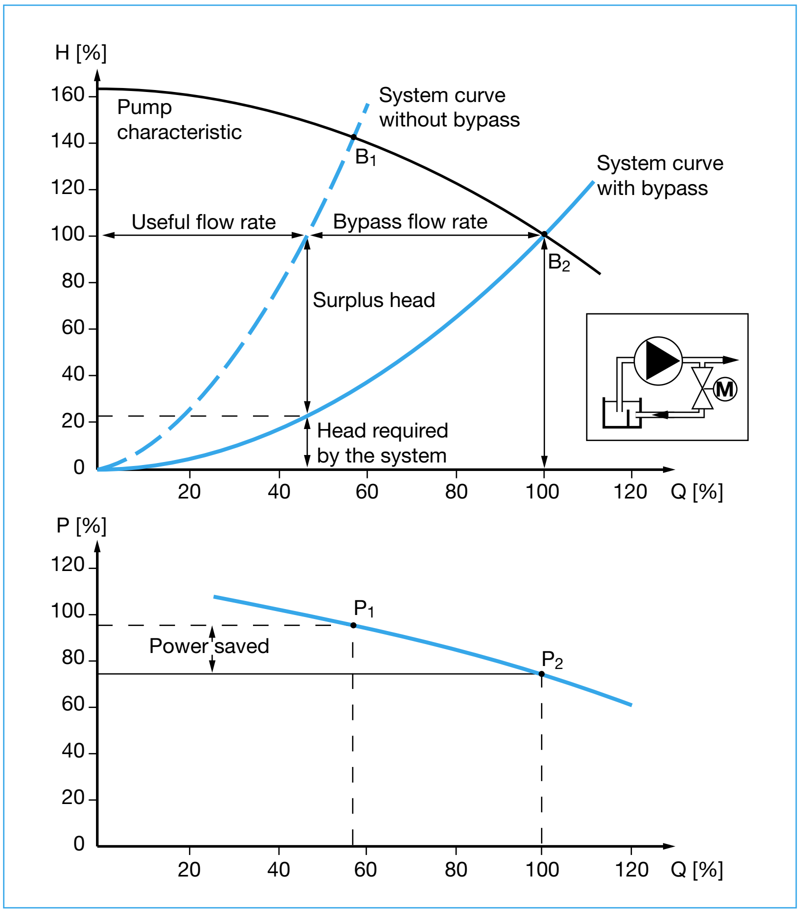

Fig. 34: Characteristic curves and operating points of a pump with a falling power curve and flow control using a bypass. (For a radial flow pump the power curve would increase towards the right and this type of control would cause an increase in power input, see Fig. 5).

3.5
Suction and Inlet Conditions [3]

NPSH = Net Positive Suction Head

3.5.1
The NPSH Value of the System: $NPSH_a$

The $NPSH_a$ value is the difference between the total pressure in the centre of the pump inlet and the vapour pressure p_v, expressed as a head difference in m. It is in certain respects a measure of the probability of vaporization at that location and it is determined only by the operating data of the system and the type of fluid. The vapour pressure of water and other liquids are shown in Table 12 and in Fig. 35 as a function of the temperature.

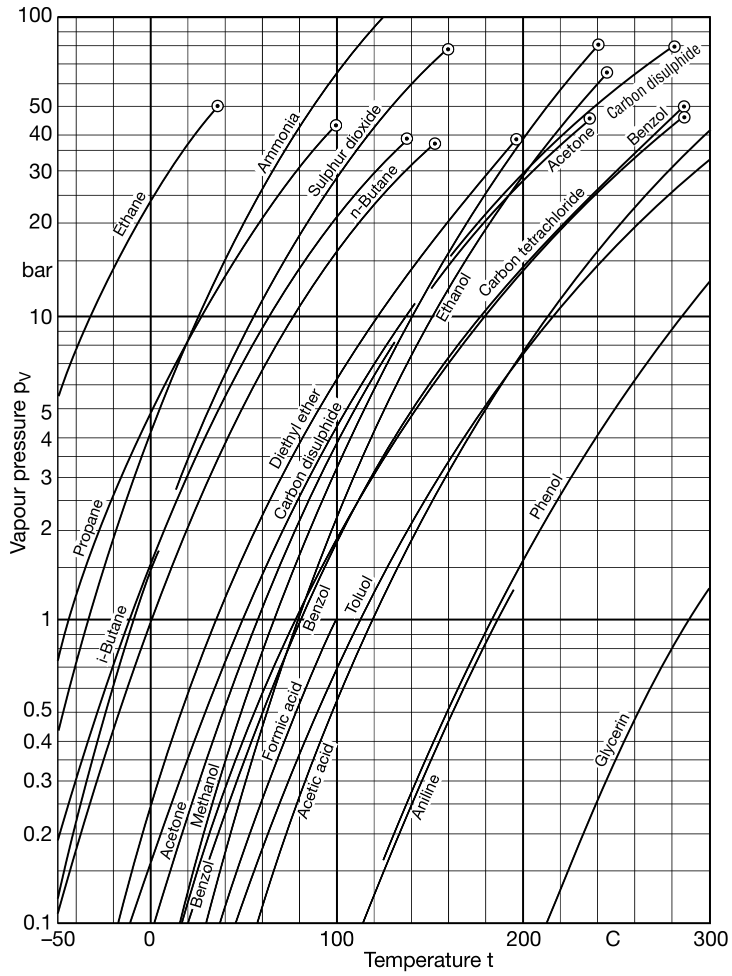

Fig. 35: Vapour pressure p_v of various fluids as a function of the temperature t (for an enlarged view see page 84)

Table 12: Vapour pressure p_v, density ϱ and kinematic viscosity ν of water at saturation conditions as a function of the temperature t

t °C	p_v bar	ϱ kg/m³	ν mm²/s
0	0.00611	999.8	1.792
1	0.00656	999.9	
2	0.00705	999.9	
3	0.00757	1000.0	
4	0.00812	1000.0	
5	0.00872	1000.0	
6	0.00935	999.9	
7	0.01001	999.9	
8	0.01072	999.8	
9	0.01146	999.7	
10	0.01227	999.6	1.307
11	0.01311	999.5	
12	0.01401	999.4	
13	0.01496	999.3	
14	0.01597	999.2	
15	0.01703	999.0	
16	0.01816	998.8	
17	0.01936	998.7	
18	0.02062	998.5	
19	0.02196	998.4	
20	0.02337	998.2	1.004
21	0.02485	997.9	
22	0.02642	997.7	
23	0.02808	997.5	
24	0.02982	997.2	
25	0.03167	997.0	
26	0.03360	996.7	
27	0.03564	996.4	
28	0.03779	996.1	
29	0.04004	995.8	
30	0.04241	995.6	0.801
31	0.04491	995.2	
32	0.04753	994.9	
33	0.05029	994.6	
34	0.05318	994.2	
35	0.05622	993.9	
36	0.05940	993.5	
37	0.06274	993.2	
38	0.06624	992.9	
39	0.06991	992.6	
40	0.07375	992.2	0.658
41	0.07777	991.8	
42	0.08198	991.4	
43	0.08639	991.0	
44	0.09100	990.6	
45	0.09582	990.2	
46	0.10085	989.8	
47	0.10612	989.3	
48	0.11162	988.9	
49	0.11736	988.5	
50	0.12335	988.0	0.553
51	0.12960	987.7	
52	0.13613	987.2	
53	0.14293	986.7	
54	0.15002	986.2	
55	0.15741	985.7	
56	0.16509	985.2	
57	0.17312	984.7	
58	0.18146	984.3	
59	0.19015	983.7	
60	0.19920	983.2	0.474

t °C	p_v bar	ϱ kg/m³	ν mm²/s
61	0.2086	982.6	
62	0.2184	982.1	
63	0.2285	981.6	
64	0.2391	981.1	
65	0.2501	980.5	
66	0.2614	980.0	
67	0.2733	979.4	
68	0.2856	978.8	
69	0.2983	978.3	
70	0.3116	977.7	0.413
71	0.3253	977.1	
72	0.3396	976.6	
73	0.3543	976.0	
74	0.3696	975.4	
75	0.3855	974.8	
76	0.4019	974.3	
77	0.4189	973.7	
78	0.4365	973.0	
79	0.4547	972.5	
80	0.4736	971.8	0.365
81	0.4931	971.3	
82	0.5133	970.6	
83	0.5342	969.9	
84	0.5557	969.4	
85	0.5780	968.7	
86	0.6010	968.1	
87	0.6249	967.4	
88	0.6495	966.7	
89	0.6749	966.0	
90	0.7011	965.3	0.326
91	0.7281	964.7	
92	0.7561	964.0	
93	0.7849	963.3	
94	0.8146	962.6	
95	0.8452	961.9	
96	0.8769	961.2	
97	0.9095	960.4	
98	0.9430	959.8	
99	0.9776	959.0	
100	1.0132	958.3	0.295
102	1.0878	956.8	
104	1.1668	955.5	
106	1.2504	954.0	
108	1.3390	952.6	
110	1.4327	951.0	
112	1.5316	949.6	
114	1.6361	948.0	
116	1.7465	946.4	
118	1.8628	944.8	
120	1.9854	943.1	0.2460
122	2.1144	941.5	
124	2.2503	939.8	
126	2.3932	938.2	
128	2.5434	936.5	
130	2.7011	934.8	
132	2.8668	933.2	
134	3.0410	931.4	
136	3.2224	929.6	
138	3.4137	927.9	
140	3.614	926.1	0.2160

t °C	p_v bar	ϱ kg/m³	ν mm²/s
145	4.155	921.7	
150	4.760	916.9	
155	5.433	912.2	
160	6.180	907.4	0.1890
165	7.008	902.4	
170	7.920	897.3	
175	8.925	892.1	
180	10.027	886.9	0.1697
185	11.234	881.4	
190	12.553	876.0	
195	13.989	870.3	
200	15.550	864.7	0.1579
205	17.245	858.7	
210	19.080	852.8	
215	21.062	846.6	
220	23.202	840.3	0.1488
225	25.504	834.0	
230	27.979	827.3	
235	30.635	820.6	
240	33.480	813.6	0.1420
245	36.524	806.5	
250	39.776	799.2	
255	43.247	791.8	
260	46.944	784.0	0.1339
265	50.877	775.9	
270	55.055	767.9	
275	59.487	759.4	
280	64.194	750.7	0.1279
285	69.176	741.6	
290	74.452	732.3	
295	80.022	722.7	
300	85.916	712.5	0.1249
305	92.133	701.8	
310	98.694	690.6	
315	105.61	679.3	
320	112.90	667.1	0.1236
325	120.57	654.0	
330	128.64	640.2	
340	146.08	609.4	0.1245
350	165.37	572.4	
360	186.74	524.4	0.1260
370	210.53	448.4	
374.2	225.60	326.0	0.1490

Density ϱ of sea water
ϱ = 1030 ÷ 1040 kg/m³

3.5.1.1 NPSH$_a$ for Suction Lift Operation

For suction lift operation (Fig. 8) the pump is installed above the suction-side water level. The value of NPSH$_a$ can be calculated from the conditions in the suction tank (index e) as follows (see Fig. 36)

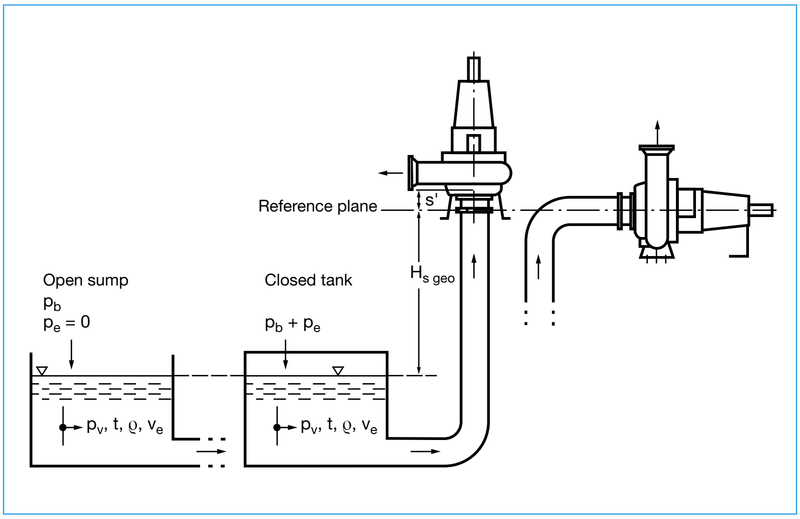

Fig. 36: Calculation of the NPSH$_a$ for suction lift operation for horizontally or vertically installed pumps

$$NPSH_a = (p_e + p_b - p_v)/(\varrho \cdot g) + v_e^2/2g - H_{L,s} - H_{s\,geo} \pm s' \quad \textbf{(29)}$$

where

- p_e Gauge pressure in suction tank in N/m^2
- p_b Absolute atmospheric pressure in N/m^2 (Table 13: consider effect of altitude!)
- p_v Vapour pressure in N/m^2 (in Table 12 as absolute pressure!)
- ϱ Density in kg/m^3
- g Gravitational constant, 9.81 m/s^2
- v_e Flow velocity in the suction tank or sump in m/s
- $H_{L,s}$ Head loss in the suction piping in m
- $H_{s\,geo}$ Height difference between the fluid level in the suction tank or sump and the centre of the pump inlet in m
- s' Height difference between the centre of the pump inlet and the centre of the impeller inlet in m

Table 13: Influence of the altitude above mean sea level on the annual average atmospheric pressure and on the corresponding boiling point (1 mbar = 100 Pa)

Altitude above mean sea level m	Atmospheric pressure p_b mbar	Boiling point °C
0	1013	100
200	989	99
500	955	98
1000	899	97
2000	795	93
4000	616	87
6000	472	81

For cold water and open sump (Fig. 36, on the left) at sea level this equation can be simplified with sufficient accuracy for most practical purposes to

$$NPSH_a = 10 - H_{L,s} - H_{s\,geo} \pm s' \quad (30)$$

The correction using s' is only necessary when the centre of the impeller inlet (which is the decisive location for cavitation risk) is not at the same height as the centre of the pump inlet (= reference plane). In Fig. 36, $H_{s\,geo}$ must be "lengthened" for the pump on the left by the value s' (i.e., same sign for $H_{s\,geo}$ and s'!). When s' is unknown, it can usually be estimated with enough accuracy by examining the pump's outline drawing.

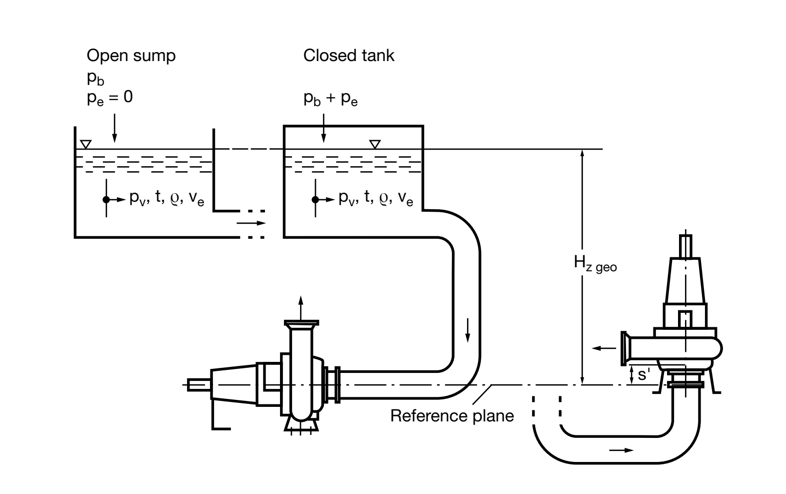

Fig. 37: Calculation of the $NPSH_a$ for suction head operation for horizontally or vertically installed pumps

3.5.1.2 $NPSH_a$ for Suction Head Operation

For operation with positive inlet pressure (also called "suction head operation"), the pump is installed below the liquid level. Eqs. (29) and (30) change by replacing $-H_{s\ geo}$ with $+H_{z\ geo}$ and then read:

$$NPSH_a = (p_e + p_b - p_v)/(\varrho \cdot g) + v_e^2/2g - H_{L,s} + H_{z\ geo} \pm s' \quad \textbf{(31)}$$

where

$H_{z\ geo}$ Height difference between the fluid level in the inlet tank and the centre of the pump inlet in m

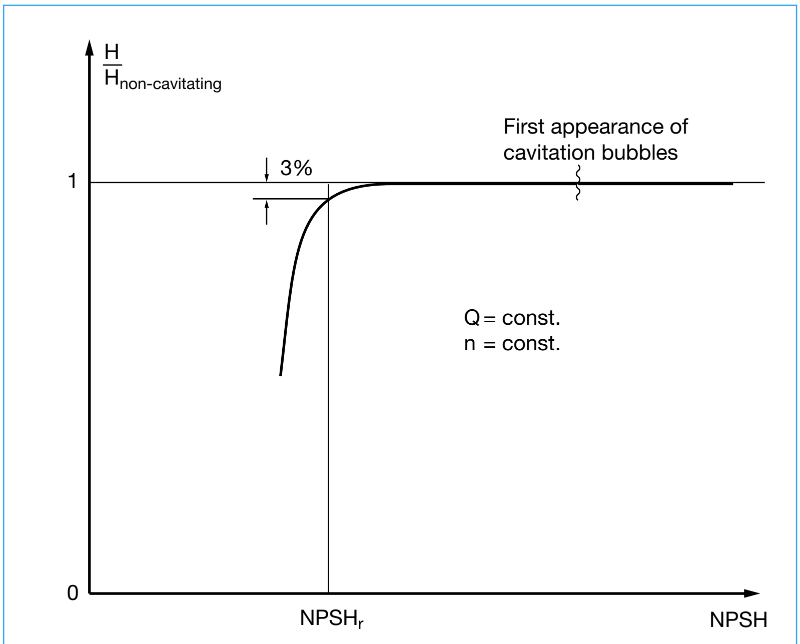

Fig. 38: Experimental determination of the $NPSH_r$ for the criterion $\Delta H = 0.03\ H_{non-cavitating}$

For cold water and open tanks (Fig. 37, on the left) at sea level this equation can also be simplified for all practical purposes to:

$$NPSH_a = 10 - H_{L,s} + H_{z\ geo} \pm s' \quad (32)$$

The comments on s' as outlined in section 3.5.1.1 apply analogously.

3.5.2 The NPSH Value of the Pump: $NPSH_r$

When the inlet pressure drops, cavitation bubbles start to develop in the pump long before their effects become apparent in the hydraulic performance. One must therefore accept the presence of a small amount of cavitation bubbles in order to operate economically. The permissible amount of cavitation can be defined with certain criteria. Often a head drop of 3% resulting from cavitation is accepted. Fig. 38 shows how this point is identified: At a constant flow rate and constant speed of rotation, the $NPSH_a$ of the test loop is reduced until the pump's discharge head has fallen by 3%. Other criteria for the cavitation limit can also be used, such as the increase in sound level due to cavitation, the amount of material erosion or a certain reduction in pump efficiency. To avoid impermissible cavitation conditions, a minimum NPSH value is required, which is shown (in units of m) in the $NPSH_r$ curves below the H/Q characteristics (see Fig. 18). The reference plane is the centre of the impeller inlet (Fig. 39), which can vary by the height s' from the reference plane of the system, for example for vertical pumps (see Figs. 36 and 37).

So as to avoid exceeding the given cavitation limit, it is necessary that

$$NPSH_a > NPSH_r \quad (33)$$

Fig. 40 shows this graphically at the intersection of the $NPSH_a$ and $NPSH_r$ curves. If the NPSH requirement is not fulfilled, the developed head will quickly decrease to the right of the intersection (i.e. at larger flow rates), which produces a "cavitation breakdown curve". Prolonged operation under these conditions can damage the pump.

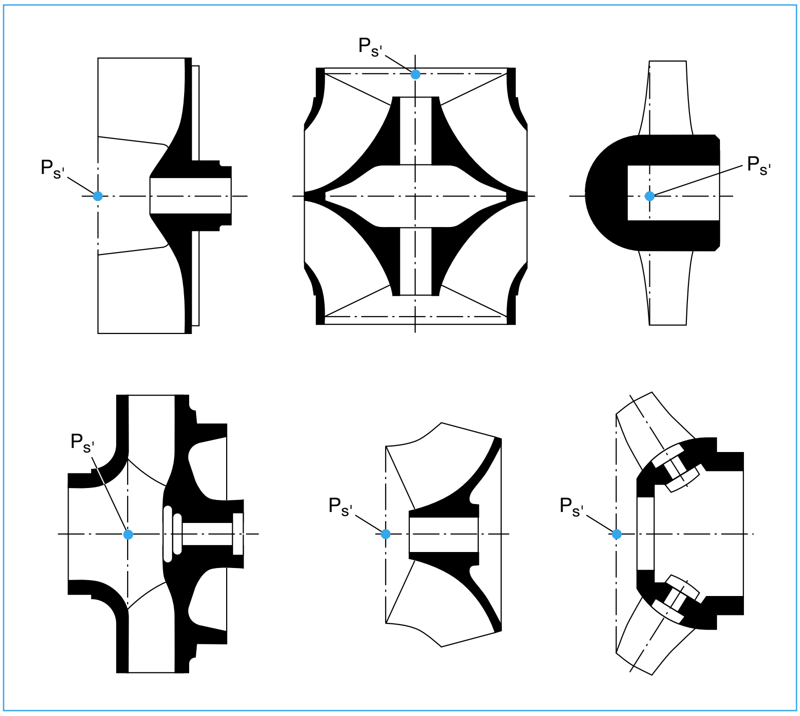

Fig. 39: Position of the reference point $P_{s'}$ for various impellers

3.5.3 Corrective Measures

The numerical values of $NPSH_a$ and $NPSH_r$ are based on the fixed design geometry of the system and of the pump, which cannot be changed after the fact, and on the particular operating point. It follows that a subsequent improvement of the $NPSH_a > NPSH_r$ condition in an installed centrifugal pump system is only possible with major design and financial expenditure for the pump or the system. Options include: increasing $H_{z\,geo}$ or reducing $H_{s\,geo}$ (by mounting the tank at

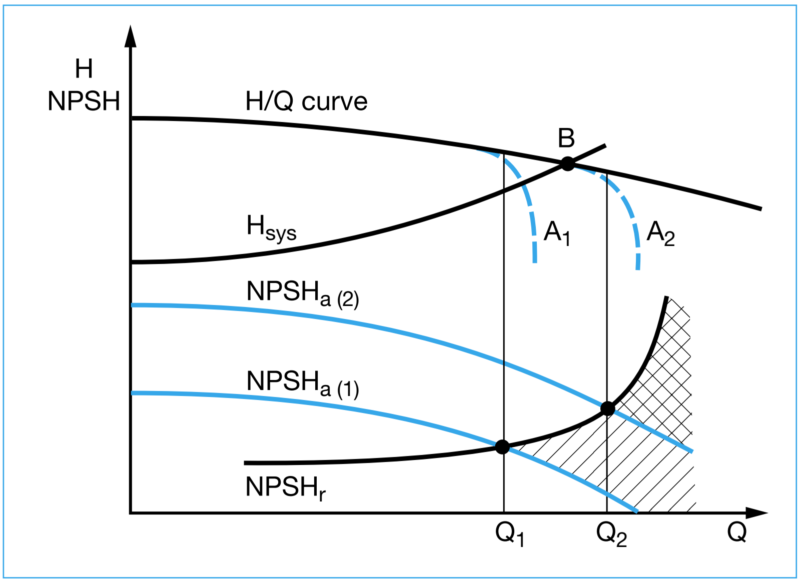

Fig. 40: "Cavitation breakdown curves" A_1 and A_2 of the H/Q curve in the case of insufficient $NPSH_a$: An NPSH deficit exists in the singly hatched (case 1) and cross-hatched regions (case 2). After increasing $NPSH_a(1)$ to $NPSH_a(2)$, the pump's useful operating range is increased from Q_1 to Q_2 and the operating point B can now be reached.

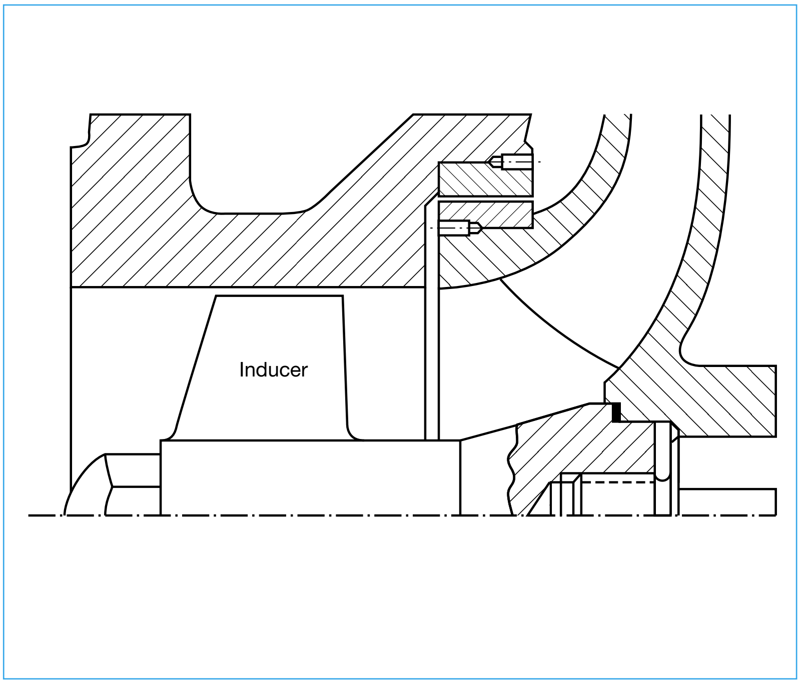

Fig. 41: Sectional drawing of a pump with an inducer (detail)

a higher level or installing the pump at a lower point), minimizing the pressure losses in the inlet piping $H_{L,s}$ or replacing the pump. In the latter case, using a special low-NPSH suction-stage impeller or installing an inducer (propeller in front of the impeller, Fig. 41) can keep the costs of the improvement within limits (a rebuild of the pump is unavoidable, however). It must be kept in mind that the $NPSH_r$ reduction by the inducer does not have an impact on the entire flow range of the pump in question, but only on a certain part of the range (see Fig. 42).

The resistance to cavitation erosion can be increased by choosing more suitable (and more expensive) materials for the impeller, in particular for larger pump sizes.

In one special case, the elimination of an NPSH problem is quite simple: For closed flow loops (for example in a heating system), the system pressure can simply be increased to improve the $NPSH_a$, as long as the system is designed to cope with the higher pressure.

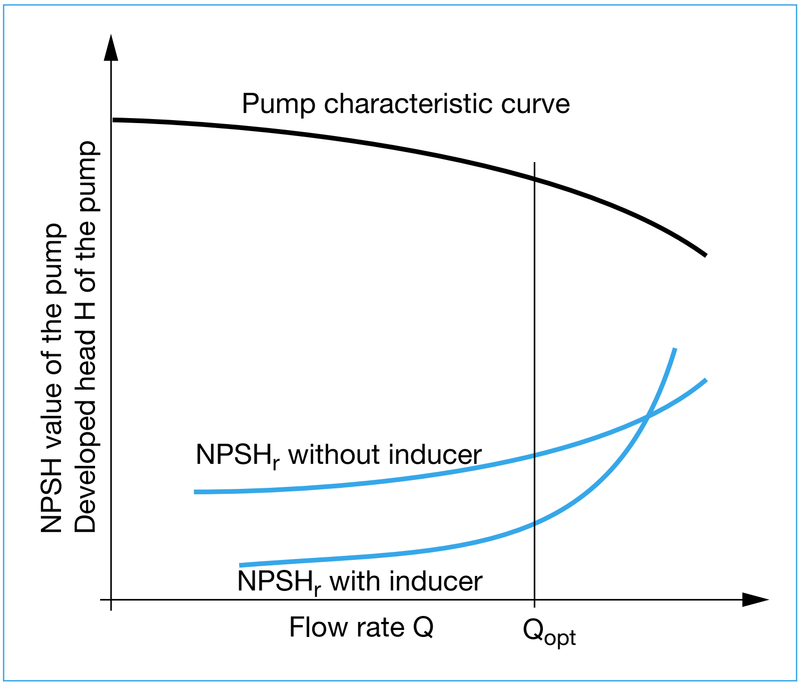

Fig. 42:
Effect of an inducer on the $NPSH_r$

3.6
Effect of Entrained Solids

If the water to be pumped (for example, domestic waste water, rainwater or mixtures) contains small amounts of entrained solids, special impeller and pump types are used (for example with cleaning covers or special shaft seals) [1].

Fig. 43 shows the most common impeller designs for these types of waste water. For pumping sludge, non-clogging channel impellers can be used up to 3% solids content, single vane impellers up to 5%, free flow impellers up to 7% and worm type impellers for even higher concentrations.

Since single vane impellers cannot be turned down to adjust the operating point (see section 3.4.6), this type of pump is often driven using a belt drive (see Fig. 59g).

Allowances added to the drive power are not shown in Fig. 20, but rather in the product literature [1], since they depend not only on the drive rating but also on the impeller design and specific speed. For example, for **single vane impellers** pumping domestic waste water or sewage the following **power reserves** are recommended:

up to	7.5 kW	approx. 30% (≧1kW)
from	11 – 22 kW	approx. 20%
from	30 – 55 kW	approx. 15%
above	55 kW	approx. 10%

When assessing the head losses in the piping (see section 3.2.1.2), adequate allowances have to be added [1].

To avoid blockages in the pipes for waste water with high solids concentrations, a minimum flow velocity of 1.2 m/s in horizontal pipes and 2 m/s in vertical pumps should be maintained. (Exact values can only be determined experimentally!). This is of particular importance for variable speed drives [1].

Impeller Types for Pumping Waste Water

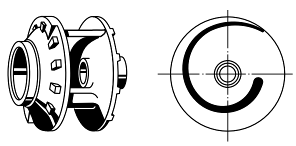

Front view shown without shroud

*Fig. 43a: **Closed single vane impeller** for waste water containing solid or stringy substances*

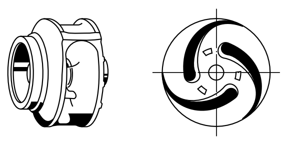

Front view shown without shroud

*Fig. 43b: **Closed non-clogging channel impeller** for sludge or non-gassing liquids containing solids without stringy components*

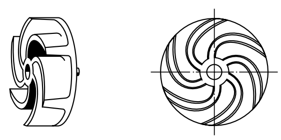

*Fig. 43c: **Free flow impeller** for fluids with coarse or stringy solids and gas content*

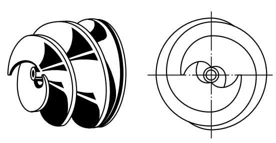

*Fig. 43d: **Worm type impeller** for waste water containing coarse, solid or stringy substances or for sludge with up to 5 to 8% solids content*

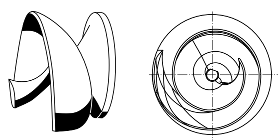

Fig. 43e: Diagonal impeller for waste water containing solid, stringy or coarse substances

4 Special Issues when Pumping Viscous Fluids

4.1 The Shear Curve

Viscosity is that property of a fluid by virtue of which it offers resistance to shear. Fig. 44 shows this process. In a fluid, a plate with a wetted surface area A is moved with speed v_0 parallel to a stationary wall at a distance y_0.

The movement requires that the resistance force F be overcome, which can be expressed as a shear stress $\tau = F/A$. If the wall distance y_0, the velocity v_0 or the type of fluid is changed, then the shear stress also changes in proportion to the velocity v_0 or inversely proportional to the distance y_0. The two easily identified parameters v_0 and y_0 are combined to yield the shear gradient v_0/y_0.

Since the viscosity of the fluid causes a shear stress τ not only at the walls, but rather at every distance from the wall within the fluid, the definition of the rate of shear is generalized as $\partial v/\partial y$ (change of velocity per change of distance). Just as for the shear stress τ, it is not the same for all wall distances y. During an experiment, pairs of values τ and $\partial v/\partial y$ are measured and can be plotted as a function, the so-called shear curve (Fig. 45).

When the shear curve is a straight line going through the origin:

$$\tau = \eta \cdot \partial v/\partial y \qquad (34)$$

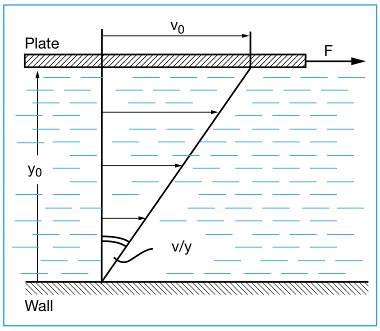

Fig. 44: Velocity profile between a plane wall and a moving parallel plate.

F = *Towing force*
v_0 = *Towing speed*
y_0 = *Distance to wall*
$\partial v/\partial y$ = *Rate of shear*

the constant factor of proportionality η is referred to as the dynamic viscosity with the units Pa s. Fluids with this type of curve (for example water or all mineral oils) are normally viscous or Newtonian fluids, for which the laws of hydrodynamics apply without restriction. If the shear curve is not a straight line through the origin, the fluid is a non-Newtonian fluid, for which the laws of hydrodynamics apply only in a limited fashion. One must therefore strictly differentiate between these two cases.

Since the quotient of dynamic viscosity η and density ϱ is often used in fluid dynamic relation-

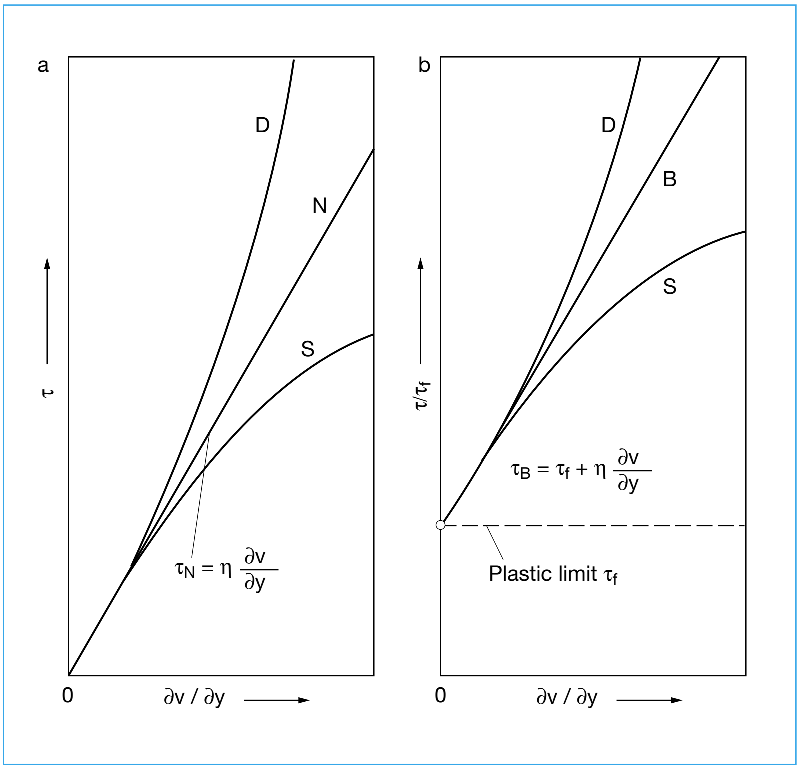

Fig. 45: Overview of the shear behaviour of viscous fluids
a without, b with a plastic shear limit τ_f
N Newtonian, B Bingham, S pseudo-plastic, D dilatant fluids

ships it is defined as the kinematic viscosity

$$\nu = \eta/\varrho \qquad (35)$$

where
ν Kinematic viscosity in m^2/s

η Dynamic viscosity in Pa s (= kg/sm)

ϱ Density in kg/m^3 (for numerical values see Fig. 48)

For water at 20°C, $\nu = 1.00 \cdot 10^{-6}\ m^2/s$. For further numerical values see Table 12. The units centistokes = mm^2/s, degrees Engler °E, Saybolt seconds S" (USA) and Redwood seconds R" (UK) are no longer used and can be converted to m^2/s using Fig. 46.

Independently of the discussion above, viscosity varies with temperature: at higher temperatures almost all liquids become "thinner"; their viscosity decreases (Figs. 47 and 48).

The dynamic viscosity η can be measured for all liquids using a rotating viscometer to determine the shear curve. A cylinder rotates with a freely chosen speed in a cylindrical container filled with the liquid in question. The required driving torque is measured at various speeds along with the peripheral speed, the size of the wetted area and the distance of the cylinder from the wall.

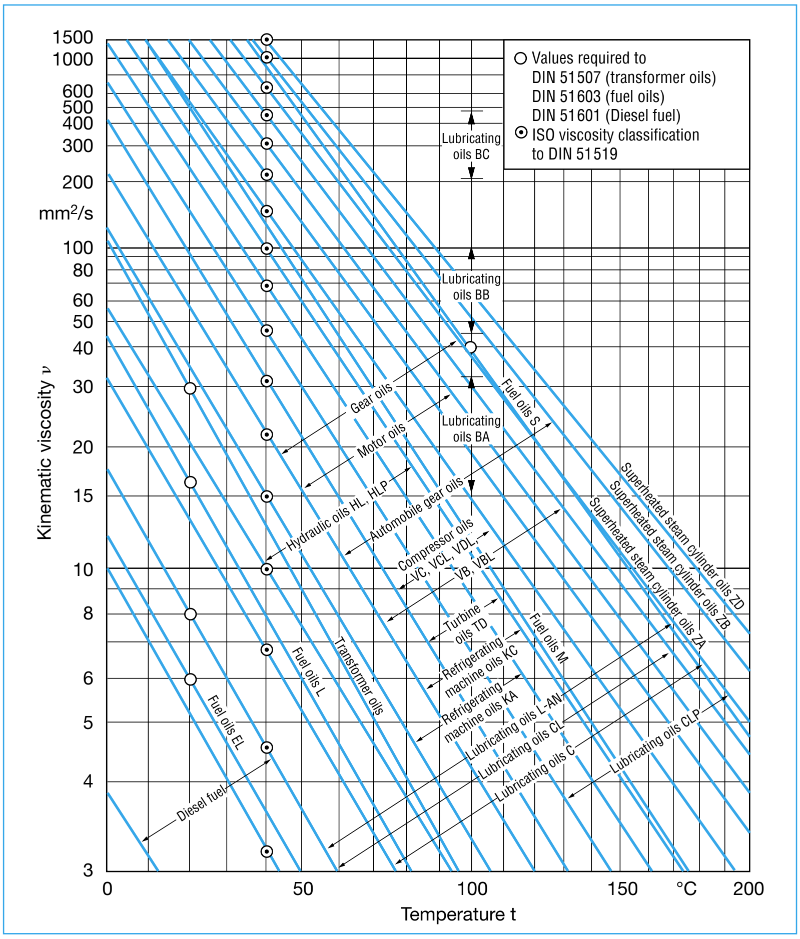

Fig. 47: Kinematic viscosity ν of various mineral oils as a function of the temperature (enlarged view on page 85)

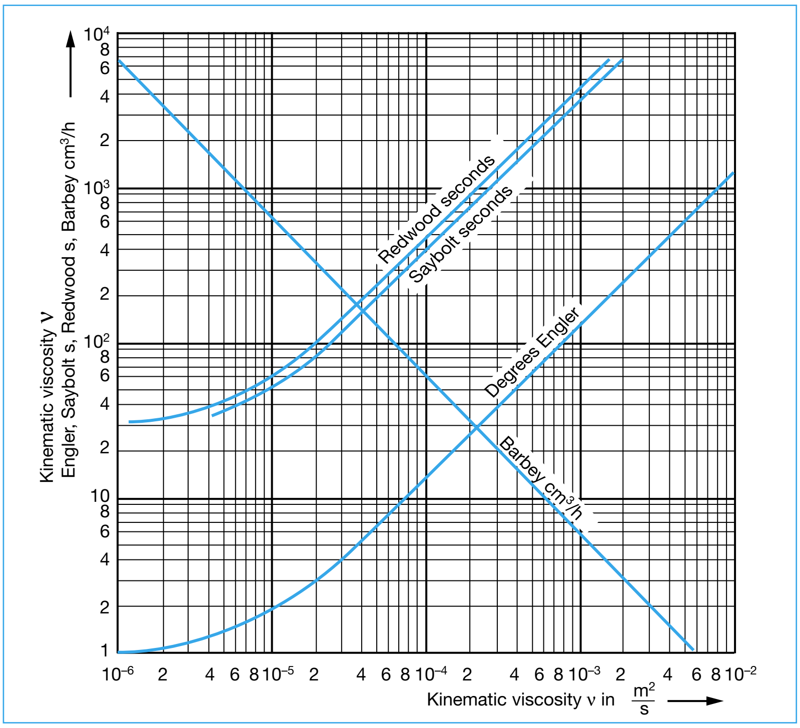

Fig. 46: Conversion between various units of kinematic viscosity ν

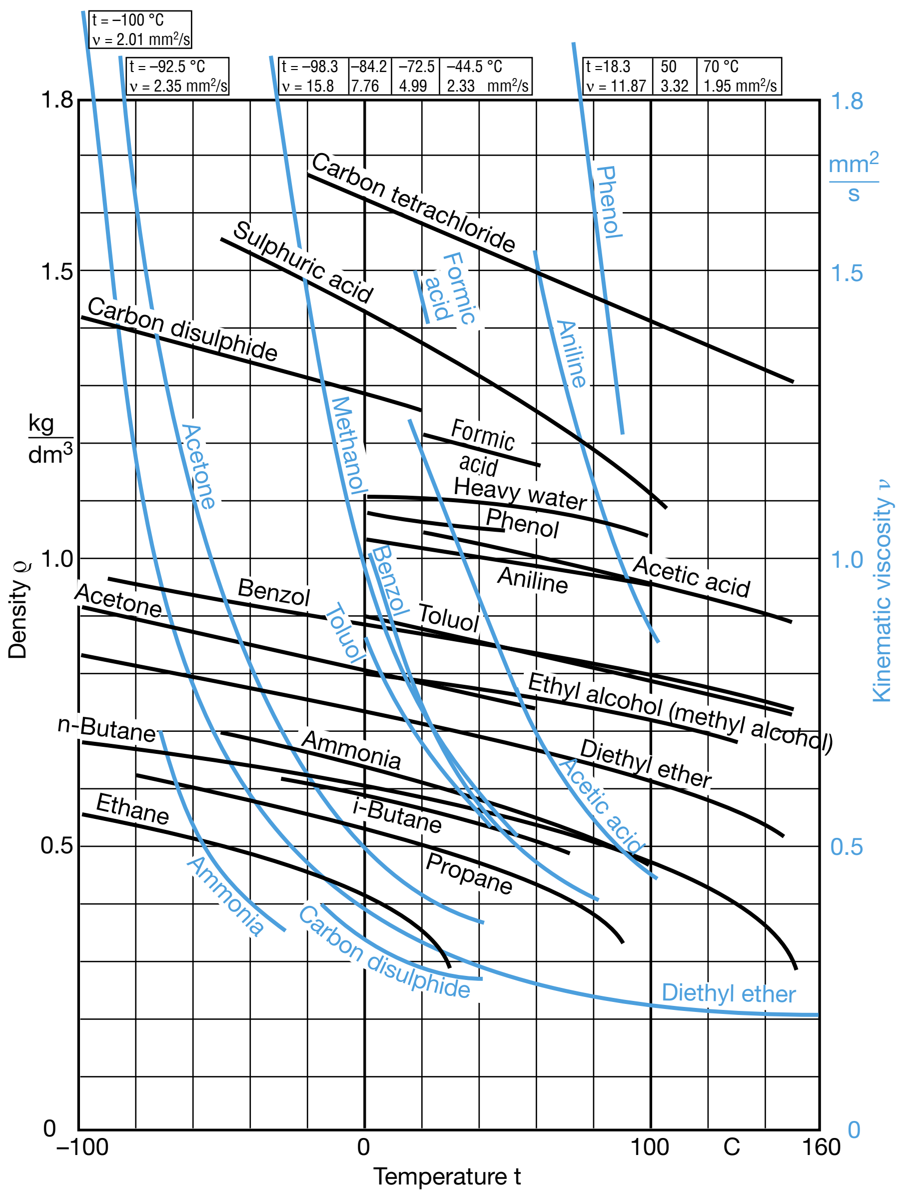

Fig. 48: Density ϱ and kinematic viscosity ν of various fluids as a function of the temperature t (enlarged view on p. 86)

4.2 Newtonian Fluids

4.2.1 Influence on the Pump Characteristics

The characteristic curves of a centrifugal pump (H, η and P as functions of Q) only start to change perceptibly at viscosities above $\nu > 20 \cdot 10^{-6}$ m²/s and only need to be corrected with empirical conversion factors above this limit. The **two most well known methods** are that described in the **Hydraulic Institute (HI) Standards** and that of **KSB.** Both methods use diagrams containing the conversion factors which are applied in a similar manner, but differ in that the KSB method not only includes the parameters Q, H and ν but also the significant influence of the specific speed n_q (see section 3.1.5). The HI method (Fig. 49) is based on measurements with n_q = 15 to 20 and gives the same numerical results as the KSB method (Fig. 50) in this narrow range. The KSB method is based on measurements with n_q from 6.5 to 45 and viscosity up to $\nu_z = 4000 \cdot 10^{-6}$ m²/s. The use of both diagrams is explained with the examples shown in them [9].

The flow rate Q, the total developed head H and the ef-

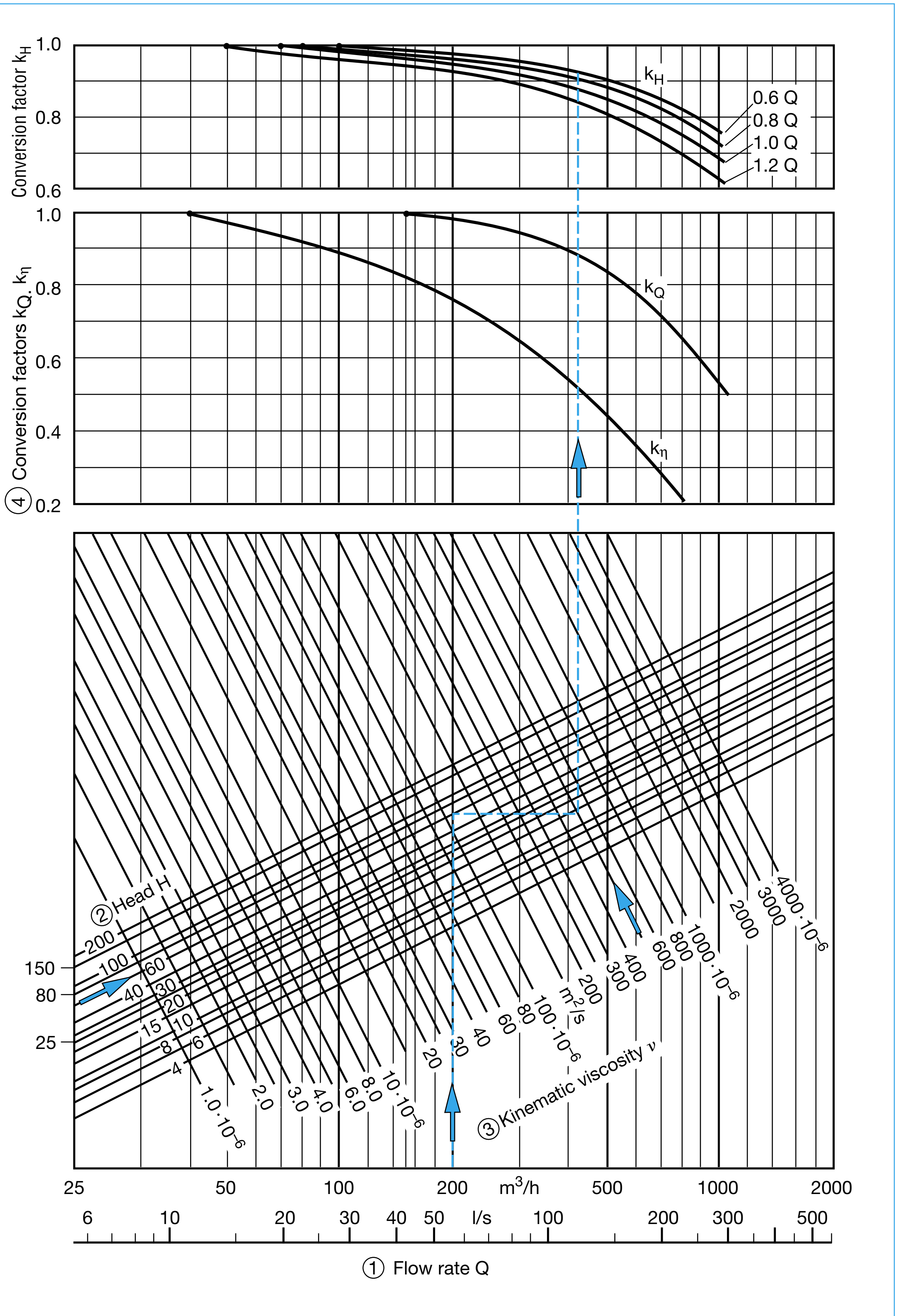

Fig. 49: Determination of the conversion factors k using the Hydraulic Institute method. Example shown for $Q = 200$ m³/h, $H = 57.5$ m, $\nu = 500 \cdot 10^{-6}$ m²/s

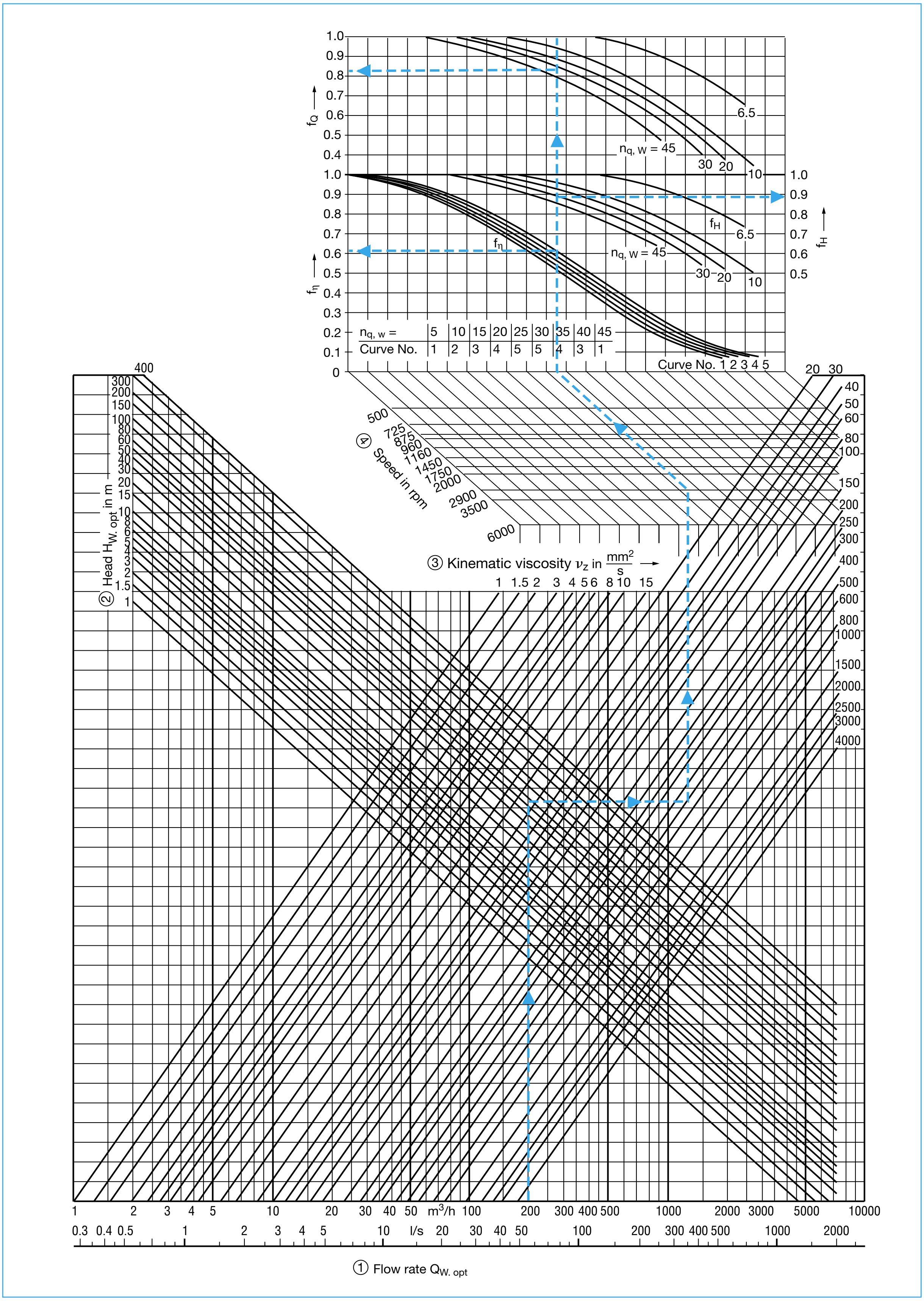

Fig. 50: Determination of the conversion factors f using the KSB method. Example shown for $Q = 200\ m^3/h$, $H = 57.5\ m$, $n = 1450\ rpm$, $\nu = 500 \cdot 10^{-6}\ m^2/s$, $n = 2900\ rpm$, $n_q = 32.8$

ficiency η, which are known for a single-stage centrifugal pump operating with water (subscript w), can be converted to the values for operation with a viscous medium (subscript z) as follows:

$$Q_z = f_Q \cdot Q_w \quad \textbf{(36)}$$

$$H_z = f_H \cdot H_w \quad \textbf{(37)}$$

$$\eta_z = f_\eta \cdot \eta_w \quad \textbf{(38)}$$

The factors f are designated with k in the HI method; both are shown graphically in Figs. 49 and 50. In Fig. 50 the speed of rotation n of the pump must be considered in the diagram and the specific speed n_q of the pump impeller must be known, for example from Fig. 3 or Eq. 3.

With these factors the known performance for water can be converted to reflect operation with a viscous fluid. The conversion is valid for the range

$$0.8\ Q_{opt} < Q < 1.2\ Q_{opt} \quad (39)$$

A simple calculation can thus be done for three flow rates, with a single exception:

At $Q = 0.8\ Q_{opt}$, $H_z = 1.03 \cdot f_H \cdot H_w$ applies (but H_z never is $> H_w$!).

At flow rate Q = 0, simply set $H_z = H_w$ and $\eta_z = \eta_w = 0$. A worksheet or spreadsheet calculation as shown in Fig. 51 can simplify the conversion.

After the power is calculated at the three flow rates (in the flow range according to Eq. 39) using

How to Find the Operating Point

Given:

Flow rate	Q_w		m^3/h
Total developed head	H_w		m
Speed of rotation	n		1/min
Kinematic viscosity	ν_z		m^2/s
Density	ϱ_z		kg/m^3
Gravitational constant	g	9.81	m/s^2

Calculation

Q/Q_{opt} =		0	0.8	1.0	1.2	–	
Q_w	from the pump characteristic for 4 points	0				m^3/h	
H_w						m	
η_w		0				–	
$n_{q,w}$	from section 3.1.5	–	–		–	1/min	
$f_{Q,w}$	from Fig. 50	–				–	
$f_{H,w}$		–				–	
$f_{\eta,w}$		–				–	
$Q_z = Q_w \cdot f_{Q,w}$		0				m^3/h	2)
H_z =		$= H_w$ ↓	$= H_w \cdot f_{H,w} \cdot 1{,}03$ ↓ 1)	$H_w \cdot f_{H,w}$ ↓	$H_w \cdot f_{H,w}$ ↓	m	2)
$\eta_z = \eta_w \cdot f_{\eta,w}$		0					2)
$P_z = \dfrac{\varrho_z \cdot g \cdot H_z \cdot Q_z}{\eta_z \cdot 1000 \cdot 3600}$		X				kW	2)

1) If H_z becomes larger than H_w, it should be set to H_w.

2) These are four values on the H_z/Q and Q/η_z curve and three points on the Q/P_z curve. Plot versus Q.

Fig. 51: Spreadsheet for calculating the pump characteristics for a viscous fluid using the KSB method (enlarged view on p. 87)

$$P_z = \varrho_z \cdot g \cdot H_z \cdot Q_z / 1000\ \eta_z \quad (40)$$

where

ϱ_z Density in kg/m^3
Q_z Flow rate in m^3/s
g Gravitational constant 9.81 m/s^2
H_z Total developed head in m
η_z Efficiency between 0 und 1
P_z Power in kW (!)

all the characteristic curves can be plotted over Q_z using the 3 or 4 calculated points, as shown in Fig. 52 on page 54.

For the inverse problem, i.e. when the operating point for the viscous fluid is known and the values for water are to be found (for example when choosing a suitable pump for the requested operating point), the water values are estimated and the solu-

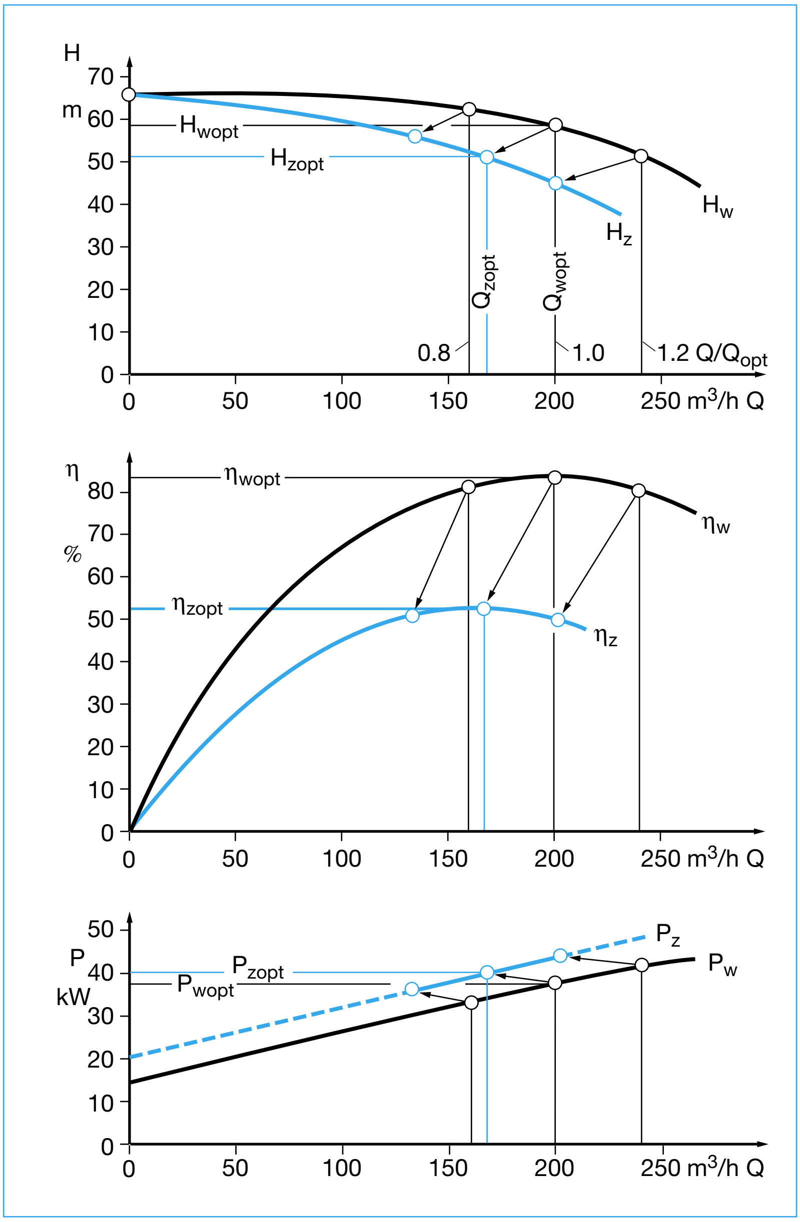

Fig. 52: Conversion of the pump characteristics for water to that for a viscous fluid

tion is approached iteratively using f_Q, f_H and f_η in two (or sometimes three) steps.

For specific speeds above $n_q \approx 20$ the more realistic KSB method results in smaller power requirements; below this limit the calculated required driving power according to HI is too small [9]!

4.2.2 Influence on the System Characteristics

Since the laws of fluid dynamics retain their validity for all Newtonian fluids, the equations and diagrams for calculating the pipe friction factor and the loss coefficients for valves and fittings are also applicable to viscous media. One must simply substitute the kinematic viscosity of the viscous liquid ν_z for the water viscosity ν_w when calculating the Reynolds number $Re = v \cdot d/\nu$. This yields a lower Reynolds number, and a larger friction factor λ_z results from Fig. 10. (Note: the influence of the wall roughness can now often be ignored because of the larger boundary layer thickness in the flow.) All of the pressure losses in the pipes, valves and fittings calculated for water in accordance with section 3.2.1.2 are to be increased by the ratio λ_z/λ_w.

Fig. 53 is also suitable for general practical use: the diagram provides a fast way of determining the pipe friction factor λ_z as a function of the flow rate Q, pipe inside diameter d and kinematic viscosity ν_z. It must be kept in mind, however, that the coefficient λ_w for water in this diagram is only valid for hydraulically smooth pipes (i.e. not for rough-surfaced pipes)! The corresponding λ_w can be used to calculate the ratio λ_z/λ_w.

Since the static component of the system characteristic curve H_{sys} (Fig. 16) is not affected by viscosity, the "dynamic" component of the system characteristic for water can be redrawn as a steeper parabola for a viscous fluid.

4.3 Non-Newtonian Fluids

4.3.1 Influence on the Pump Characteristics

Since the local velocity gradients in all the hydraulic components of a pump are not known, a cal-

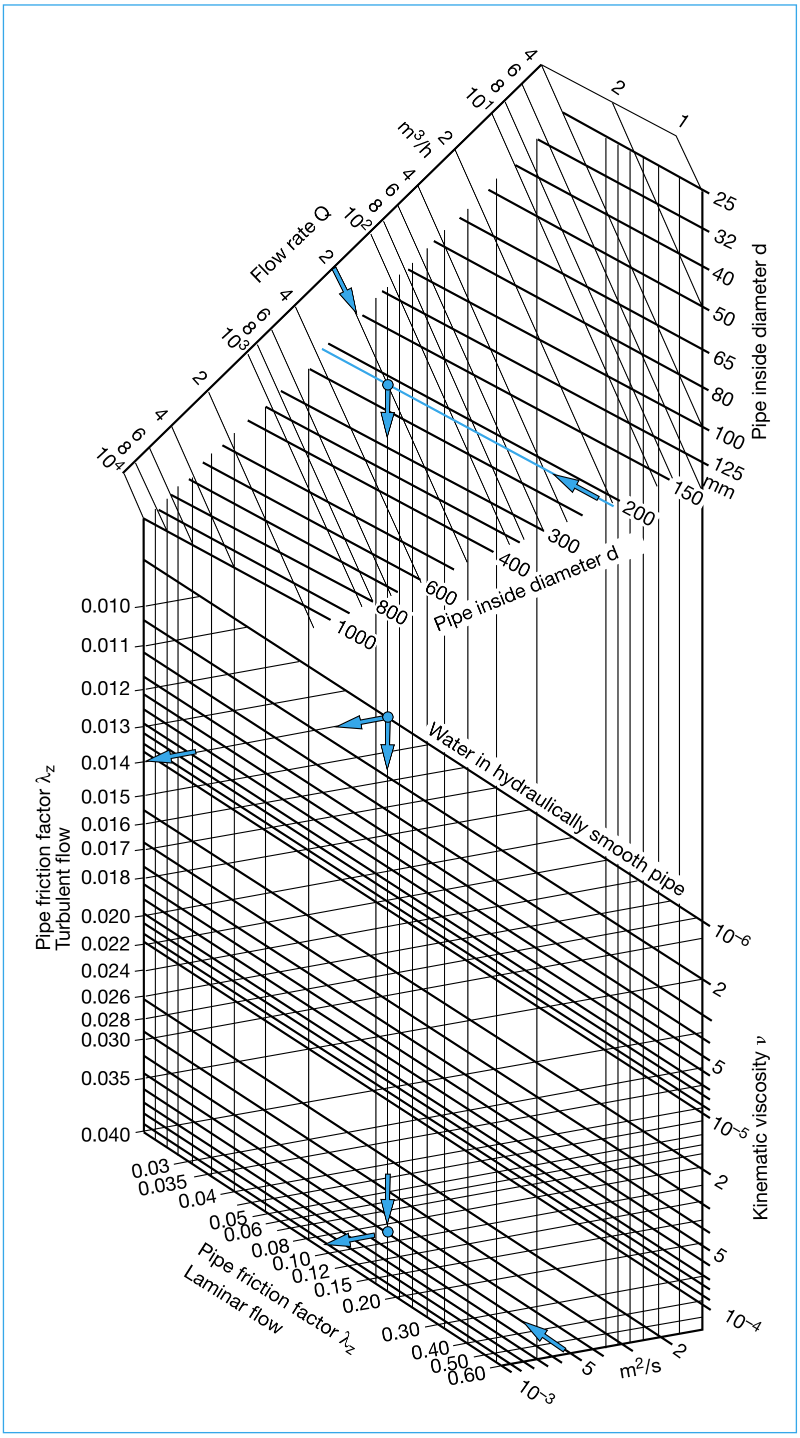

Fig. 53: Finding the pipe friction factor λ_z for viscous liquids
Example: $Q = 200\ m^3/h$; $d = 210\ mm$; $\nu_z = 5 \cdot 10^{-4}\ m^2/s$

culation of the influence of non-Newtonian fluids on the pump characteristics is not generally possible. Only for a limited number of special fluids, such as fibre pulp, is a prediction based on knowledge gained during years of experience with this fluid feasible. The selection of a suitable pump must therefore be done by the design department.

4.3.2 Influence on the System Characteristics

When the shear curves are not straight lines of constant linear viscosity, one must divide them into sections and determine the coefficient (= stiffness number) and the exponent n (= structural number) for each section individually (easiest when plotted on double-logarithmic scales). Using a special diagram (analogous to Fig. 10), which shows the pipe friction factors λ_z as a function of the generalized Reynolds number Re_n for various exponents n, the value of λ_z can be read and the system curve H_{sys} determined for a particular flow rate Q. Since this process is very laborious, in particular because of the need for multiple iterations, it cannot be recommended for general use.

Just as for the pump characteristics, in most cases diagrams with a narrow range of application based on experience with a particular fluid are used to find the head loss H_L. The more the application differs from the particular conditions of the diagram, the more uncertain will the head loss analysis become, so that in such cases the experience of the design department must be tapped.

5 Special Issues when Pumping Gas-laden Fluids

Unlike dissolved gases, a non-dissolved gas in a liquid (expressed as a volume percentage) can change the design parameters, the characteristic curve and the general performance of a centrifugal pump dramatically, as shown in Fig. 54 using a non-clogging impeller pump as an example. The gas content may be caused by the production process itself but also by leaking flanges or valve stems in the suction line or from air-entraining vortices in an open sump inlet when the water level is too low (see section 7.2).

In the centrifugal force field of an impeller, the gas bubbles tend to accumulate in certain locations and to disturb the flow there. This effect is reinforced

- the more the pump operates at a reduced flow rate, since the lower velocities exert less carrying force on the gas,
- the smaller the impeller inlet diameter is, since the throttling effect of the gas volume is increased,
- the lower the specific speed n_q of the pump impeller is, and
- the lower the speed of rotation of the pump is.

These effects cannot be calculated. When significant gas volumes are expected in the pumpage, the following measures can be useful:

- A sufficiently large settling tank in the suction line can allow the gas to separate out of the fluid and thus mitigate its disturbing effects.
- Pipes which are used to fill an open inlet sump must end below the liquid level so that there is no free fall of water that might entrain air bubbles in the tank. In addition, a baffle can prevent the entry of vortices in the suction piping (see Figs. 64 and 65).
- Low-flow operation of the main pump can be prevented by installing a special part-load pump. When this pump is only needed occasionally, it is advantageous to use a self-priming pump (whose efficiency is lower, though).
- A gas removal line in front of the impeller hub requires a vacuum system, is only of limited use for large gas quantities and disturbs the normal operation of the pump.
- In the pump, open impellers (see Fig. 4) with few vanes are advantageous, as is the installation of an inducer (Fig. 41). Without any special precautions, non-clogging impeller pumps (Fig. 43) can pump up to 3%$_{vol}$ and free flow impellers up to 6 to 7%$_{vol}$ of gas.
- If a large gas content is to be expected under normal operating conditions, side channel pumps or water-ring pumps (positive displacement principle) operate more reliably.

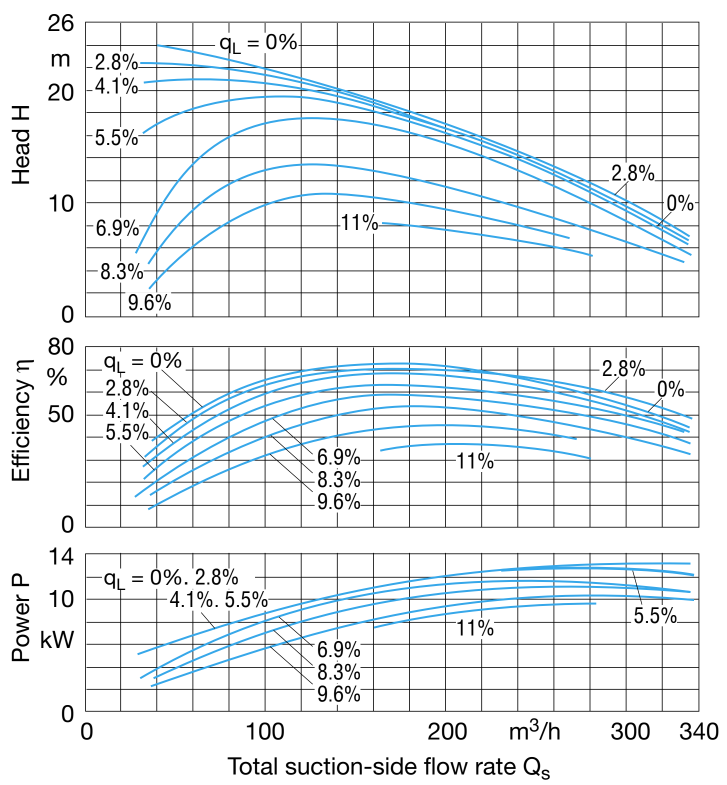

Fig. 54: Influence of non-dissolved air on the operation of a non-clogging impeller pump when pumping pre-treated sewage (open three-channel impeller, D = 250 mm, n = 1450 rpm, n_q = 37)
q_{air} = Gas volume in suction piping as % of the mixture.

6 Special Issues When Pumping Solids-laden Fluids

6.1 Settling Speed

Solids (which are heavier than water) are most easiest to pump when their settling speed is lowest and their flow velocity highest. Because of the large number of influencing parameters, the settling speed can only be calculated based on simplifying assumptions: the settling speed of a single sphere in an unlimited space (subscript 0) results from force equilibrium as

$$w_{s0} = \sqrt{\frac{4\,g\,d_s}{3\,c_D} \cdot \frac{\varrho_s - \varrho_f}{\varrho_f}} \qquad (41)$$

where

- w_{s0} Settling speed in m/s
- g Gravitational constant 9.81 m/s
- d_s Diameter of sphere in m
- c_D Resistance coefficient of the sphere dependent on Re_s
- ϱ_s Density of the solid in kg/m^3
- ϱ_f Density of the fluid in kg/m^3

$$Re_s = w_{s0} \cdot d_s/\nu_f \qquad (42)$$

where

- ν_f Kinematic viscosity of the liquid in Pa s

The settling speed w_{s0} is shown graphically in Fig. 55.

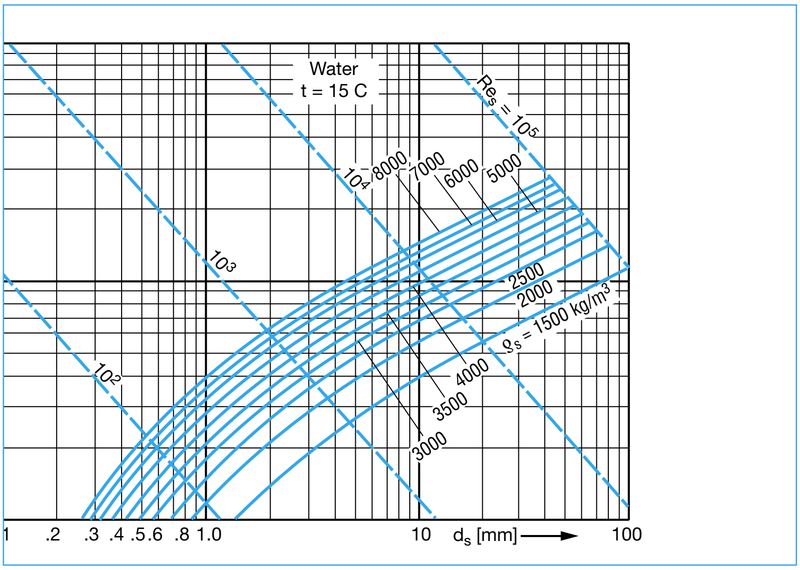

Fig. 55: Settling speed w_{s0} of individual spherical particles (spherical diameter d_s) in still water

The solids concentration:

$$c_T = Q_s/(Q_s + Q_f) \qquad (43)$$

has a large effect, where

- c_T Flow-based solids concentration (transport concentration)
- Q_s Flow rate of the solid in m^3/s
- Q_f Flow rate of the fluid in m^3/s

The solids concentration and the boundary effect of the pipe walls reduce the settling speed considerably because of the mutual repulsion of the particles, approximately according to the following empirical relationship

$$w_s = w_{s0} \cdot (1 - c_T)^5 \qquad (44)$$

The effect of an irregular particle shape cannot be estimated; the shape may differ substantially from that of a sphere.

The effect of the particle size distribution can also hardly be calculated. Fig. 56 shows an example of the distribution of

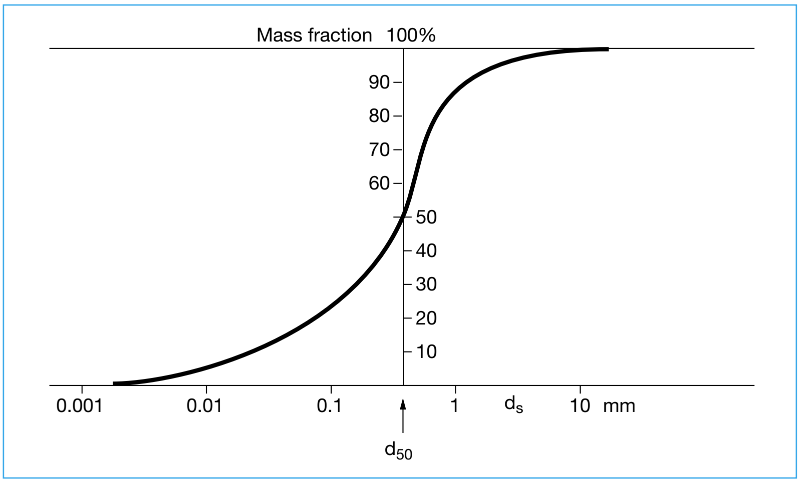

Fig. 56: Example of a particle size distribution

particle sizes d_s plotted logarithmically for the portion which passed through a sieve of a given mesh size. Transported solids are almost always composed of particles of various sizes, so that the size distribution has a more or less distinct S-shape. To simplify the analysis, it can be assumed that the particle size for 50% mass fraction, designated d_{50}, is representative of the mixture. This assumption is the most important source of disparities in the planning phase.

After all these assumptions and gross approximations, no exact predictions of the effects of solids on the flow behaviour, the system curve, the total developed head and the efficiency of pumps are to be expected. The design and selection of pumps for solids transport must therefore be left to experts who have sufficient experience with similar cases. Even then, experiments are often necessary to attain a measure of certainty. Only certain general tendencies can be stated.

6.2 Influence on the Pump Characteristics

The solids behave differently under the influence of the centrifugal force field in an impeller than the carrier fluid (usually water) does. The solids cross the streamlines or collide with and rub against the walls of the flow passages. They thus reduce the head H produced in the impeller by the difference ΔH.

Experimental data exist on the effects of the particle diameter d_s, the concentration c_T and the density ϱ_s of the solids as well as the specific speed n_q. The empirical relationship for the relative head reduction ΔH/H is approximately

$$\Delta H/H = c_T / \psi \cdot \sqrt[3]{Re_s} \cdot (11.83/n_q)^3 \cdot (\varrho_s/\varrho_f - 1) \qquad \textbf{(45)}$$

where

- c_T Transport concentration according to Eq. 43
- ψ Head coefficient of the pump; here approx. = 1
- Re_s Reynolds number of the solids flow according to Eq. 42
- n_q Specific speed of the pump according to Eq. 3
- ϱ_s Density of the solid in kg/m^3
- ϱ_f Density of the fluid in kg/m^3

When conveying solids hydraulically, the pump characteristic curve needs to be shown as developed pressure Δp versus flow rate Q, not as developed head H, since the average density ϱ_m of the solids / water mixture (in contrast to pumping clean water) is not constant. As simplifications, the geodetic head difference $z_{s,d}$ between the pump inlet and discharge as well as the velocity head difference $(c_d^2 - c_s^2)/2\,g$ are ignored, i.e., the static head is set to equal the total head ($H_p \approx H$):

$$\Delta p = \varrho_m \cdot g \cdot (H - \Delta H) \qquad \textbf{(46)}$$

where

- ϱ_m Average density of the solids/ water mixture given by Eq. 47 in kg/m^3
- g Gravitational constant 9.81 m/s^2
- H Total developed head in m
- ΔH Head reduction according to Eq. 45 in m
- Δp Pressure in N/m^2 (to convert to bar: 1 bar = 100 000 N/m^2)

The average density of the mixture is given by

$$\varrho_m = c_T \cdot \varrho_s + (1 - c_T) \cdot \varrho_w \qquad \textbf{(47)}$$

where

- ϱ_m Average density in kg/m^3
- ϱ_s Density of the solid in kg/m^3
- ϱ_w Density of water in kg/m^3
- c_T Transport concentration according to Eq. 43

Since the pressure rise in the pump is the product of the density and the developed head (which is reduced when transporting solids), two independent influences are at work in Eq. 46: the increased average density due to the presence of the solids, and the reduced developed head (H – ΔH). Both changes are caused by the solids concentration, but they have opposite effects, since the density raises the pressure while the head deficit decreases it. Therefore, no general prediction can be made as to whether the pump pressure rise will be higher or lower than the water curve when the solids concentration increases. Heavy, small-grained solids (for example ores) are likely to produce an increase, while light, large solids (for example coal) and low specific speeds tend to decrease the pressure.

6.3 Influence on the System Characteristics

When the flow velocity drops, solids tend to settle to the bottom of horizontal pipe runs and collect on the pipe wall. The flow resistance increases and the free flow passage becomes smaller, so that despite the decreasing flow rate, the flow resistance can actually increase. This results in the unusual shape of the system curves as shown in Fig. 57. The minimum in the curves measured at various concentrations is a sure sign that a solids accumulation is taking place and that the pipes will soon be clogged. The curve minimum is therefore generally considered to be the lower limit of operation. Exact predictions are only possible with sufficient experience or by experiment.

6.4 Operating Performance

Fig. 57 shows the typical behaviour of a centrifugal pump transporting solids through a horizontal pipe: with increasing concentration, the intersection of the pump and system characteristic curves shifts to ever lower flow rates, so that the lower limit of operation could be exceeded. To avoid this, a control system must intervene promptly. Throttle valves would be subject to high wear, however, so only a change of rotational speed remains as a feasible control method for the hydraulic transport of solids. Speed control has an additional advantage: when the head developed by the pump impeller drops as the impeller wears, it is possible to compensate by merely increasing the speed.

In vertical pipes, the settling of the solids poses much greater risk, since the pipe can suddenly become plugged if the flow falls below the minimum required, even if only due to stopping the pump.

The high erosion rates when pumping granular solids are the decisive parameter for the design of the pumps used. An example of their typical robust design is shown in Fig. 58. The risk of erosion also limits the permissible operating range to near Q_{opt}.

High solids concentrations put constraints on the use of centrifugal pumps; the limit values can only be found by experience.

The above considerations should have convinced the reader that the selection of pumps for hydraulic solids transport is risky without a solid base of experience and should be left to experts who do this frequently!

6.5 Stringy, Fibrous Solids

If long, stringy solids are present in the flow, problems can occur, in particular for axial flow (propeller) pumps, when these materials (plant fibres, plastic sheets and rags for example) are caught on the propeller blade leading edge and accumulate

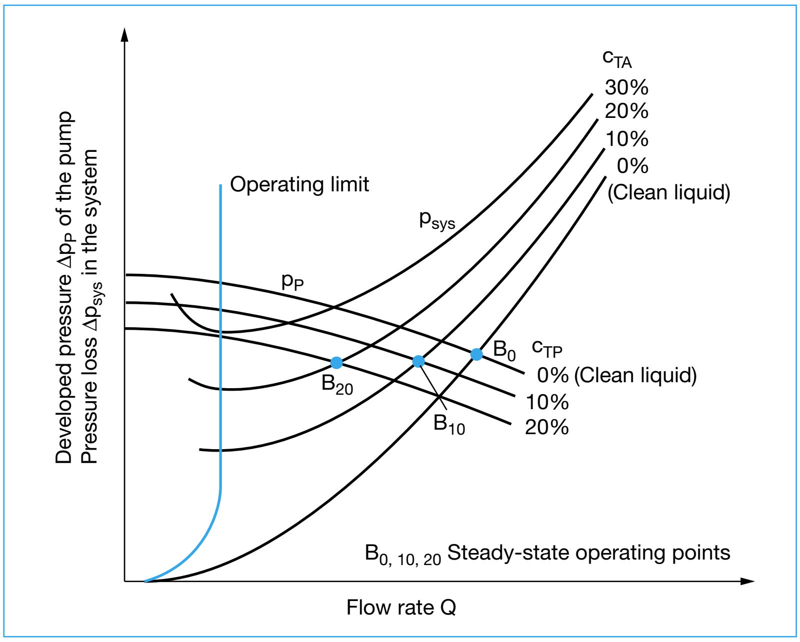

Fig. 57: Pressure developed by the pump Δp_P and pressure losses of the system Δp_{sys} for various solids concentrations (concentrations c_{Tsys}, c_{TP}) of the flow Q. The developed pressure $\Delta p_P = f(c_T)$ can also increase with increasing concentration c_{TP} for solids with high density (here shown decreasing for 10 and 20%).

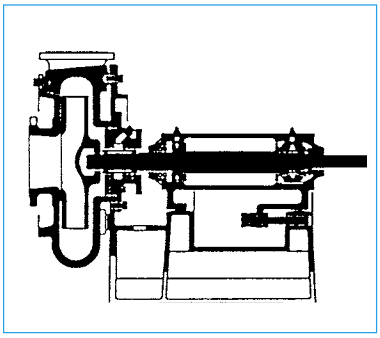

Fig. 58: Typical centrifugal pump for the hydraulic transport of solids

there. The consequences are an increasing head loss and power input, which continue until the driving motor must be stopped due to overloading.

The problem can be solved by slanting the leading edges of the propeller blades backwards by shifting the individual profile planes during blade design, just as for a backswept airfoil. During operation, the fibres can slide along the blade leading edge until they are shredded in the clearance gap at the outside diameter of the propeller and flushed out. These self-cleaning blades are called "ECBs" (= ever clean blades) [5].

Untreated municipal sewage often contains textiles which tend to form braids and plug impellers with multiple vanes or other flow-dividing devices. Single vane impellers, worm type (screw) impellers, or free flow impellers (see Fig. 43) are the better choice for these applications.

Figs. 59 a to o: Typical installation arrangements

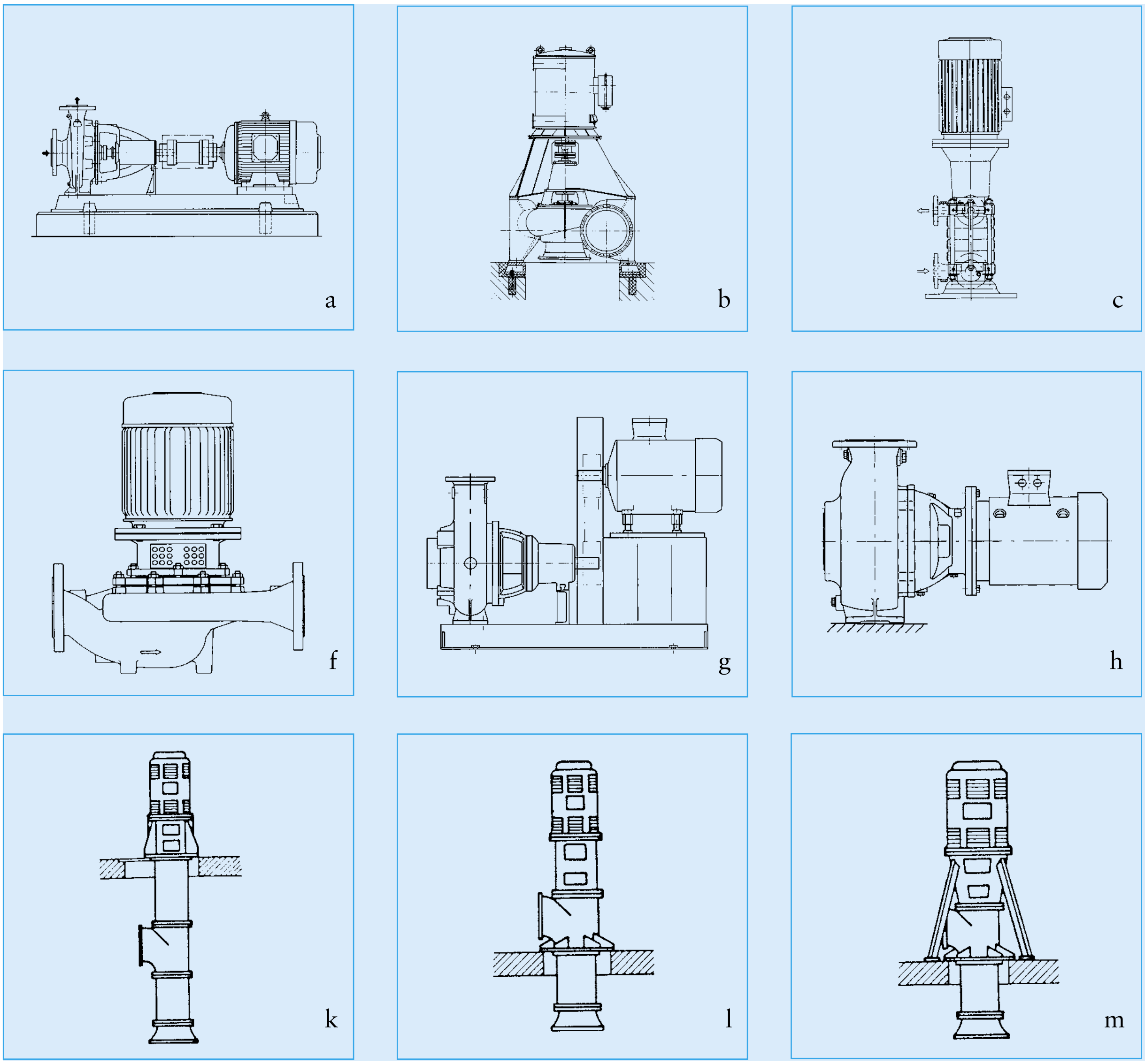

7 The Periphery

7.1 Pump Installation Arrangements

Pump installation arrangements are design features in which pumps of the same type (in general of the same series) may differ. Figures 59 a to o provide typical examples of the most frequent installation arrangements for horizontal and vertical centrifugal pumps [1].

The major parameters classifying the pump installation arrangement are:

- the position of the shaft, i. e. horizontal or vertical (see Figs. a and b, also i and c or h and f),
- the arrangement of the feet, i. e. underneath or shaft centreline (see Figs. d and e),
- the mode of installation of the pump set, i. e. with or without foundation (see Figs. b and f),
- the arrangement of the drive, i. e. on its own or a common baseplate or flanged to the pump (see Figs. g, a, h and i),
- the weight distribution of the pump and drive,

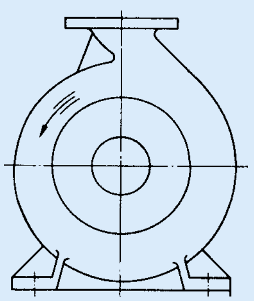
d

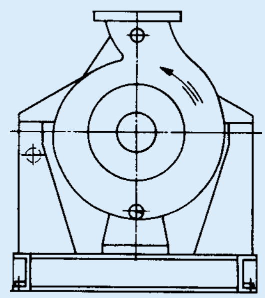
e

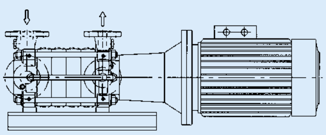
i

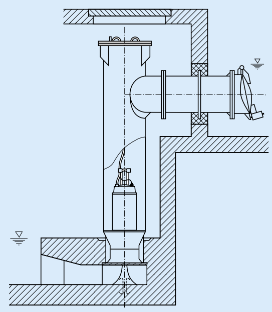
j

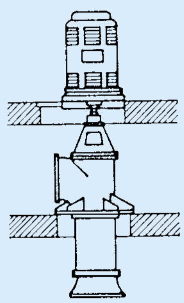
n

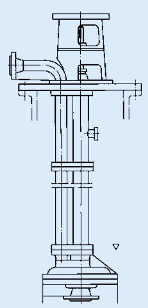
o

- the arrangement of the discharge nozzle on tubular casing pumps (see Figs. k, l, m and n),
- the environment of the pump casing, i. e. dry or wet (see Figs. b and o).

7.2 Pump Intake Structures

7.2.1 Pump Sump

Pump sumps (or suction tanks) are designed to collect liquids and be intermittently drained if the mean inlet flow is smaller than the pump flow rate. The sump or tank size depends on the pump flow rate Q and the permissible frequency of starts Z of the electric motors, see section 3.3.3.1.

The useful volume V_N of the pump sump is calculated using:

$$V_N = Q_{in} \cdot \frac{Q_m - Q_{in}}{Q_m \cdot Z} \qquad \textbf{(48)}$$

where

- Z Max. permissible frequency of starts per hour
- Q_{in} Inlet flow in m^3/h
- Q_m $= (Q_{on} + Q_{off}) / 2$
- Q_{on} Flow rate at switch-on pressure in m^3/h
- Q_{off} Flow rate at switch-off pressure in m^3/h
- V_N Useful volume of pump sump including potential backwash volume in m^3

The maximum frequency of starts occurs when the flow rate Q_m is twice the incoming flow Q_{in}. The max. frequency of starts per hour is therefore:

$$Z_{max} = Q_m/4V_N \qquad \textbf{(49)}$$

With dirty liquids, solids must be prevented from being deposited and collecting in dead zones and on the floor. Walls arranged at a 45°, or better still 60° angle, help prevent this (Fig. 60).

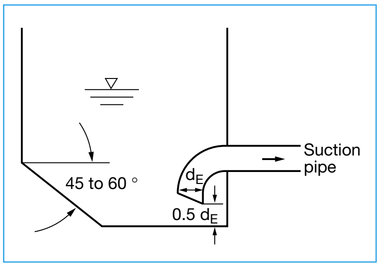

Fig. 60: Inclined sump walls to prevent deposits and accumulation of solids

7.2.2
Suction Piping

The suction pipe should be as short as possible and run with a gentle ascending slope towards the pump. Where necessary, eccentric suction piping as shown in Fig. 61 should be provided (with a sufficient straight length of pipe upstream of the pump $L \geq d$) to prevent the formation of air pockets. If, on account of the site conditions, fitting an elbow immediately upstream of the pump cannot be avoided, an accelerating elbow (Fig. 62) helps to achieve a smooth flow. For the same reason, an elbow with multiple turning vanes (see Fig. 63) is required in front of double-entry pumps or pumps with mixed flow (or axial flow) impellers unless this is impossible because of the nature of the medium handled (no stringy, fibrous solids, see 6.5).

The suction and inlet pipes in the suction tank or pump sump must be sufficiently wide apart to prevent air from being entrained in the suction pipe; positive deflectors (Figs. 64 and 65) should be provided, if required. The mouth of the inlet pipe must always lie below the liquid level, see Fig. 65.

If the suction pipe in the tank or pump sump is not submerged adequately because the liquid level is too low, rotation of the medium might cause an air-entraining vortex (hollow vortex) to develop. Starting as a funnel-shaped depression at the surface, a tube-shaped air cavity forms within a short period of time, extending from the surface to the suction pipe. This will cause the pump to run very unsteadily and the output to decrease. The required minimum submergence (minimum depth

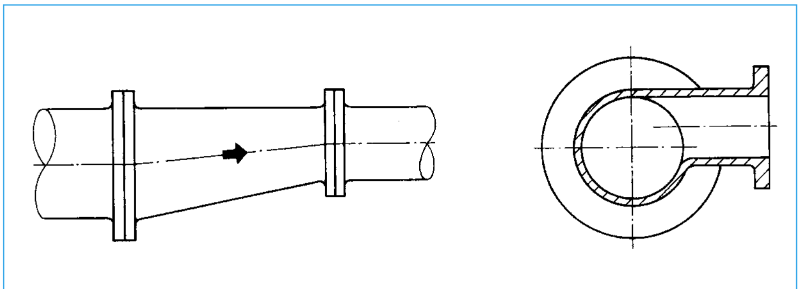

Fig. 61: Eccentric reducer and branch fitting to avoid air pockets

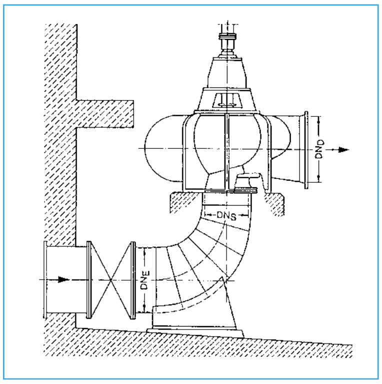

Fig. 62: Flow-accelerating elbow upstream of a vertical volute casing pump with high specific speed

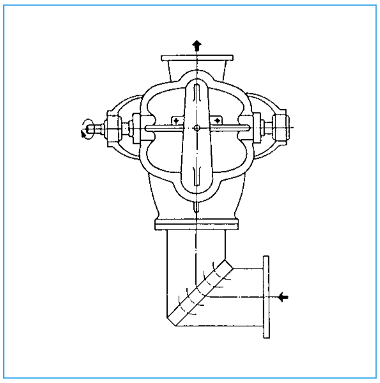

Fig. 63: Intake elbow with multiple turning vanes upstream of a double-entry, horizontal volute casing pump (plan view)

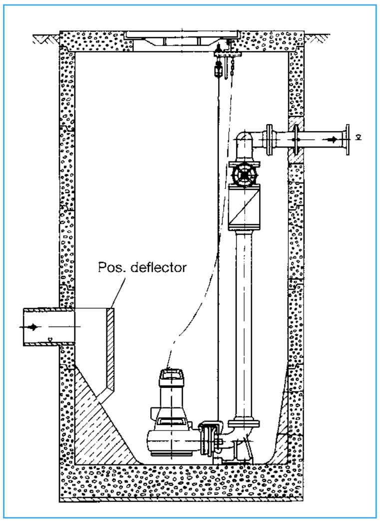

Fig. 64: Installation of a positive deflector in the intake chamber of a submersible motor pump

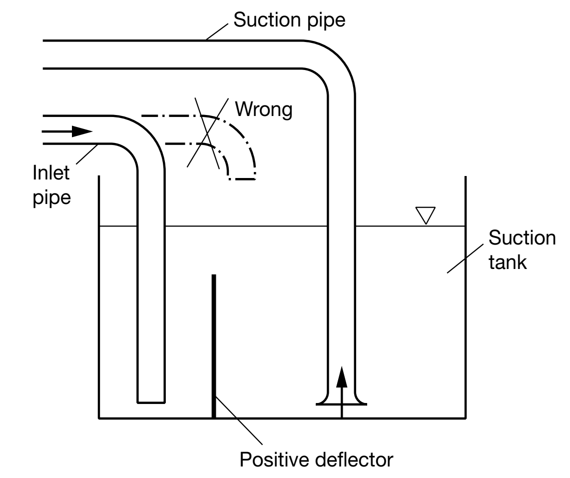

Fig. 65: Piping arrangement in the suction tank / pump sump to prevent air entrainment

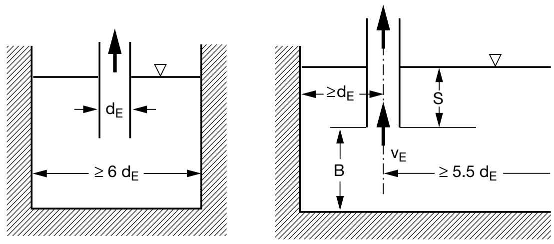

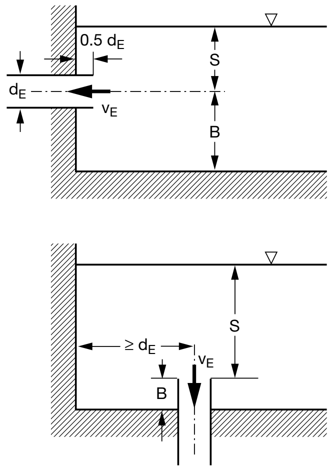

DN	B mm
65	80
80	80
100	100
150	100
200	150
250	150
300	200
400	200
500	200

Fig. 66: Clearances between wall and suction pipe in the suction tank or pump sump according to relevant German regulations. S_{min}, as shown in Fig. 67. 2 suction pipes arranged side by side require a distance of ≥ 6 d_E.

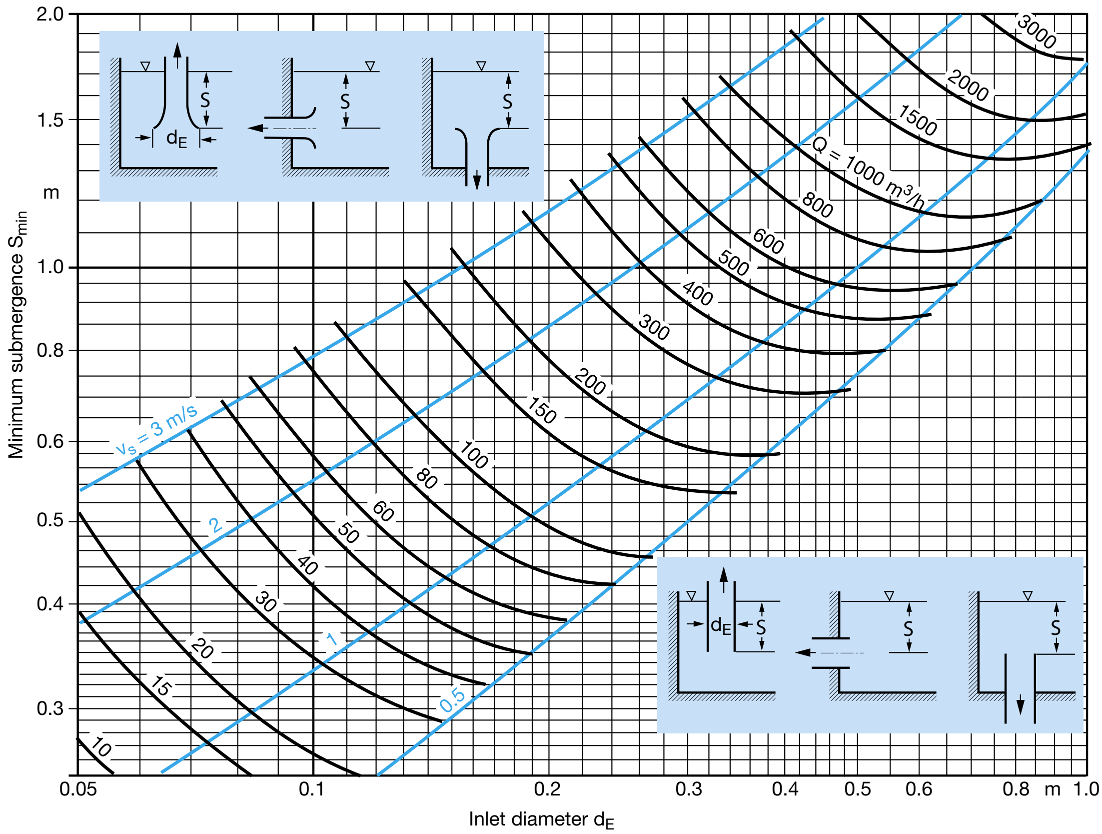

Fig. 67: Minimum submergence S_{min} of horizontal and vertical suction pipes (with and without entry nozzle) required for suction tanks to avoid hollow vortices (to Hydraulic Institute standards)

of immersion) is specified in Fig. 67, the minimum clearance between suction pipes and walls / sump floor in Fig. 66. (Special measures must be taken for tubular casing pumps, see 7.2.3).

The minimum submergence S_{min} can be read from Fig. 67 as a function of the intake diameter d_E (this is the pipe inside diameter of straight, flangeless pipes) or, where available, the inlet diameter of the entry nozzle and the flow rate Q. It can also be calculated according to the following equation given by the **Hydraulic Institute:**

$$S_{min} = d_E + 2.3 \cdot v_s \cdot \sqrt{\frac{d_E}{g}} \quad (50)$$

where

S_{min} Minimum submergence in m

v_s Flow velocity $= Q/900\,\pi\,d_E^2$ in m/s, recommended 1 to 2 m/s but never exceeding 3 m/s

Q Flow rate in m^3/h

g Gravitational constant 9.81 m/s^2

d_E Inlet diameter of suction pipe or entry nozzle in m

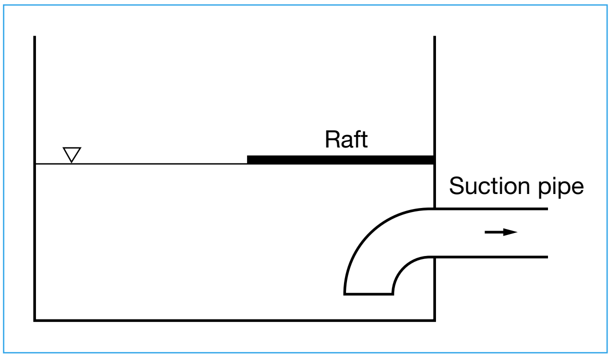

Fig. 68: Raft to prevent air-entraining hollow vortices

At flow velocities of 1 m/s, the minimum submergence levels specified by the relevant German regulations agree well with the data given above [13].

Wherever the required minimum submergence cannot or not always be ensured, measures as shown in Figs. 68 and 69 have to be taken to prevent air-entraining vortices. Irrespective of the aspects mentioned before, it should be checked whether the submergence levels also meet the $NPSH_a$ requirements laid down in 3.5.2.

Round tanks with tangential inlet pipes are special cases but used frequently. The liquid discharged via the inlet pipe causes the contents of the tank to rotate. For this reason baffles as illustrated in Fig. 70 should be provided.

7.2.3 Intake Structures for Tubular Casing Pumps [1]

For tubular casing pumps, the minimum submergence and the design of the intake chamber are of particular importance because impellers with high specific speeds react very sensitively to uneven inlet flows and air-entraining vortices.

Fig. 71 shows the arrangement of suction pipes in intake chambers of tubular casing pumps.

Refer to Fig. 72 for the minimum water level required for open, unlined intake chambers

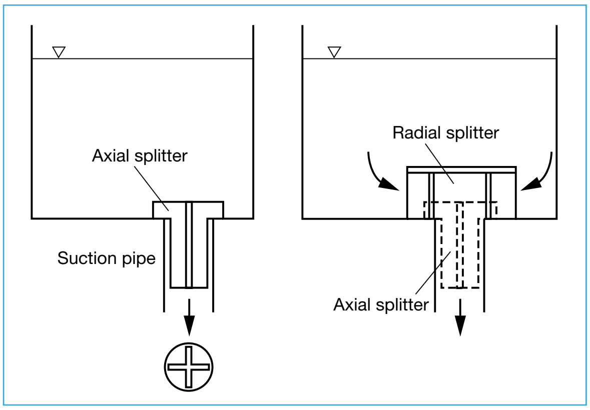

Fig. 69: Use of swirl preventers

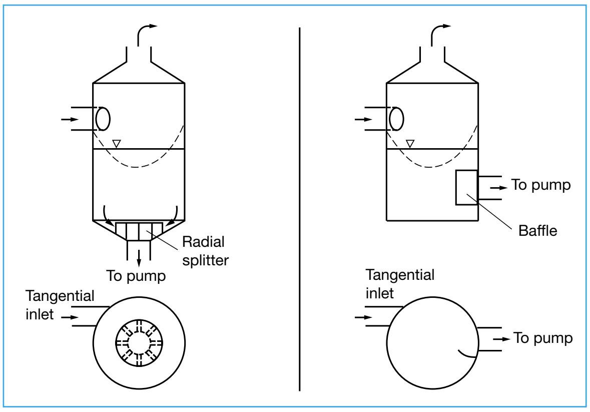

Fig. 70: Use of swirl preventers in cylindrical tanks to ensure smooth flow to pump

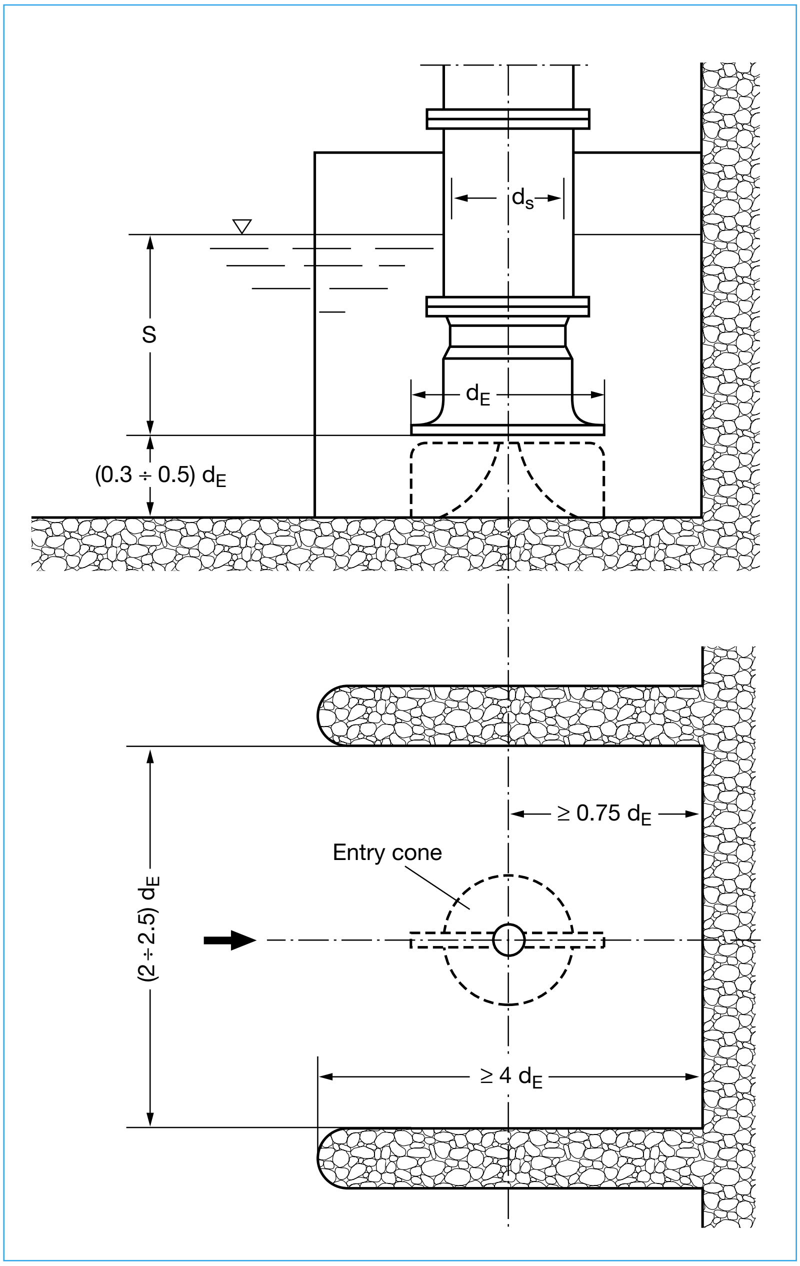

Fig. 71: Suction pipe arrangement in intake chambers of tubular casing pumps. S_{min} as shown in Fig. 72
$d_E \approx (1.5 \div 1.65)\ ds$
2 suction pipes arranged side by side require a distance of > 3 d_E

with and without entry cones or calculate it using the following equation:

$$S_{min} = 0.8\ d_E + 1.38 \cdot v_s \cdot \sqrt{\frac{d_E}{g}} \quad (51)$$

where
S_{min} Minimum submergence in m
v_s Flow velocity $= Q / 900\ \pi\ d_E^2$ in m/s
Q Flow rate in m^3/h
g Gravitational constant 9.81 m/s^2
d_E Inlet diameter of bellmouth in m

Lined or covered intake chambers or Kaplan intake elbows are more expensive, but allow pump operation at lower submergence levels [1].

Irrespective of the aspects mentioned before, it should be checked whether the submergence levels also meet the $NPSH_a$ requirements laid down in 3.5.2.

7.2.4 Priming Devices

Most centrifugal pumps are not self-priming; i. e. their suction pipes and suction-side casings must be deaerated prior to start-up unless the impeller is arranged below the liquid level. This often inconvenient procedure can be avoided by installing a foot valve (functioning as a non-return valve) at the suction pipe mouth (Fig. 73). Deaerating is then only necessary prior to commissioning and after a long period of standstill.

A closed suction tank (static tank) serves the same purpose, in particular when contaminated liquids are handled (it does, however, increase the flow losses and therefore reduces the $NPSH_a$). The tank is under negative pressure and mounted upstream of the pump suction nozzle (Fig. 74). Prior to commissioning it must be filled with liquid. When the pump is started up, it empties the tank, and the air in the suction or siphon pipe is drawn into the suction tank across the apex until the liquid to be pumped follows. After the pump has been stopped, the tank is refilled with liquid via the discharge pipe either manually or automatically. The air stored in the tank escapes into the suction pipe.

The suction tank volume V_B depends on the suction pipe volume and the suction lift capacity of the pump:

$$V_B = d_s^2 \frac{\pi}{4} \cdot L_s \cdot \frac{p_b}{p_b - \varrho g H_s} \tag{52}$$

where

V_B Suction tank volume in m^3

d_s Inside diameter of the air-filled inlet pipe in m

L_s Straight length of air-filled piping in m

p_b Atmospheric pressure in Pa (≈ 1 bar = 100 000 Pa)

ϱ Density of the liquid handled in kg/m^3

g Gravitational constant $9.81\ m/s^2$

H_s Suction lift of pump in m according to equation

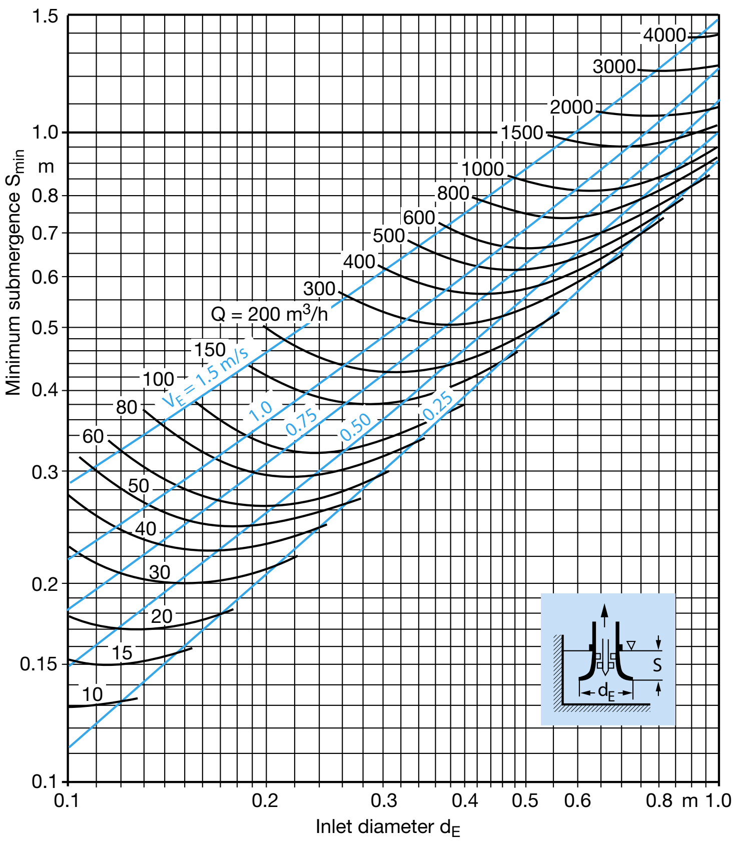

Fig. 72: Minimum submergence S_{min} of tubular casing pump suction pipe to avoid hollow vortices

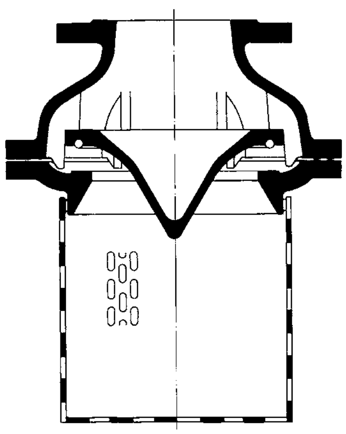

Fig. 73: Foot valve (cup valve) with suction strainer

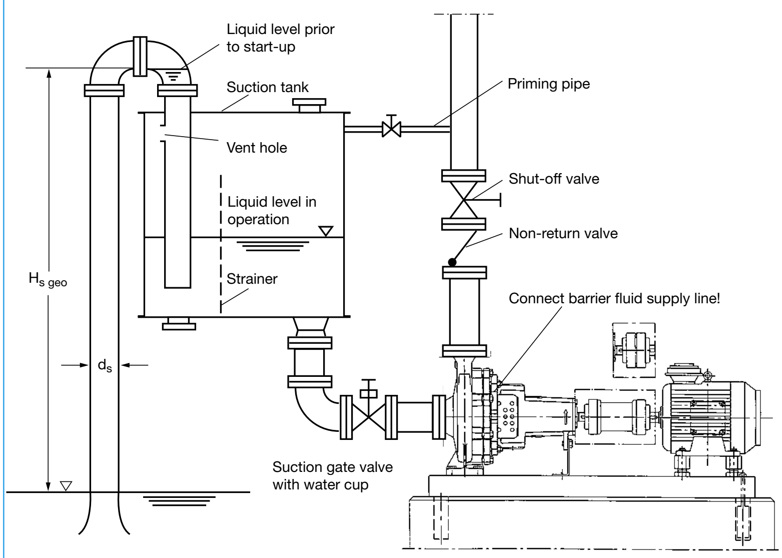

Fig. 74: Suction tank arrangement

$$H_s = H_{s\,geo} + H_{L,s} \qquad (53)$$

where

$H_{s\,geo}$ Vertical distance between water level and pump reference plane for suction lift operation in m, see Fig. 36

$H_{L,s}$ Head loss in the suction piping in m (refer to 3.2.1.1).

As $H_{L,s}$ is in most cases notably smaller than $H_{s\,geo}$, Eq. 53 can be neglected and H_s equated with $H_{s\,geo}$. In this case, Fig. 75 provides a much faster way of finding the required tank size.

For safety reasons the suction tank volume should be multiplied by a factor of 2 to 2.5, or by a factor of up to 3 in the case of smaller pumping stations. The liquid pressure must never reach its specific vaporization pressure at any point in the system.

7.3 Arrangement of Measurement Points

In order to achieve a certain accuracy in pressure and velocity measurement, the flow must be smooth and regular at the measuring points. Therefore, undisturbed straight lengths of piping need to be arranged upstream and downstream of the measurement point(s), as shown in Fig. 76 and indicated in Table 14. All pipe components which may impede a straight, parallel and non-swirling flow of liquid are considered a disturbance.

Relevant German regulations (**VdS** – Association of German

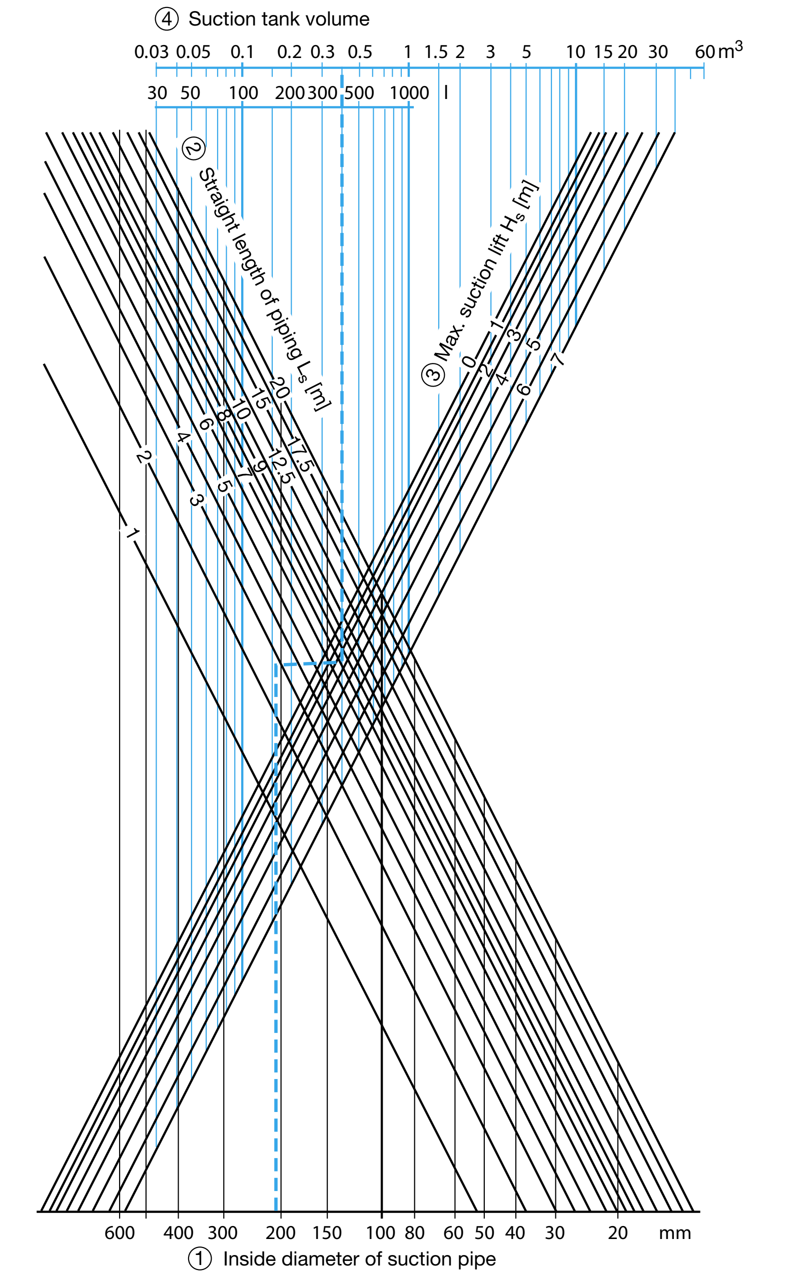

Fig. 75: Graph to determine the size of the suction tank. Follow the numbers from ① to ④ for selection. A safety factor of 3.0 has already been considered in the above diagram (head losses $H_{L,s}$ in the suction piping were neglected).

Table 14: Minimum values for undisturbed straight lengths of piping at measurement points in multiples of the pipe diameter D

Source	Distance from pump flange		Undisturbed pipe length		
	A_s/D	A_d/D	U_s/D	U_d/D	
VdS 2092-S	0.5	1.0	2.5	2.5	In-service measurement
ISO 9906	2.0	2.0	$5+n_q/53$	–	Acceptance test measurement

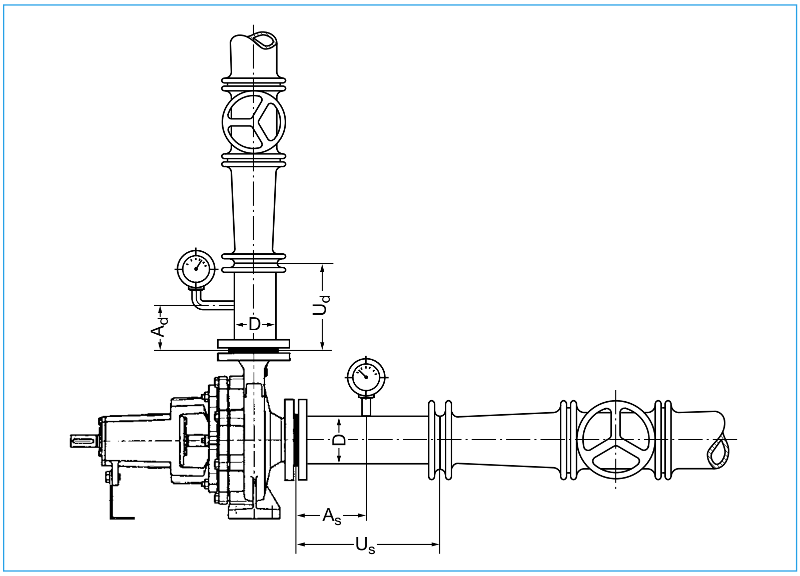

Fig. 76: Arrangement of pressure measurement points up- and downstream of the pump

Property Insurance Companies) stipulate pipe lengths in multiples of the pipe diameter for in-service measurements, while **ISO 9906** specifies pipe lengths for **acceptance test measurements.** The data from both sources are listed in Table 14.

If the required straight pipe lengths cannot be provided, the measuring results are likely to be less accurate. Consequently, pump flanges are not suitable as measurement points.

The pressure measuring points should consist of a 6 mm diameter hole and a weld socket to fit the pressure gauge. Even better still are annular measuring chambers with four drilled holes spread evenly across the circumference.

7.4 Shaft Couplings

In centrifugal pump engineering, both rigid and flexible shaft couplings are used. Rigid couplings are mainly used to connect shafts in perfect alignment, since the smallest degree of misalignment will cause considerable stress on the coupling and on the adjacent shaft sections.

Flexible couplings to DIN 740 are elastic, slip-free connecting elements between drive and pump which accommodate axial, radial and angular misalignment and damp shock loads. Flexibility is usually achieved by the deformation of damping and rubber-elastic spring elements whose life is governed to a large extent by the degree of misalignment. Fig. 77 shows two of the most common types of flexible shaft coupling. Fig. 78 shows a spacer coupling between a volute casing pump and drive. It permits removal of the pump rotating assembly without having to dismantle the suction and discharge piping or move the pump casing or drive (back pull-out design).

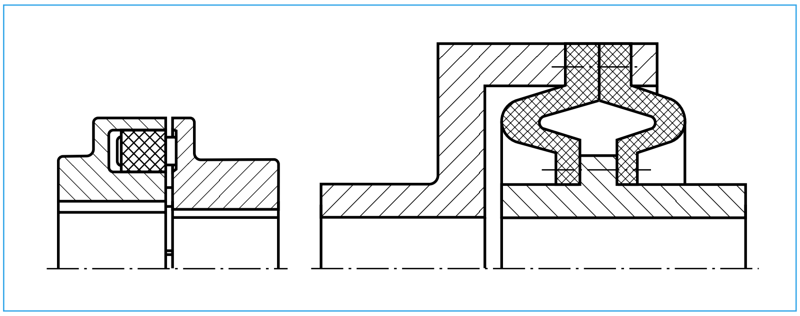

Fig. 77: Flexible (left) and highly flexible coupling

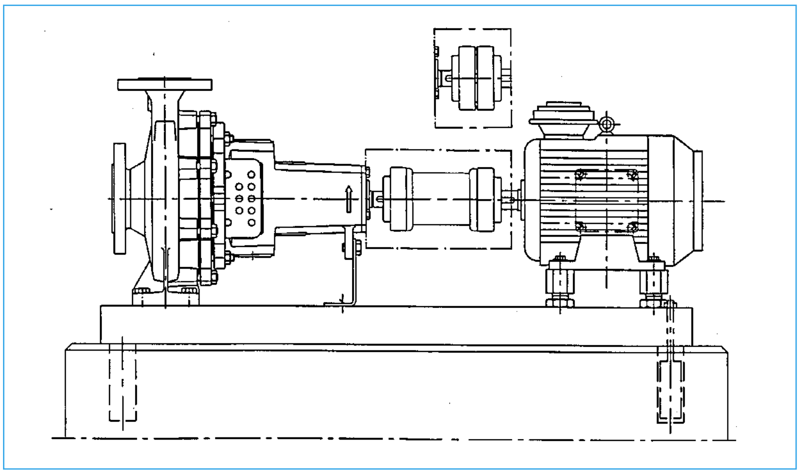

Fig. 78: Pump with spacer coupling compared with normal coupling

7.5 Pump Nozzle Loading

A centrifugal pump mounted on the foundation should not be used as an anchorage point for connecting the piping. Even if the piping is fitted to the nozzles without transmitting any stresses or strains, forces and moments, summarized as nozzle loading, will develop under actual operating conditions (pressure and temperature) and as a result of the weight of the liquid-filled piping. These cause stresses and deformation in the pump casings, and above all changes in coupling alignment, which, in turn, may affect the pump's running characteristics, the service life of the flexible elements in the shaft coupling, as well as the bearings and mechanical seals. For this reason limits have been defined for permissible nozzle loading [1].

As the loading profile for each pump nozzle is made up of three different forces and moments, it is not possible to specify theoretical nozzle loading limits for all conceivable combinations. Therefore, operators either need to check whether the nozzle loading imposed by the system is still within the pump's permissible limits, or have to contend with the considerably reduced general limits specified in several national and international standards and codes (EUROPUMP brochure "Permissible flange forces and moments for centrifugal pumps", 1986; API 610; ISO 5199).

Fig. 79 shows the permissible nozzle loading for single-stage volute casing pumps to ISO 5199 (solid line for pumps on grouted baseplate, broken line for pumps on non-grouted baseplates).

7.6 National and International Standards and Codes

A series of national standards and other technical codes have been introduced in Germany since the early sixties which govern the dimensions, manufacture, design, procurement and use of centrifugal pumps. Many of the requirements laid down have been included in European and international standards and codes. Drawn up by both operators and manufacturers, these are now well-established in virtually all sectors of industry using or producing pumps. The most important standards are tabulated in Fig. 80 on page 70.

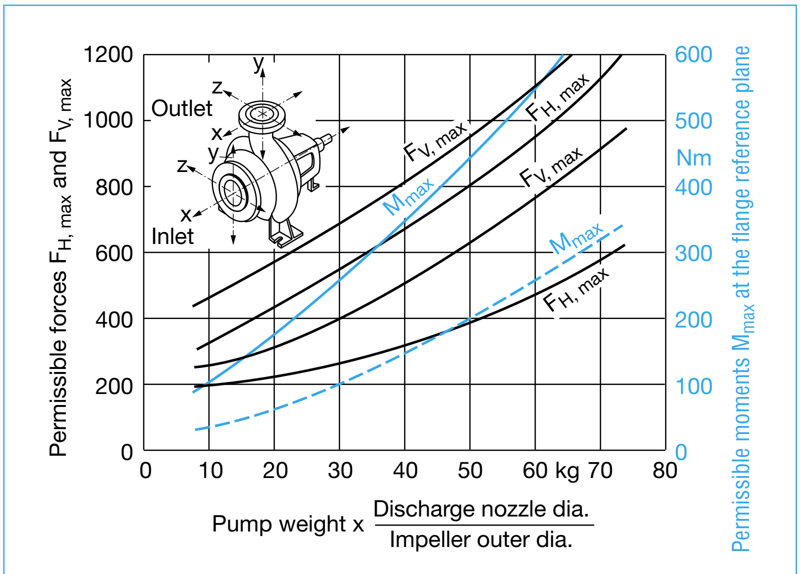

Fig. 79: Permissible moments M_{max} at the flange reference plane, as well as permissible forces $F_{H,max}$ (at x,z plane) and $F_{V,max}$ (in y direction) to ISO 1599 for single-stage volute casing pumps made of ferritic cast steel or nodular cast iron at room temperature. Lower numerical values apply to austenitic cast steel, lamellar graphite cast iron or higher temperatures.

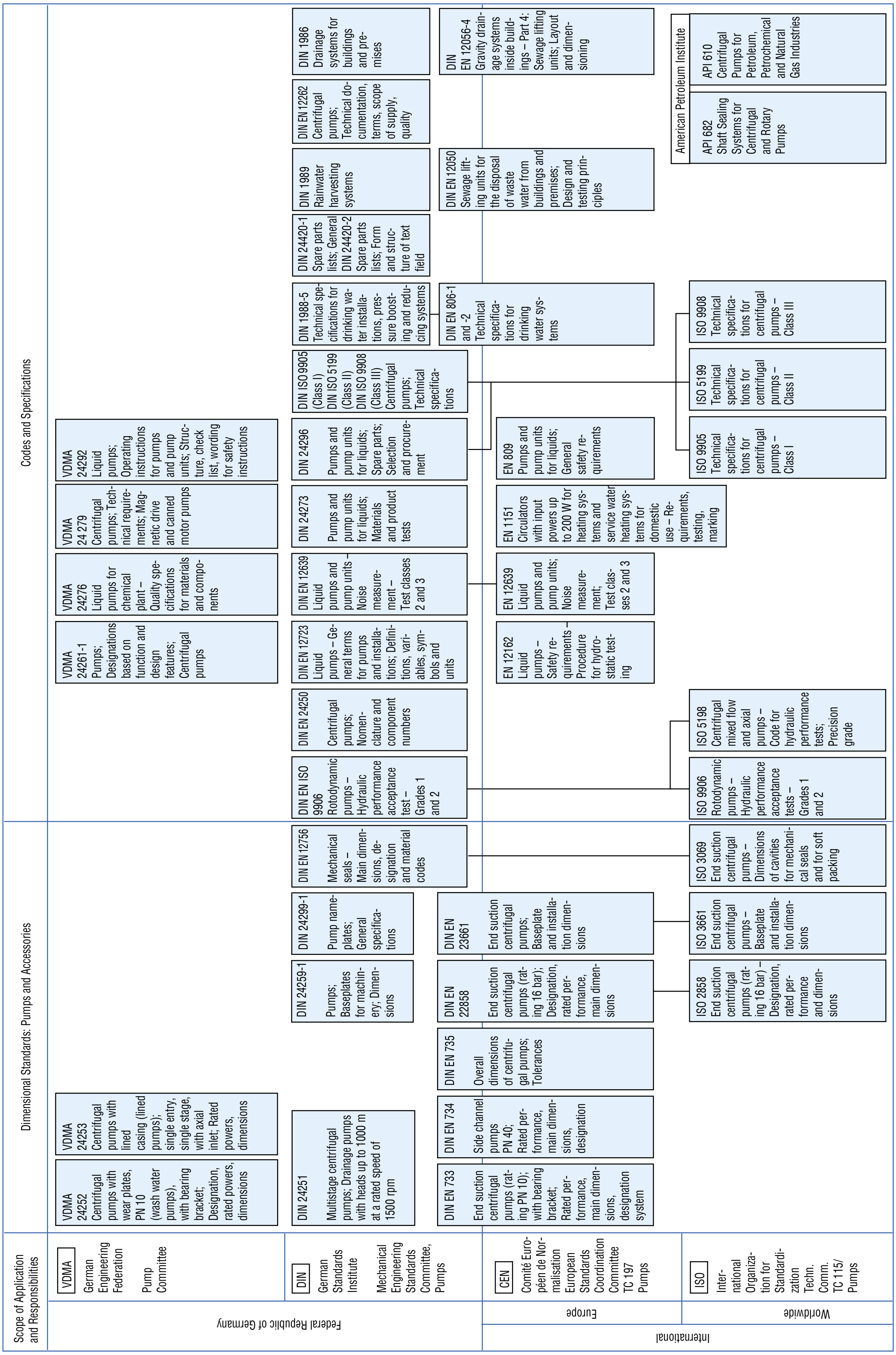

Fig. 80: National and international standards and codes for centrifugal pumps (last update: 2005)

8. Calculation Examples

The consecutive numbers of the calculation examples in this chapter are identical to the numbers of the respective equations in the text. For example, the application dealt with in exercise 8.3 refers to Equation (3).

8.1 Pressure Differential

Given: A volute casing pump Etanorm 80–200 with characteristic curves as per Fig. 18, speed of rotation n = 2900 rpm, impeller diameter D_2 = 219 mm, operating point at the point of best efficiency: Q = 200 m^3/h, H = 57.5 m, η = 83.5%, water temperature t = 20 °C, density ϱ = 998.2 kg/m^3. Nominal nozzle diameters DN_d = 80; DN_s = 100; inside nozzle diameter d_d = 80 mm, d_s = 100 mm [1]. Height difference between suction and discharge nozzles $z_{s,d}$ = 250 mm, Fig. 8.

Sought: The pressure differential between the discharge and suction sides indicated by the pressure gauges.

(Taking $z_{s,d}$ = 250 mm into account presupposes that the pressure gauges are fitted exactly at the respective nozzle levels to keep the same difference in height. If they are mounted at the same level, $z_{s,d}$ must be set to zero. Refer to paragraph 7.3 and ISO DIS 9906 for the correct location of the pressure measurement taps).

Flow velocities

$v_d = 4\ Q / \pi\ d_d^2 = 4 \cdot (200/3600) / \pi\ 0.08^2 = 11.1$ m/s

$v_s = 4\ Q / \pi\ d_s^2 = 4 \cdot (200/3600) / \pi\ 0.10^2 = 7.08$ m/s.

According to Eq. **(1)** the pressure differential is:

$\Delta p = \varrho \cdot g \cdot [H - z_{s,d} - (v_d^2 - v_s^2) / 2g]$

$= 998.2 \cdot 9.81 \cdot [57.5 - 0.250 - (11.1^2 - 7.08^2)/(2 \cdot 9.81)]$

$= 524\,576$ Pa $= 5.25$ bar

8.2 Input Power

Given: The data as per exercise 8.1.

Sought: The input power P.

According to Eq. **(2)** the input power is:

$$P = \varrho \cdot g \cdot Q \cdot H / \eta$$
$$= 998.2 \cdot 9.81 \cdot (200/3600) \cdot 57.5/0.835$$
$$= 37\,462 \text{ W} = 37.5 \text{ kW}$$

8.3 Specific Speed

Given: The data as per 8.1; the specific speed n_q is calculated using Eq. **(3)**

$$n_q = n \cdot \sqrt{Q_{opt}} / H_{opt}^{3/4} = 2900 \cdot \sqrt{(200/3600)} / 57.5^{3/4}$$
$$= 2900 \cdot 0.236/20.88 = 32.8 \text{ rpm}$$

or

$$= 333 \cdot (n/60) \cdot \sqrt{Q_{opt}} / (gH_{opt})^{3/4}$$
$$= 333 \cdot 48.33 \cdot \sqrt{(200/3600)} / 9.81 \cdot 57.5^{3/4}$$
$$= 333 \cdot 48.33 \cdot 0.236/115.7 = 32.8 \text{ (dimensionless)}$$

8.5
Bernoulli's Equation

Given: A centrifugal pump system as shown in Fig. 8 with tanks B and D, designed for a flow rate of $Q = 200$ m³/h for pumping water at 20 °C. The discharge-side tank is under a pressure of 4.2 bar (positive pressure), the suction tank is open to atmosphere, $v_e \approx 0$. The geodetic difference in height is 11.0 m; the welded discharge piping has a nominal diameter of DN 200 (d = 210.1 mm acc. to Table 4). The system head loss is 3.48 m.

Sought: The system head H_{sys}.

Eq. **(5)** gives:

$$H_{sys} = H_{geo} + (p_a - p_e)/(\varrho \cdot g) + (v_a^2 - v_e^2)/2g + \sum H_L$$

where

Density $\varrho = 998.2$ kg/m³ according to Table 12

Pressure in tank B: $p_a = 4.2$ bar = 420 000 Pa

Pressure in tank D: $p_e = 0$

$(p_a - p_e)/(\varrho \cdot g) = 420\,000/(998.2 \cdot 9.81) =$	42.89 m
$v_a = 4\,Q/(3600 \cdot \pi \cdot d^2) = 4 \cdot 200/(3600 \cdot \pi \cdot 0.2101^2)$ $= 1.60$ m/s	
$(v_a^2 - v_e^2)/2g = (1.60^2 - 0)/(2 \cdot 9.81) =$	0.13 m
$H_{geo} =$	11.00 m
$\sum H_L =$	3.48 m
$H_{sys} =$	57.50 m

8.9
Head Loss in Pipes

Given: The data as per 8.1 and: suction pipe DN 200, d = 200.1 mm according to Table 4, length = 6.00 m, average absolute roughness k = 0.050 mm.

Sought: The head loss H_L according to Fig. 11 or Eq. **(9)**.

The diagram in Fig. 11 gives: $H_L = 1.00 \cdot 6.00/100 = 0.060$ m

The calculation according to Fig. 10 would be more complex and involved, but also **absolutely necessary for other roughness values.**

Relative roughness $d/k = 210.1/0.050 = 4202$

According to Eq. (11), the Reynolds number is $Re = v \cdot d/\nu$

where

$\nu = 1.00 \cdot 10^{-6}$ m²/s,

$v = Q/A = (Q/3600) \cdot 4/(\pi d^2) = (200/3600) \cdot 4/(\pi \cdot 0.2101^2)$
$= 1.60$ m/s,

$Re = v \cdot d/\nu = 1.60 \cdot 0.2101/10^{-6} = 3.37 \cdot 10^5$.

From Fig. 10, $d/k = 4202 \rightarrow \lambda = 0.016$.

Eq. **(9)** gives

$$H_L = \lambda\,(L/d) \cdot v^2/2g$$
$$= 0.016 \cdot (6.00/0.2101) \cdot 1.60^2/2 \cdot 9.81 = 0.060 \text{ m}$$

8.15 Head Loss in Valves and Fittings

Given:
The suction pipe described in 8.9, including
a slide disc valve DN 200,
a 90° elbow with smooth surface and R = 5 d,
a foot valve DN 200
and a reducer DN 200 / DN 100 according to Table 8,
type IV with an opening angle of $\alpha = 30°$.

Sought: The head losses H_L.

According to Table 5, the loss coefficient of the slide disc valve is	$\zeta = 0.20$
Acc. to Table 6, the loss coefficient of the 90° elbow is	$\zeta = 0.10$
Acc. to Table 5, the approx. loss coefficient of the foot valve is	$\zeta = 2.0$
Acc. to Table 5, the loss coefficient of the reducer is	$\zeta = 0.21$
The total of all loss coefficients is	$\sum \zeta = 2.51$

Eq. **(15)** then gives the following head loss:

$$H_L = \sum\zeta \cdot v^2 / 2\,g = 2.51 \cdot 1.60^2 / (2 \cdot 9.81) = 0.328 \text{ m}$$

8.20 Orifice Plate

Given:
The pump described in exercise 8.1 is provided with a welded discharge pipe DN 80, the inside diameter being d = 83.1 mm. The discharge head is to be constantly throttled by $\Delta H = 5.00$ m.

Sought: The inside diameter of the orifice plate d_{Bl}.

Eq. **(20)** gives

$$d_{Bl} = f \cdot \sqrt{Q / \sqrt{(g \cdot \Delta H)}} \text{ with f according to Fig. 25.}$$

As an iterative calculation is necessary, d_{Bl} is estimated in the first instance, and this value is compared with the calculated diameter. If the two values differ, the value selected for the second estimate lies between the initially estimated and calculated diameters.

The following is calculated first of all:

$$\sqrt{Q / \sqrt{g \cdot \Delta H}} = \sqrt{200 / \sqrt{9.81 \cdot 5.0}} = 5.34 \text{ m.}$$

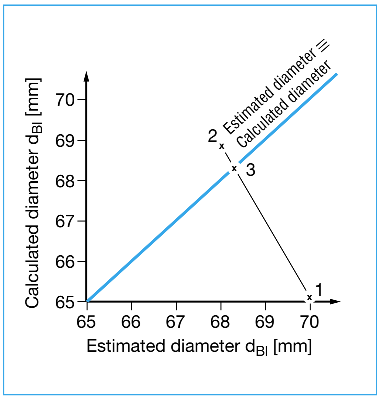

First estimate d_{Bl} = 70 mm; $(d_{Bl} / d)^2 = 0.709$; f = 12.2;
Result: $d_{Bl} = 12.2 \cdot 5.34 = 65.1$ mm

Second estimate d_{Bl} = 68 mm; $(d_{Bl} / d)^2 = 0.670$; f = 12.9;
Result: $d_{Bl} = 12.9 \cdot 5.34 = 68.9$ mm

Third estimate d_{Bl} = 68.4; $(d_{Bl} / d)^2 = 0.679$; f = 12.8;
Result: $d_{Bl} = 12.8 \cdot 5.34 = 68.4$ mm

For a faster solution, it is recommended to plot the calculated versus the corresponding estimated diameters in a diagram so that the third estimate already provides the final result in the intersection of connecting line and diagonal, see adjacent diagram.

8.21 Change of Speed

Given:
The pump speed as per 8.1 (operating data with index $_1$) is to be reduced from n_1 = 2900 rpm to n_2 = 1450 rpm.

Sought: The data for flow rate Q_2, discharge head H_2 and driving power P2 after change of speed.

Eq. **(21)** gives
$Q_2 = Q_1 \cdot (n_2/n_1) = 200 \ \ (1450 / 2900) = 100 \text{ m}^3/\text{h}$

Eq. (22) gives
$H_2 = H_1 \cdot (n_2/n_1)^2 = 57.5 \cdot (1450 / 2900)^2 = 14.4 \text{ m}$

Eq. (23) gives
$P_2 = P_1 \cdot (n_2/n_1)^3 = 37.5 \cdot (1450 / 2900)^3 = 4.69 \text{ kW}$,

on the assumption that the efficiency is the same for both speeds.

8.27 Turning Down Impellers

Given:
The flow rate of the pump at BEP described in 8.1, i.e. Q_t = 200 m^3/h, is to be reduced to Q_r = 135 m^3/h by turning down the original impeller diameter D_t = 219 mm.

Sought: The reduced diameter D_r and the discharge head H_r at BEP after turning down the impeller (H_t = 57.5 m).

Eq. **(27)** gives
$D_r \approx D_t \cdot \sqrt{(Q_r / Q_t)} = 219 \cdot \sqrt{(135 / 200)} = 180 \text{ mm}$

Eq. (26) gives
$H_r \approx H_t \cdot (Q_r / Q_t) = 57.5 \cdot 135 / 200 = 38.8 \text{ m}$

8.29 $NPSH_a$ for Suction Lift Operation

Given:
The centrifugal pump system described in exercise 8.5 plus the following data: place of installation 500 m above M.S.L.; $H_{L,s}$ (refer to exercises 8.9 and 8.15) = 0.39 m; $H_{s\ geo}$ = 3.00 m; $v_e \approx 0$. The pump described in 8.1 is installed horizontally with an open suction tank, as shown in Fig. 36. According to Fig. 18, the pump's $NPSH_r$ is 5.50 m at a flow rate of Q = 200 m^3/h.

Question: Is $NPSH_a$ sufficient?

According to Eq. **(29)**,
$NPSH_a = (p_e + p_b - p_v)/(\varrho \cdot g) + v_e^2/2g - H_{L,s} - H_{s\ geo} \pm s'$
where

Gauge pressure in suction tank p_e = 0			
Atmospheric pressure p_b	= 955 mbar	= 95 500 Pa	acc. to Table 13
Vapour pressure p_v	= 0.02337 bar	= 2337 Pa	acc. to Table 12
Density ϱ		= 998.2 kg/m^3	acc. to Table 12

$(p_e + p_b - p_v)/(\varrho \cdot g) = (0 + 95\,500 - 2337)/(998.2 \cdot 9.81) = 9.51 \text{ m}$
$v_e^2/2g = 0$
$H_{L,s} = 0.39 \text{ m}$
$H_{s\ geo} = 3.00 \text{ m}$
s' = 0, as the centre of the impeller inlet is at the same height as the centre of the pump inlet.

$NPSH_a = 6.12 \text{ m}$

With an $NPSH_r$ of 5.50 m,
$NPSH_a$ is larger than $NPSH_r$ in this case and therefore sufficient.

8.31 NPSH$_a$ for Suction Head Operation

Given: The pump system described in exercise 8.29 is be operated in suction head operation with a closed tank as shown in Fig. 37. The system data are as follows: place of installation 500 m above M. S. L.; $H_{L,s}$ (refer to exercises 8.9 and 8.15) = 0.39 m; $H_{z\ geo}$ = 2.00 m; ve ≈ 0. The pump described in 8.1 is installed horizontally with a closed suction tank, as shown in Fig. 37. According to Fig. 18, the pump's NPSH$_r$ is 5.50 m at a flow rate of Q = 200 m^3/h.

Question: Is NPSH$_a$ sufficient?

According to Eq. **(31)**

$$NPSH_a = (p_e + p_b - p_v) / (\varrho \cdot g) + v_e^2 / 2g - H_{L,s} + H_{z\ geo} \pm s'$$

where

Gauge pressure in suction tank p_e	= –0.40 bar	= –40 000 Pa	
Atmospheric pressure p_b	= 955 mbar	= 95 500 Pa	acc. to Table 13
Vapour pressure p_v	= 0.02337 bar	= 2337 Pa	acc. to Table 12
Density ϱ	= 998.2 kg/m^3		acc. to Table 12

$(p_e + p_b - p_v) / (\varrho \cdot g)$

= (–40 000 + 95 500 – 2337) / (998.2 · 9.81) = 5.43 m

$v_e^2/2g$ = 0

$H_{L,s}$ = 0.39 m

$H_{z\ geo}$ = 2.00 m

s' = 0, as the centre of the impeller inlet is at the same height as the centre of the pump inlet.

NPSH$_a$ = 7.04 m

With an NPSH$_r$ of 5.50 m,
NPSH$_a$ is larger than NPSH$_r$ in this case and therefore sufficient.

8.36 Pump Characteristics When Pumping Viscous Fluids

Given: A mineral oil with a density of ϱ_z = 0.897 kg/m^3 and a kinematic viscosity of ν_z = 500 · 10-6 m^2/s is to be pumped by the centrifugal pump described in 8.1; characteristic curves according to Fig. 19.

Sought: The characteristics for discharge head, efficiency and input power when pumping this viscous fluid, using the spreadsheet calculation as per Fig. 51.

The data for handling water (index w) are required first to find the conversion factors:

Flow rate at BEP	$Q_{w,\ opt}$	= 200 m^3/h
Head at BEP	$H_{w,\ opt}$	= 57.5 m
Optimum efficiency	$\eta_{w,\ opt}$	= 0.835
Power	$P_{w,\ opt}$	= 37.5 kW
Speed	n	= 2900 min^{-1}
Specific speed (as per exercise 8.3)	n_q	= 32.8
Kinematic viscosity	ν_z	= 500 · 10^{-6} m^2/s
Density of mineral oil	ϱ_z	= 897 kg/m^3

The three conversion factors f_Q = 0.84, f_H = 0.88, f_η = 0.62 are taken from Fig. 51.

The calculation is continued using the table below:

Q/Q_{opt}	0	0.8	1.0	1.2	
Q_w } refer to Fig. 18	0	160	200	240	m^3/h
H_w } refer to Fig. 18	66.5	62.0	57.5	51.0	m
η_w } refer to Fig. 18	0	0.81	0.835	0.805	
$Q_z = Q_w \cdot f_Q$	0	134.4	168	201.6	m^3/h
H_z	= H_w	= 1.03 $H_w \cdot f_H$	= $H_w \cdot f_H$	= $H_w \cdot f_H$	
	66.5	56.2	50.6	44.9	m
$\eta_z = \eta_w \cdot f_\eta$	0	0.502	0.518	0.499	
$P_z = \varrho_z \cdot Hz \cdot Q_z / (\eta_z \cdot 367)$	÷	36.8	40.1	44.3	kW

To calculate the power P_z, the values for flow rate Q_z in m^3/h and the density ϱ_z in kg/m^3 are inserted into the equation.

These calculated points can be used to plot the characteristic curve for a viscous fluid, cf. Fig. 52 and Fig. 18 (this chart is applicable for handling water with an impeller diameter of 219 mm).

8.45
Head Reduction for Hydrotransport

Given: Grit with a density of $\varrho z = 2700$ kg/m^3 and an average particle size of $d_s = 5$ mm is to be pumped in cold water (kinematic viscosity $\nu_f = 1.00 . 10^{-6}$ m^2/s) at a concentration of $c_T = 15\%$ with a centrifugal pump (hydraulic data as per 8.1, specific speed $n_q = 33$, head coefficient $\psi = 1.0$).

Sought: The head reduction ΔH/H at H = 57.5 m.

According to Fig. 55, the settling speed w_{s0} of a single sphere under the conditions described above is 0.5 m/s. Thus, the Reynolds number is $Re_s = w_{s0} \cdot d_s / \nu_f = 0.5 \cdot 0.005 / 1.0 \cdot 10 - 6 = 2500$.

The head reduction is calculated using Eq. **(45)**:

$$\Delta H/H = c_T / \psi \cdot \sqrt[3]{Re_s} \cdot (11.83/n_q)^3 \cdot (\varrho_s/\varrho_f - 1)$$
$$= (0.15 / 1.0) \cdot \sqrt[3]{2500} \cdot (11.83 / 33)^3 \cdot (2700 / 1000 - 1)$$
$$= 0.15 \cdot 13.6 \cdot 0.0461 \cdot 1.70 = 0.16$$

$$\Delta H = 0.16 \cdot 57.5 = 9.2 \text{ m}$$

Under the above conditions the pump discharge head of $H_{w,\,opt}$ = 57.7 m would be reduced by 16%, i.e. 57.5 – 9.2 = 48.3 m.

8.47
Average Density

Given: Hydrotransport as described in exercise 8.45.

Sought: The average density ϱ_m and its effect on the pump discharge pressure; will it rise or fall?

According to Eq. **(47)** the average density is $\varrho_m = c_T \cdot \varrho_s + (1 - c_T) \cdot \varrho_f$

where

$\varrho_f \equiv \varrho_w = 998{,}2$ kg/m^3 for water at 20 °C
$\varrho_m = 0.15 \cdot 2700 + 0.85 \cdot 998.2 = 1253$ kg/m^3

The pressure differential according to equation (46)
$$\Delta p = \varrho_m \cdot g \cdot (H - \Delta H)$$
$$= 1253 \cdot 9.81 \cdot (57.5 - 9.2) = 593\,700 \text{ Pa} = 5.94 \text{ bar}$$

This is higher than the discharge pressure for handling water (Δp = 5.25 bar) as per exercise 8.1. Hence, the characteristic curve $\Delta p = f(Q)$ has increased by 13% for hydrotransport of solids.

8.48
Pump Sump

Given: The pump sump for a pump as per 8.1 with the following data:

Inlet flow $Q_{in} = 120$ m^3/h

Flow rate at switch-on pressure $Q_{on} = 220$ m^3/h and

Flow rate at switch-off pressure $Q_{off} = 150$ m^3/h

The maximum permissible number of start-ups of a pump unit is given in Table 10 (section 3.3.3.1, dry motor with P > 30 kW, in this case Z = 10/h).

Sought: The useful volume V_N of the pump sump according to equation **(48)** (all flow rates in m^3/h):

$$V_N = Q_{in} \cdot (Q_m - Q_{in}) / (Q_m \cdot Z)$$

where

$$Q_m = (Q_{on} + Q_{off}) / 2 = (220 + 150) / 2 = 185 \text{ m}^3/\text{h}$$

$$V_N = 120 \cdot (185 - 120) / (185 \cdot 10) = 4.22 \text{ m}^3/\text{h}$$

8.50
Minimum Submergence

Given: The vertical unflanged suction pipe according to 8.9 and Fig. 8D, inside pipe diameter $d = d_E = 210.1$ mm at a flow rate of $Q = 200\ m^3/h$.

Sought: The minimum submergence S_{min} in the open suction tanks. The flow velocity v_s in the suction pipe inlet is

$$v_s = Q/A = (Q/3600)/(\pi \cdot d_E^2/4) = (200/3600) \cdot (\pi \cdot 0.2101^2/4) = 1.60\ m/s$$

Eq. **(50)** gives the minimum submergence as

$$\begin{aligned} S_{min} &= d_E + 2.3 \cdot v_s \cdot \sqrt{d_E / g} \\ &= 0.2101 + 2.3 \cdot 1.60 \cdot \sqrt{0.2101 / 9.81} \\ &= 0.75\ m. \end{aligned}$$

The same result can be obtained faster from the diagram in Fig. 67.

Fig. 66 provides the required distance to the wall with > 0.21 m, the channel width with > 1.26 m and the distance to the floor with > 0.150 m.

8.52
Suction Tank Volume

Given: A centrifugal pump system, data according to 8.1 and 8.9, including a suction tank as per Fig. 74. The straight length of the air-filled suction pipe DN 200 (inside diameter d_s = 210.1 mm according to Table 4) is $L_s = 3.00$ m, with $H_{s\ geo} = 2.60$ m (= vertical distance between pump reference plane and water level for positive inlet pressure operation). The atmospheric pressure $p_b = 989$ mbar = 98900 Pa; density of the water at 20° C = 998.2 kg/m^3, vapour pressure $p_v = 2337$ Pa.

Sought: The volume of the suction tank according to Eq. **(52)**:

$$V_B = (d_s^2\, \pi /4) \cdot L_s \cdot p_b / (p_b - \varrho \cdot g \cdot H_s)$$

The suction lift Hs is defined by Eq. (53):
$H_s = H_{s\ geo} + H_{L,s}$
Given is $H_{s\ geo} = 2.60$ m, the suction pipe head loss $H_{L,s}$ is to be calculated from $H_{L,s1}$ and $H_{L,s2}$ as follows:

1) Head loss $H_{L,s}$ of the pipe as per 8.9:

$$H_{L,s1} = \lambda \cdot (L / d_s) \cdot v_s^2 / 2g$$

where

- λ = 0.016 from 8.9
- L = $H_{s\ geo}$ = 2.6 m (not 3.0 m because the elbow length is taken into account in $H_{L,s2}$)
- d_s = 0.2101 m.
- v_s = 1.60 m from exercise 8.9.

$$H_{L,s1} = 0.016 \cdot (2.60 / 0.2101) \cdot 1.60^2 / (2 \cdot 9.81) = 0.026\ m$$

$H_{L,s2}$ covers the 180° elbow (2 x 90° elbow according to Table 6 as in 8.15) and inlet pipe fittings according to Table 7.

Loss coefficient ζ of 180° elbow (factor 1.4) = $1.4 \cdot 0.10$ = 0.14

Loss coefficient ζ of inlet pipe fitting (broken inlet edge) = 0.20

$$H_{L,s2} = \Sigma\zeta \cdot v_s^2 / 2g = (0.14 + 0.20) \cdot 1.60^2 / (2 \cdot 9.81) = 0.044\ m$$

3) The total head loss $H_{L,s} = H_{vs1} + H_{L,s2} = 0.026 + 0.044 = 0.070$ m

and therefore

$$H_s = H_{s\ geo} + H_{L,s} = 2.60 + 0.07 = 2.67\ m$$

The example shows that the head loss $H_{L,s}$ (= 0.070) can be neglected for short suction pipes, since $H_{s\ geo}$ (2.60 m) is considerably higher. This simplifies the calculation. The volume of the suction tank V_B can be calculated using Eq. (52) or can simply be determined using the graphs of Fig. 75 (provided the head loss $H_{L,s}$ is neglected).

$V_B = (d_s^2\pi / 4) \cdot L_s \cdot p_b / (p_b - \varrho g H_s)$

$= (0.2101^2 \cdot \pi/4) \cdot 3.0 \cdot 98\,900 / (98\,900 - 998.2 \cdot 9.81 \cdot 2.67)$
$= 0.141\ m^3$

The chosen tank size is 2.8 times the volume of 0.40 m^3 (cf. example in Fig. 75).

Check
The lowest pressure is = $p_b - \varrho g H_s$ = 72 828 Pa
The vapour pressure is 0.02337 bar = 2337 Pa

This means the pressure does not fall below vapour pressure during venting.

9. Additional Literature

[1] Product literature (KSB sales literature)

[2] KSB Centrifugal Pump Lexicon

[3] Cavitation in Centrifugal Pumps. KSB publication No. 0383.051

[4] Gebäudetechnik von KSB. Pumpenregelung und Anlagenautomation. Planungshinweise. (Building Services Products from KSB. Pump Control and Plant Automation. Planning Information). KSB publication No. 2300.024 (2005)

[5] Bernauer J., M. Stark, W. Wittekind: Improvement of Propeller Blades Used for Handling Liquids Containing Fibrous Solids. KSB Technische Berichte 21e (1986), pp. 16 – 21

[6] Bieniek K., Gröning N.: Controlling the Output of Centrifugal Pumps by Means of Electronic Speed Control. KSB Technische Berichte 22e (1987), pp. 16 – 31

[7] Bieniek K.: Submersible Motors and Wet Rotor Motors for Centrifugal Pumps Submerged in the Fluid Handled. KSB Technische Berichte 23e (1987), pp. 9 – 17

[8] Holzenberger K., Rau L.: Parameters for the Selection of Energy Conserving Control Options for Centrifugal Pumps. KSB Technische Berichte 24e (1988), pp. 3 – 19

[9] Holzenberger K.: A Comparison of Two Conversion Methods Applied to the Characteristics of Centrifugal Pumps While Pumping Viscous Liquids. KSB Technische Berichte 25e (1988), pp. 45 – 49

[10] Holzenberger K.: How to Determine the Starting Torque Curve of Centrifugal Pumps by Using Characteristic Factors. KSB Technische Berichte 26 (1990), pp. 3 – 13

[11] Kosmowski I., Hergt P.: Förderung gasbeladener Medien mit Hilfe von Normal- und Sonderausführungen bei Kreiselpumpen (Pumping Gas-laden Fluids by Standard and Special Design Centrifugal Pumps). KSB Technische Berichte 26 (1990), pp. 14 – 19

[12] Schreyer H.: Glandless Chemical Pump with Magnetic Drive. KSB Technische Berichte 24e (1988), pp. 52 – 56

10.
Technical Annex

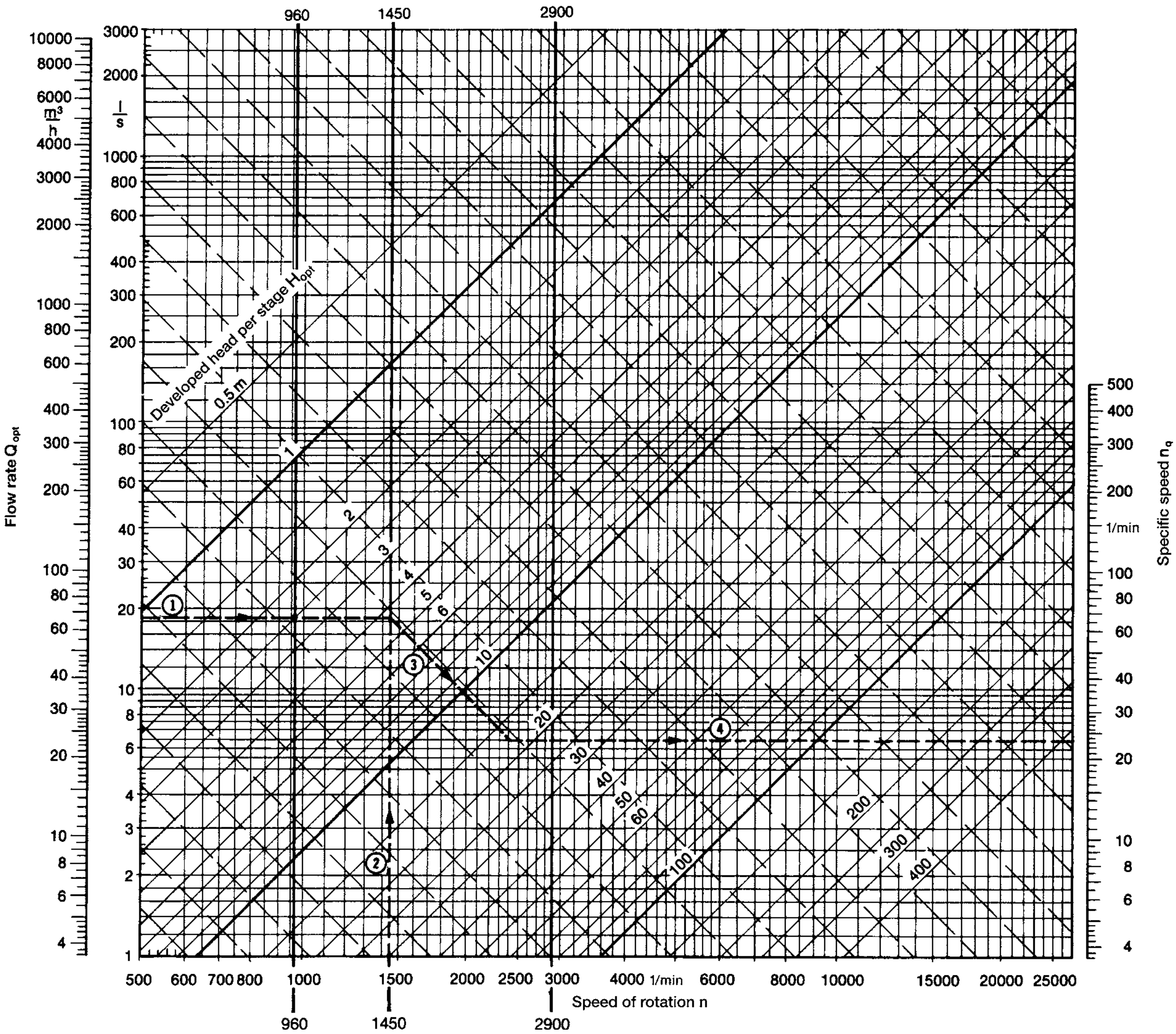

Fig. 3: Nomograph to determine the specific speed n_q
Example: Q_{opt} = 66 m^3/h = 18.3 l/s; n = 1450 rpm, H_{opt} = 17.5 m. Found: n_q = 23 (metric units).

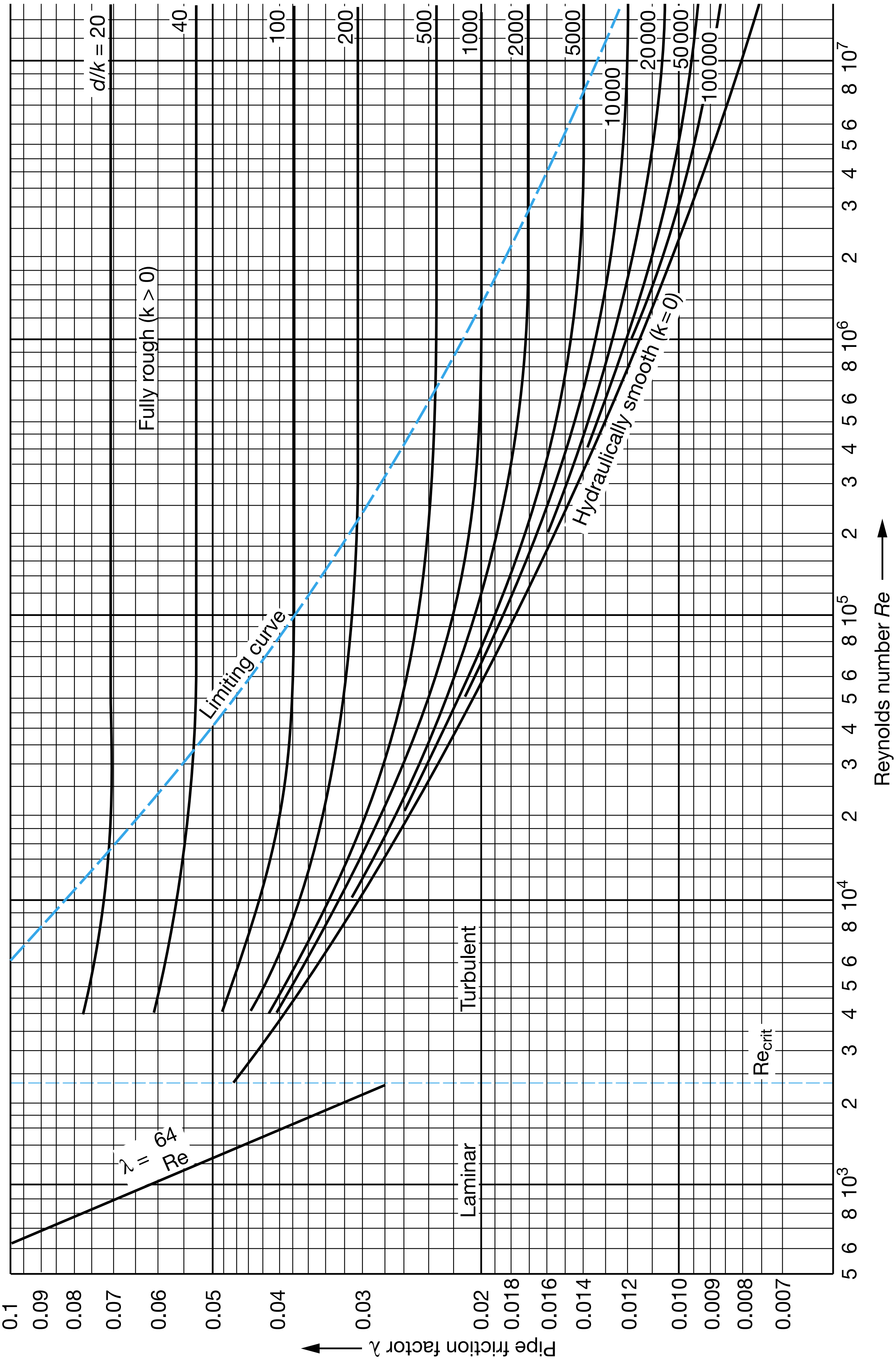

Fig. 10: Pipe friction factor λ as a function of the Reynolds number Re and the relative roughness d/k

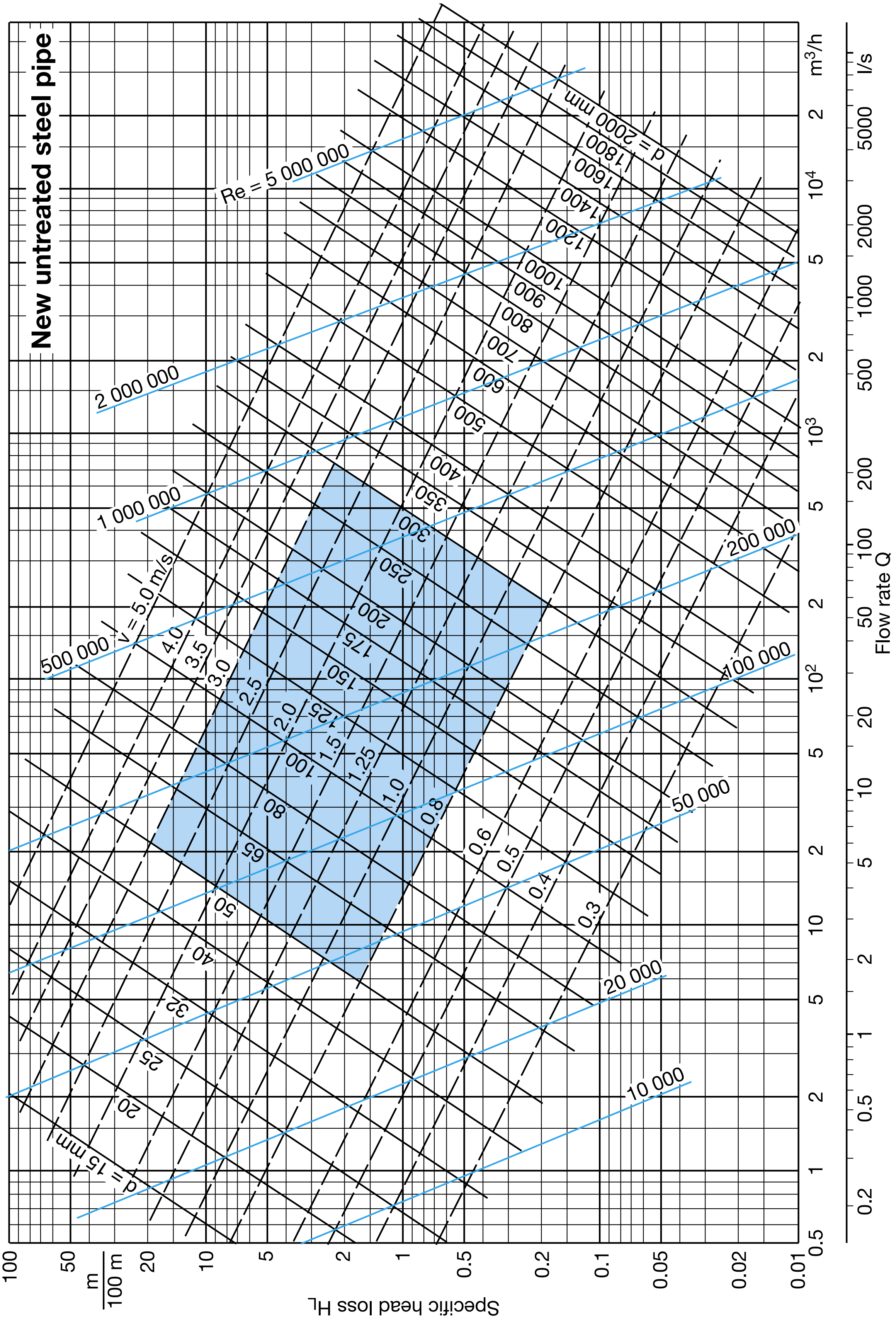

Fig. 11: Head losses H_L for new steel pipes (k = 0.05 mm)

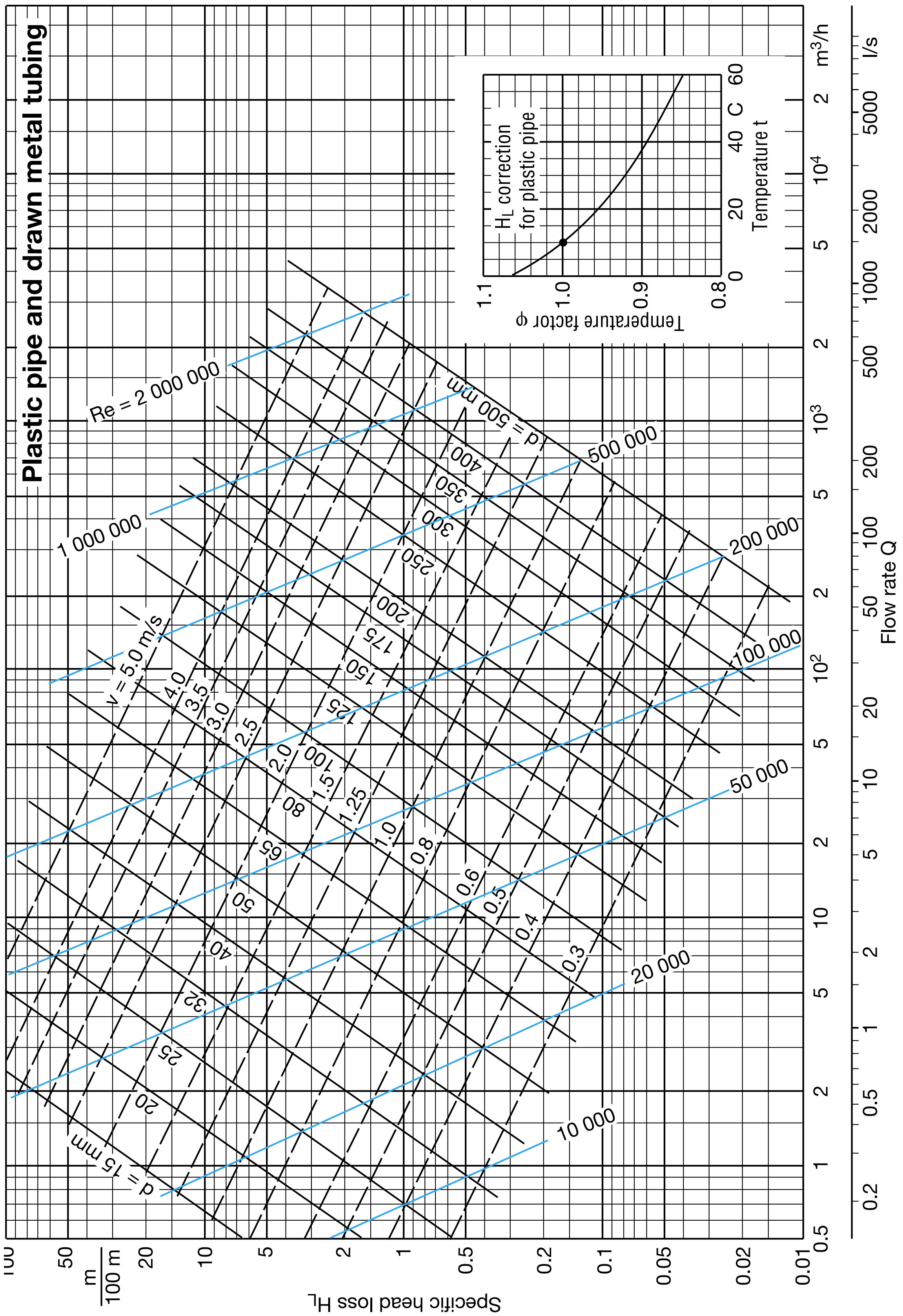

Fig. 12: Head losses H_L for hydraulically smooth pipes (k = 0)
For plastic pipe when t ≠ 10 °C multiply by the temperature factor φ

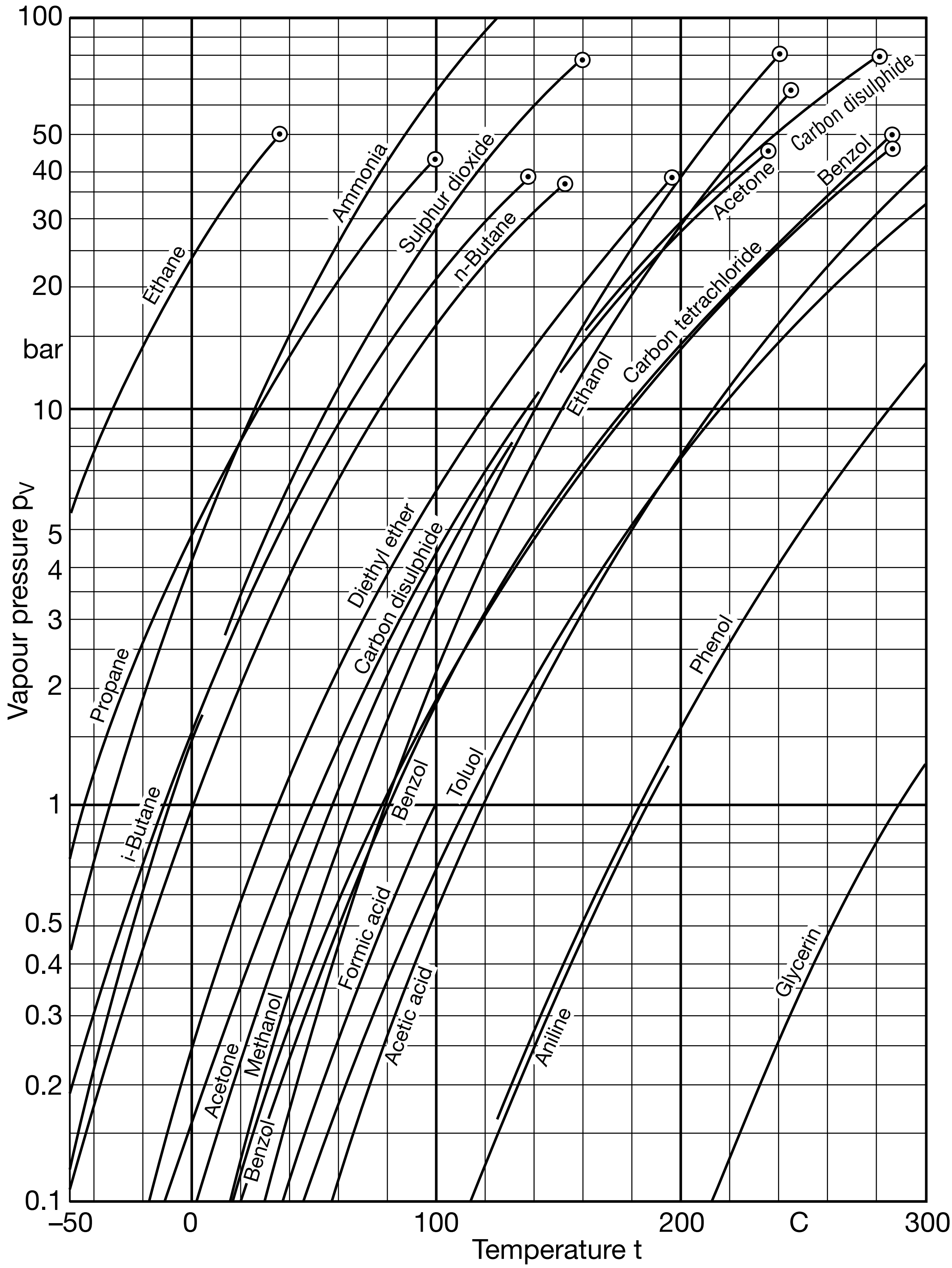

Fig. 35: Vapour pressure p_v of various fluids as a function of the temperature t

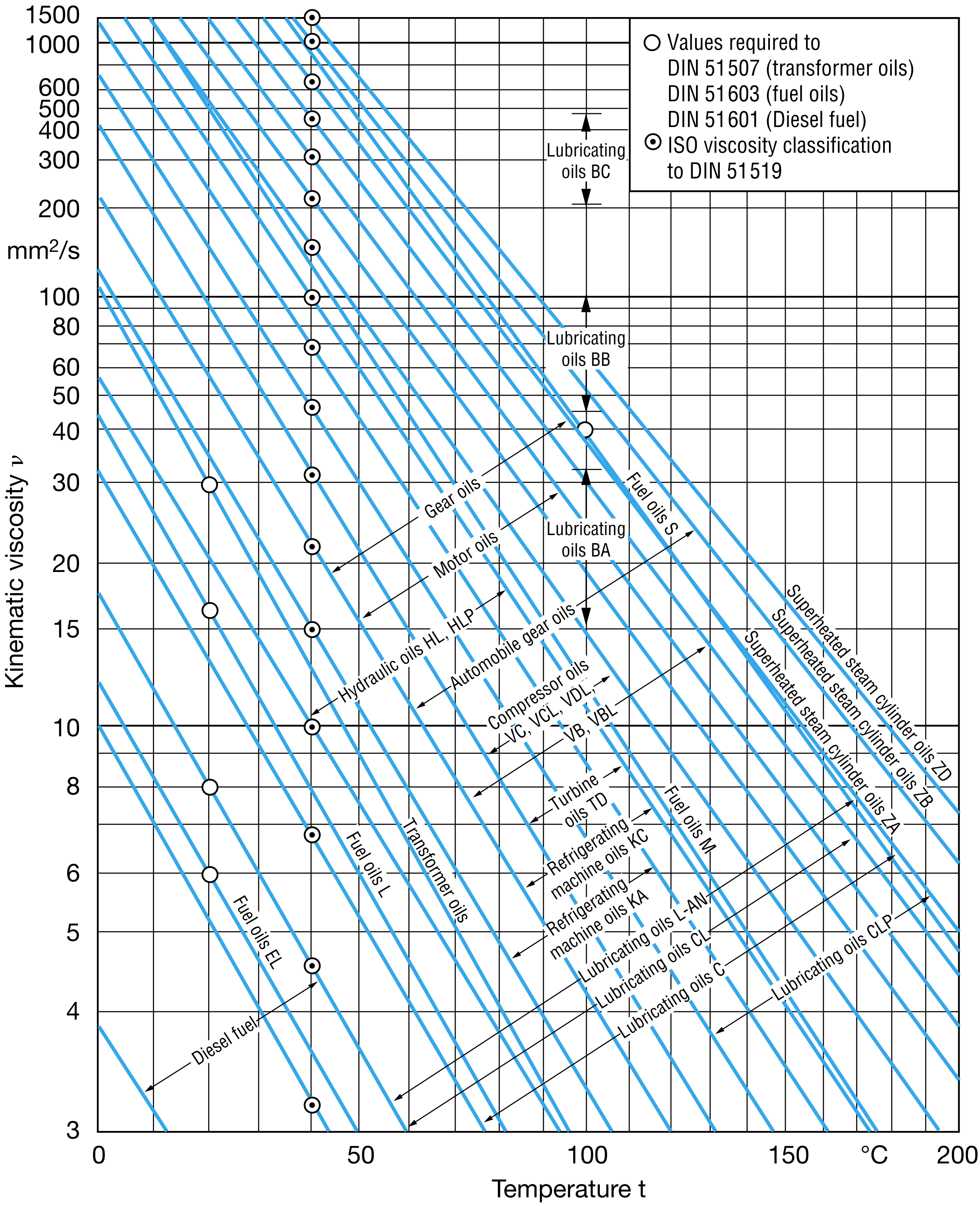

Fig. 47: Kinematic viscosity ν of various mineral oils as a function of the temperature t

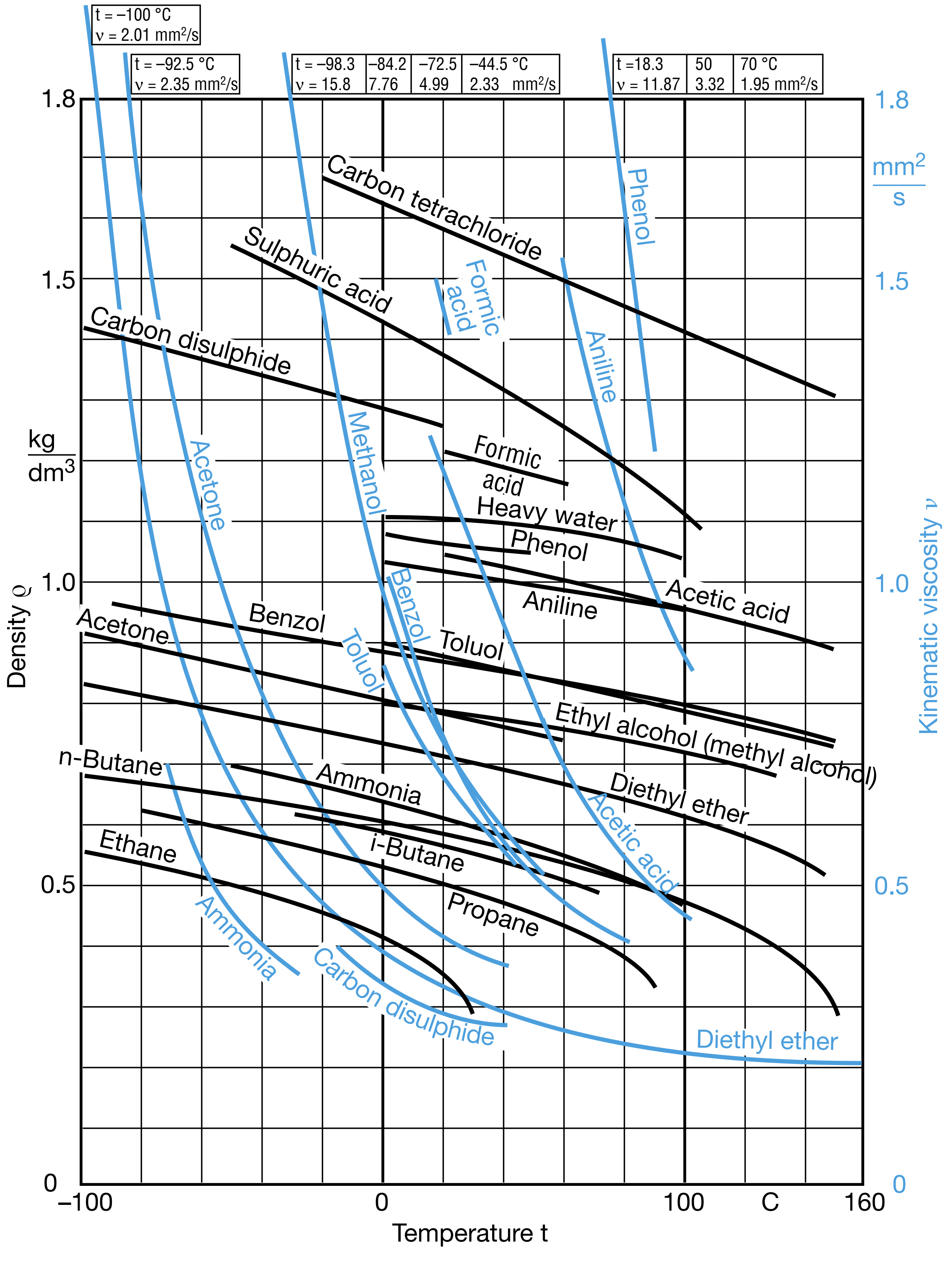

Fig. 48: Density ϱ and kinematic viscosity ν of various fluids as a function of the temperature t

How to Find the Operating Point

Given:

Flow rate	Q_W		m^3/h
Total developed head	H_W		m
Speed of rotation	n		1/min
Kinematic viscosity	ν_Z		m^2/s
Density	ϱ_Z		kg/m^3
Gravitational constant	g	9.81	m/s^2

Calculation

Q/Q_{opt} =	0	0.8	1.0	1.2	–	
Q_W from the pump characteristic for 4 points	0				m^3/h	
H_W					m	
η_W	0				–	
$n_{q,W}$ from section 3.1.5	–	–		–	1/min	
$f_{Q,W}$ from Fig. 50	–				–	
$f_{H,W}$	–				–	
$f_{\eta,W}$	–				–	
$Q_Z = Q_W \cdot f_{Q,W}$	0				m^3/h	
H_Z =	$= H_W$	$= H_W \cdot f_{H,W} \cdot 1{,}03$ 1)	$H_W \cdot f_{H,W}$	$H_W \cdot f_{H,W}$	m	2)
$\eta_Z = \eta_W \cdot f_{\eta,W}$	0					
$P_Z = \frac{\varrho_Z \cdot g \cdot H_Z \cdot Q_Z}{\eta_Z \cdot 1000 \cdot 3600}$					kW	

1) If H_Z becomes larger than H_W, it should be set to H_W.

2) These are four values on the H_Z/Q and Q/η_Z curve and three points on the Q/P_Z curve. Plot versus Q.

Fig. 51: Spreadsheet for calculating the pump characteristics for a viscous fluid using the KSB method

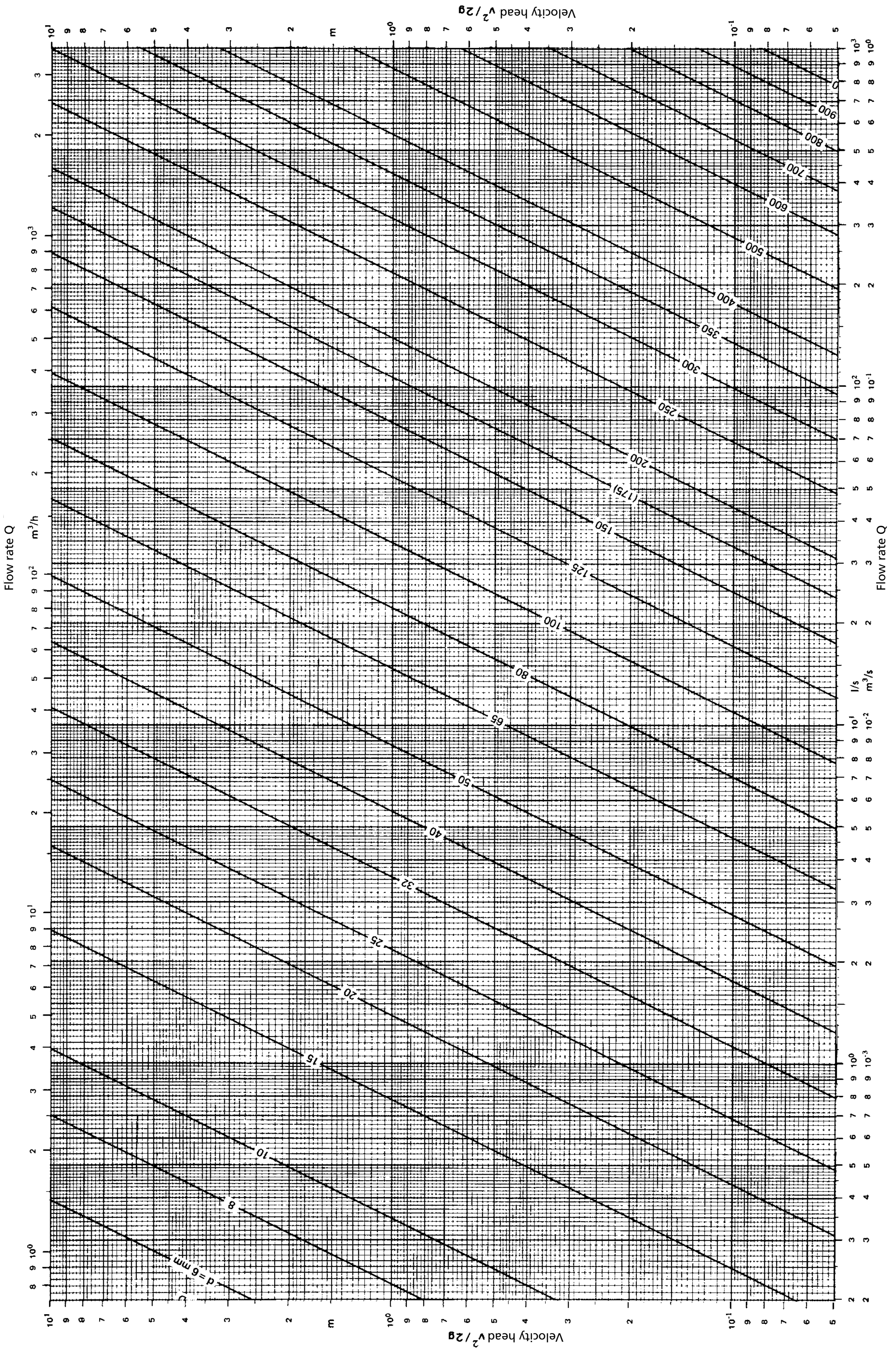

Velocity head $v^2/2$ g as a function of flow rate Q and inside pipe diameter d

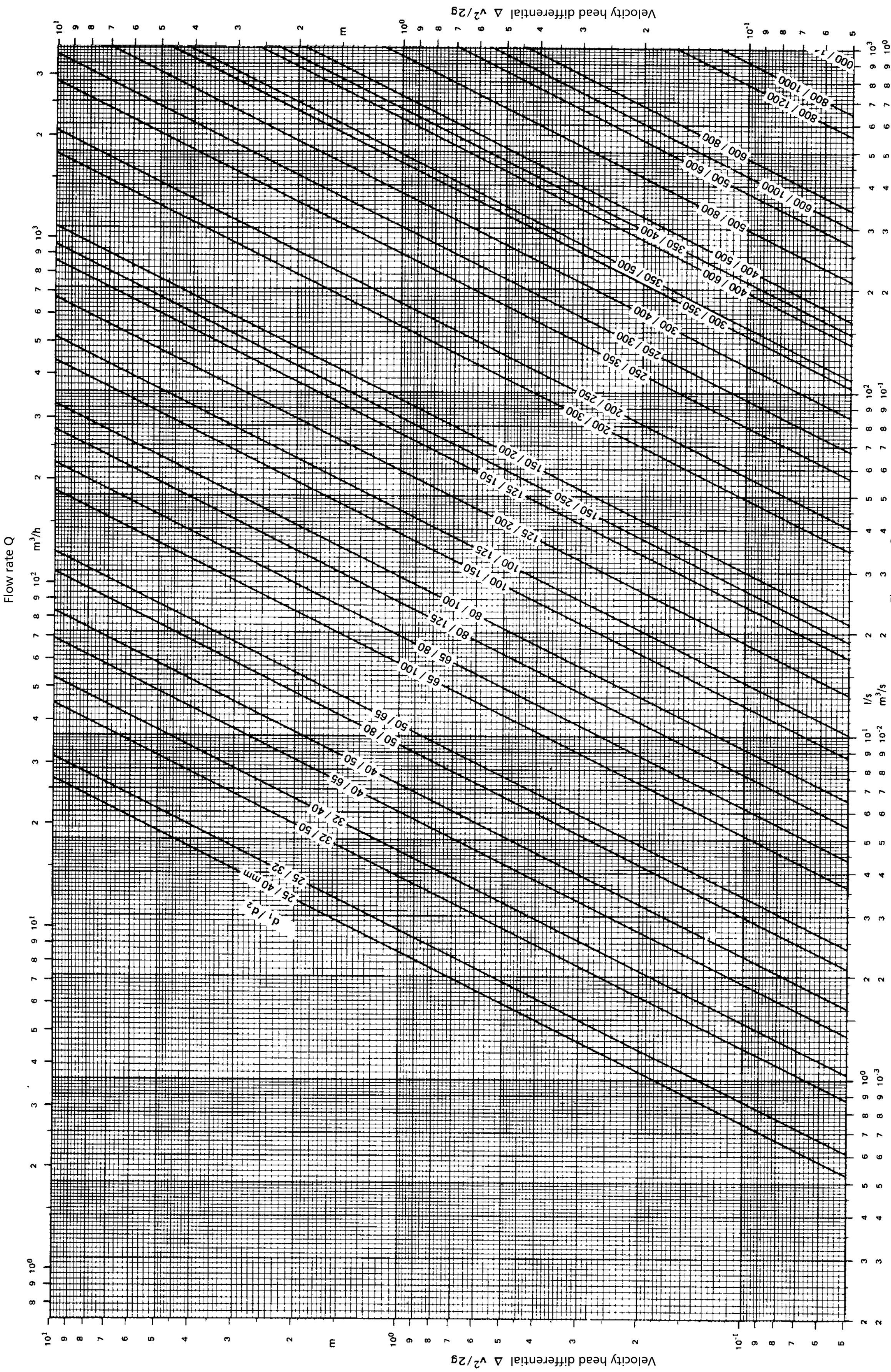

Velocity head differential Δ (v^2/2 g) as a function of flow rate Q and inside pipe diameters d_1 and d_2

11. Excerpt of Important Units for Centrifugal Pumps

Physical dimension	Symbol	Units			Units not to be used any longer	Recommended units	Comments
		SI units		Other units (not complete)			
Length	l	m	Metre	km, dm, cm, mm, µm		m	Base unit
Volume	V	m^3		dm^3, cm^3, mm^3, litre (1 l = 1 dm^3)	cbm, cdm…	m^3	
Flow rate, capacity, volume flow	Q, $\dot{V}$	m^3/s		m^3/h, l/s		l/s and m^3/s	
Time	t	s	Second	s, ms, µs, ns,… min, h, d		s	Base unit
Speed of rotation	n	1/s		1 /min (rpm)		1 /s, 1 /min	
Mass	m	kg	Kilogram	g, mg, µg, metric ton (1 t = 1000 kg)	Pound, hundredweight	kg	Base unit The mass of a commercial commodity is described as weight.
Density	ϱ	kg/m^3		kg/d m^3		kg/dm^3 und kg/m^3	The term “spezifice gravita” must no longer be employed, because it is ambiguous (see DIN 1305).
Mass moment of inertia	J	kg m^2				kg m^2	Mass moment, 2. order
Mass rate of flow	$\dot{m}$	kg/s		t/s, t/h, kg/h		kg/s and t/s	
Force	F	N	Newton (= kg m/s^2)	kN, mN, µN,…	kp, Mp,…	N	1 kp = 9.81 N. The weight force is the product of the mass m by the local gravitational constant g.
Pressure	p	Pa	Pascal (= N/m^2)	bar (1 bar=10^5 Pa)	kp/cm^2, at, m w.c., Torr, …	bar	1 at = 0.981 bar = 9.81 · 10^4 Pa 1 mm Hg = 1.333 mbar 1 mm w.c. = 0.098 mbar
Mechanical stress (strength)	σ, τ	Pa	Pascal (= N/m^2)	N/mm^2, N/cm^2…	kp/cm^2,	N/mm^2	1 kp/mm^2 = 9.81 N/mm^2
Bending moment, torque	M, T	N m			kp m, …	N m	1 kp m = 9.81 N m
Energy, work, quantity of heat	W, Q	J	Joule (= N m = W s)	kJ, Ws, kWh, … 1 kW h = 3600 kJ	kp m kcal, cal, WE	J und kJ	1 kp m = 9.81 J 1 kcal = 4.1868 kJ
Total head	H	m	Metre		m l. c.	m	The total head is the work done in J = N m applied to the mass unit of the fluid pumped, referred to the weight force of this mass unit in N.
Power	P	W	Watt (= J/s = N m/s)	MW, kW,	kp m/s, PS	kW	1 kp m/s = 9.81 W 1 PS = 736 W
Temperature difference	T	K	Kelvin	°C	°K, deg.	K	Base unit
Kinematic viscosity	ν	m^2/s			St (Stokes), °E, …	m^2/s	1 St = 10^{-4} m^2/s 1 cSt = 1 mm^2/s
Dynamic viscosity	η	Pas	Pascal second (= N s/m^2)		P (Poise)	Pa s	1 P = 0.1 Pa s
Specific speed	n_q	1				1	$n_q = 333 \cdot n \cdot \frac{\sqrt{Q_{opt}}}{(g\, H_{opt})^{3/4}}$ SI units (m und s)

€ 46,–

ISBN 3-00-017841-4

KSB Aktiengesellschaft
D-67225 Frankenthal (Pfalz) / Germany
Telephone +49 6233 86-0 • Fax +49 6233 86-3401 • www.ksb.com

0101.5/4-10 / 12.05 / Ottweiler